Mini-Review

Genotoxicity of metal oxide nanomaterials: Review of Recent data and discussion of possible mechanisms

Nazanin Golbamaki[1], Bakhtiyor Rasulev[2], Antonio Cassano[3], Richard L. Marchese Robinson[3], Emilio Benfenati[1], Jerzy Leszczynski[2], Mark T.D. Cronin[3]

Affiliations

[1] Laboratory of Environmental Chemistry and Toxicology at the Mario Negri Institute, Milan, Italy

[2] Interdisciplinary Center of Nanotoxicity, Jackson State University, Jackson, MS, USA

[3] School of Pharmacy and Biomolecular Sciences, Liverpool John Moores University, Liverpool, UK

Abstract

Nanotechnology has rapidly entered into human society, revolutionized many areas, including technology, medicine and cosmetics. This progress is due to the many valuable and unique properties that nanomaterials possess. In turn, these properties might become an issue of concern when considering potentially uncontrolled release to the environment. The rapid development of new nanomaterials thus raises questions about their impact on the environment and human health. This review focuses on the potential of nanomaterials to cause genotoxicity and summarizes recent genotoxicity studies on metal oxide nanomaterials. Though the number of genotoxicity studies on metal oxide/silica nanomaterials is still limited, this endpoint has recently received more attention for nanomaterials and the number of related publications has increased. Analysis of these peer reviewed publications over nearly two decades shows that the test most employed to evaluate the genotoxicity of these nanomaterials is comet assay, followed by Micronucleous, Ames and Chromosome aberration tests.

Analysis of the literature shows an increasing number of genotoxicity studies for nanomaterials every year. Based on the data studied we concluded that experimental data for genotoxicity for nanomaterials with the same core chemical composition, may vary to some extent due to: 1) variation in size of the nanoparticles; 2) variations in size distribution; 3) varying purity of nanomaterials ; 4) variation in surface areas for nanomaterials with the same average size; 5) differences in coatings; 6)

differences in crystal structures of the same types of nanomaterials; 7) differences in sizes of aggregates in solution/media; 8) differences in assays; 9) different concentrations of nanomaterials in assay tests; 10) variation in concentration of analytes in assays. As a result, due to the considerable inconsistencies in the recent literature and the lack of standardized test methods - reliable genotoxicity assessment of NPs is still challenging.

Keywords: comet assay, micronucleus test, Ames test, nanoparticles, nanomaterials, metal oxides, silica

1. Introduction

Nanotechnology is currently utilized in many areas of industry, medicine, and military applications [1, 2]. Nanomaterials (NMs) form the basis of nanotechnology and may be described as materials "with any external dimension in the nanoscale or having internal structure or surface structure in the nanoscale", where the "nanoscale" may be considered to be 1-100 nm [3]. However, it should be noted that variations of this definition exist [3]. For example, the recently proposed definition from the European Commission takes account of the fact that NMs will typically be composed of particles with a distribution across different sizes [4] and particles with larger sizes, up to 1000 nm (to include aggregates and agglomerates), may also be considered to be NMs [5]. Nanoparticles (NPs), as a sub-category of NMs, may be defined as particles with all three external dimensions in the range 1-100 nm although, again, variations on this definition exist [3]. The special physicochemical properties of NMs due to their small size and structure confer novel capabilities to these materials, suitable for a wide range of applications [6-12]. The development of NMs is also driven by hope that these chemicals will offer improved performances and new functionalities leading, e.g., to smart drugs and to their aiding in achieving sustainable development, e.g., by reducing the consumption of energy and materials and reducing environmental contamination [13]. At the same time, despite the huge benefits of nanotechnology, there is current concern regarding NMs' potential hazardous effects on biological systems [14-20].

The same properties that make these particles exciting for technological research and development may also make them problematic from a toxicological perspective: NMs are relatively unexplored with regard to long term, low dose, exposure [1, 15, 21-25]. However, it should be noted that the question of whether or not NMs exhibit novel mechanisms of toxic action is currently a subject of considerable debate, as noted in the recent paper of Donaldson and Poland [26] and elsewhere within the literature [1, 27-30]. Even NMs that have the same chemical composition differ in their toxicological properties; the differences in toxicity depend upon NMs' size, shape, and surface charge, type of coating material and reactivity [16, 31]. The potential toxicity and mechanisms of toxic action of NMs are still topics of particular interest due to the lack of sufficient toxicity data and mechanistic understanding. Indeed, uncertainties around the safe use of NMs are considered a major obstacle to innovations and investment in nanotechnology [32].

As well as hazard considerations, exposure is also a critical factor which affects the risk, to the environment and human health, associated with the use of NMs. As for conventional chemicals, a thorough risk assessment would require "effects assessment" (i.e. determination of the toxicity associated with a given dose, exposure duration and exposure route) in a toxicology study followed by consideration of realistic exposure estimates for the environment and human populations [33]. In addition to challenges associated with environmental/human exposure estimation [34], "effects assessment" is complicated for NMs, as compared to conventional small molecule chemicals, by problems with the toxicity data as well as the challenge of determining appropriate dose metrics [35] [26].

Since the available data on NMs' toxicity (the focus of this review) and environmental/human exposure [34] are unfortunately limited, they do not allow for significant quantitative risk assessment of the safety of synthesized NMs to be made. Moreover, the problem of the lack of data becomes even more complicated by the questionable suitability of tests used for NMs' toxicity evaluation, including the common genotoxicity tests which are the focus of this review. For example, some inconsistencies in data from different tests are found in the supporting literature and the validity of some OECD genotoxicity Test Guidelines for NMs has been called into question [36, 37]. Indeed, the OECD Working Party on Manufactured Nanomaterials is, at the time of writing, currently reviewing possible modifications or additions to existing OECD Test Guidelines and/or OECD Guidance Documents for a number of different (eco)toxicological and physicochemical endpoints which may be required for NMs [38-40] [40].

It should be noted, when considering the toxicity of NMs, that a variety of different kinds of NMs exist. NMs may initially be differentiated based upon their chemical composition. For example, Stone *et al.* [41] suggested NMs might be categorized as carbon based (e.g. carbon black, carbon nanotubes and fullerenes), mineral based (e.g. metals, metal oxides), organic (e.g. polymers, dendrimers and surfactant coatings), composites/hybrids (e.g. multicomponent NMs, such as quantum dots, or doped metal/metal oxides) with nanoclays suggested to be difficult to assign.

In this article, we concentrate on metal oxide and silica NMs for which experimental investigations were reported in the literature and summarize the *in vivo* and *in vitro* studies of genotoxic effects that these NMs exhibit. Metal oxide NMs are an important group of engineered NMs, as they are used in various areas of human life such as cosmetics, sunscreens, self-cleaning coatings, textiles and paints. Other applications include their use as water-treatment agents, as materials for solar batteries and, more recently, automobile catalytic converters [42]. Silica (silicon dioxide) based NMs are also of significant commercial relevance, as recognized by the Organisation for Economic Co-operation and Development (OECD) [43], and concerns regarding their use in cosmetics were recently raised by the European Commission, which requested a safety assessment of "nano silica" from the Scientific Committee on Consumer Safety (SCCS) in October 2013 [44]. Whilst there is precedence in the nanotoxicology literature for considering silica to be a metal oxide [10, 45], silicon is technically a metalloid [46]. It is included in our review due to its various industrial applications.

The importance of metal oxide/silica NMs is demonstrated by their large use in consumer products. Indeed, according to The Project on Emerging Nanotechnologies online database [47], at the time of writing 1809 different products containing NMs (including metal oxides) are currently marketed. Moreover, it is expected that the nano-market will grow exponentially and will reach an annual turnover of $2.6 trillion in 2014. As far as metal oxide NMs are concerned, their widespread use is highlighted by the fact that five classes of this specific category of NMs are represented in the repository. To be more precise, 180 out of 1809 (i.e. 10% of the total number) unique consumer products found in the aforementioned online database are metal oxide/silica NMs, including titanium dioxide (91 products), silicon dioxide (41 products), zinc oxide (38 products), aluminium oxide (8 products) and cerium oxide (2 products).

NMs represent high tonnage materials. For instance, Hendren and colleagues [48] estimated upper and lower bounds for annual U.S. production volumes of five classes of NMs, including cerium oxide and titanium dioxide. The results of this investigation showed that titanium dioxide NMs was estimated to reach the greatest annual production among the considered NMs, ranging between 7,800 and 38,000 tons/year. Furthermore, a study of the Dutch National Institute for Public Health and the Environment (RIVM) estimated the amount of NMs used in consumer products on the market at the time of their analysis (2009) as well as the amount of NMs which were expected to be used in consumer products in the near future [49]. In order to assess the most relevant “exposure characteristics”, i.e. factors of most relevance to estimated exposure, within the considered categories of NMs, a working group of seven RIVM experts on NM consumer exposure was consulted. The individual estimations from the seven experts were combined with the ranking of NMs in consumer products, based on the amount used within all considered products, as well as data from product inventories to identify high priority NMs for future exposure studies. As a result, product categories with a high priority for future exposure studies were as follows: sun screens (which often contain zinc oxide and titanium dioxide NMs), coatings and adhesives. In addition, cerium oxide (motor vehicles consumer category) was labelled as high priority as well as titanium dioxide and alumina contained in cleaning products.

Many industrial chemicals are capable of causing genetic damage to living organisms [50].The potential for NMs to exhibit genotoxicity has been discussed in several reviews [17, 51-55]. Among them, metal oxide/silica NMs were found to cause genotoxicity in some, but by no means all studies [17, 19]. Various kinds of features can influence the mechanism(s) of metal oxide/silica NMs’ genotoxicity - for example, their size, surface charge (and other surface properties), composition, shape, solubility, aggregation and agglomeration [41, 56]. All these properties can affect both primary and secondary genotoxicity [57]. (Primary and secondary genotoxicity mechanisms are discussed in section 5 of the current review.) A key genotoxicity mechanism that is often described is ability of the particles to cause oxidative stress, a term that can be described as an imbalance in the oxidative and antioxidative status of a cell in favor of the former [11]. However, there is a need for a more detailed understanding of NM toxicity mechanisms, including genotoxicity, and an appreciation of how the physico-chemical properties of NMs are responsible for interactions with cells. Therefore, there is an urgent need for as many toxicity data as possible to ultimately allow for the risk assessment of metal oxide NPs to be undertaken.

Despite the need, obtaining reliable genotoxicity data for NMs, including metal oxide/silica NMs, is a challenging task as there are many various complications associated with their testing. A number of short term test systems, which were originally designed for conventional chemical compounds and have subsequently been applied to NMs, are available for the assessment of genetic hazard [2, 13, 17, 19, 51-54, 58-61]. These systems are often characterized by the endpoints that they measure: gene mutation, chromosome damage, or deoxyribonucleic acid (DNA) damage [13, 17, 52, 54, 58, 60]. At the same time, none of these tests are ideal for the estimation of NMs' genotoxicity: some show low reproducibility, some need specifically adjusted protocols for NMs and discussions on this are ongoing as indicated above [2, 13, 58].

In this paper, we have gathered and discussed the latest experimental data on metal oxide/silica NMs' genotoxicity. In updating this fast-changing research area, we concentrate in particular on the discussion of genotoxicity study calls among these metal oxide/silica NMs, methods of investigation and possible mechanisms of genotoxicity. The genotoxicity profiles considered in this paper are based on common test systems used for genotoxicity studies: the comet assay [62], micronucleous test (MN) [63], Ames test [64], and chromosome aberration test [65]. When considering the data from these assays, the potential limitations of these test systems for NMs must be remembered [37].

2. Metal oxide structures and key physical properties of their NM counterparts.

A metal oxide is a chemical compound that contains at least one metal atom and one or more oxygen atoms. The metal oxides can adopt a vast number of structural geometries with an electronic structure that can exhibit metallic, semiconductor or insulator characteristics [66, 67]. Oxides of most metals adopt polymeric structures with M-O-M crosslinks. Moreover, because these crosslinks are characterized by strong interactions, the solids tend to be insoluble in solvents, though they are attacked by acids and bases. In metal oxides, the coordination number of the oxide ligand is two for most electronegative elements and 3–6 for most metals [66]. (WHAT ABOUT METALS FROM THE FIRST AND SECOND GROUP?) A selection of representative structures of metal oxides are shown in Figure 1. Some metal oxides are composed of oxygen atoms bound to transition metals (for example, titanium oxide, Figure 1a). These metal oxides are commonly utilized for their catalytic activity and semi-conductive properties [68, 69]. Transition metal oxides are also frequently used as pigments in paints and plastics, most notably - titanium dioxide [7, 70, 71]. Transition metal oxides have a wide variety of surface structures which affect the surface energy of these compounds and influence their chemical properties. Interestingly, there is very little known about the surface structures of metal oxides (transition metal oxides), however their bulk crystal structures are well researched.

Metal oxide NPs mostly have similar crystal structures to bulk-sized metal oxides but with particles sizes between 1 and 100 nm [72]. A metal oxide of NM size can have a very large surface size, which affects its reactivity and other physico-chemical properties. In order to display mechanical or structural stability, a NM must have a low surface free energy. Due to this feature, even phases that have a low stability in bulk materials can become very stable in nanostructure materials. For example, this structural

phenomenon has been detected in TiO_2, VOx, Al_2O_3 or MoOx oxides [67, 73-76]. Size-induced structural distortions associated with changes in cell parameters have been observed, for example, in NMs of Al_2O_3, NiO, Fe_2O_3, ZrO_2, MoO_3, CeO_2, and Y_2O_3 [76]. The second important effect of size is related to the electronic properties of the oxide. In any material, the nanostructure produces so-called quantum size or confinement effects which essentially arise from the presence of discrete, atom-like electronic states [67, 76]. Thus, in their bulk state, many oxides have wide band gaps and low reactivity [77]. A decrease in the average size of an oxide particle does, in fact, change the size of the band gap, with a strong influence on conductivity and chemical reactivity [78, 79]. This can dramatically affect the behavior of metal oxide NMs and their interactions, including interactions with biomolecules of cell systems [80].

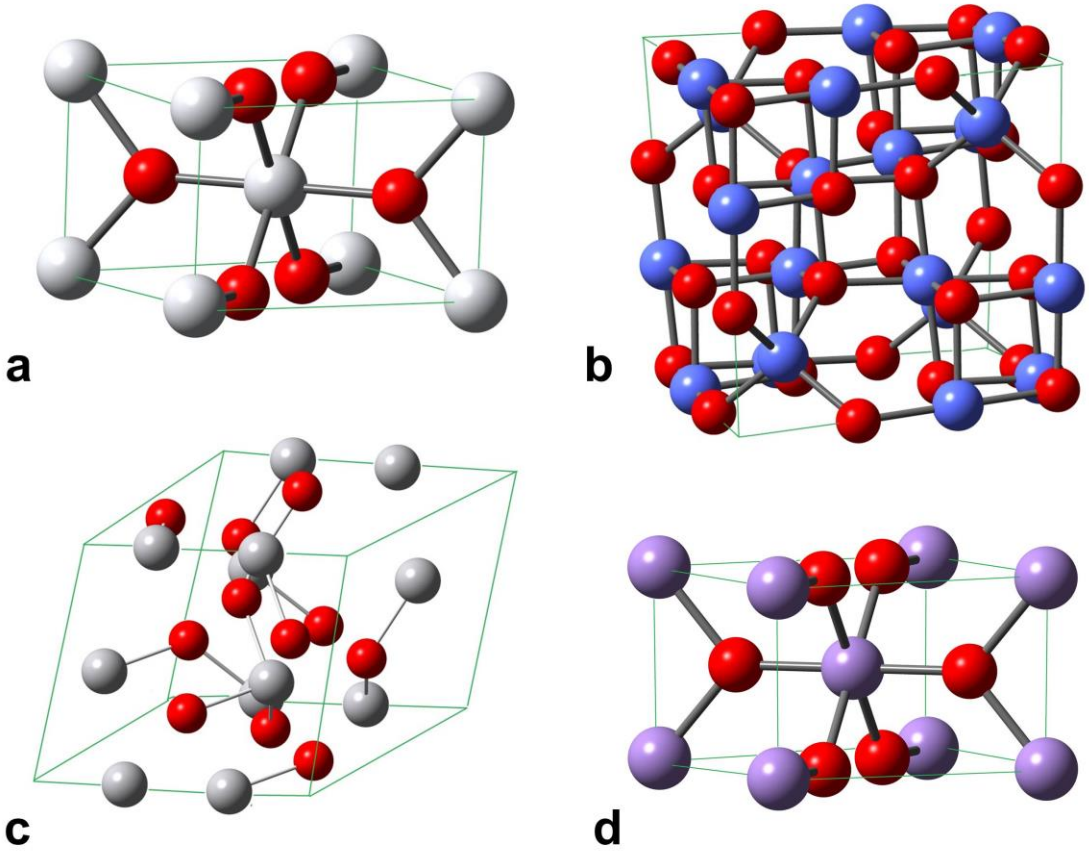

Figure 1. The crystal structures of selected metal oxides: (a) TiO_2, (b) Cr_2O_3, (c) V_2O_3, (d) MnO_2.

3. Methods used for *in vitro* genotoxicity studies

This review considers experimental genotoxicity data for NMs. Most of the data obtained were from three methods used to test primary genotoxicity (as opposed to secondary genotoxicity, which is discussed in section 5): the comet assay, micronucleus and Ames tests. The chromosome aberration test

is also discussed briefly, but limited data were obtained from this test and so it was not considered in detail.

The data obtained for the comet assay, micronucleus and Ames tests are summarized in tables 1, 2 and 3 respectively. In these tables, each row contains data for all nano metal oxides (or silica), reported in a given publication, with a single core chemical composition. If a paper comprised results for NMs with more than one core chemical composition, these data were spread over different rows. However, one single row of the table may summarize data for multiple NMs, reported in the same publication, corresponding to the same core composition but with differences in other characteristics such as size, surface functional groups etc. Hence, the column "Result" indicates whether any of the NMs, corresponding to a given core composition and reported in the corresponding publication, produced a single positive result in the relevant assay (i.e. Comet, Micronucleus or Ames depending upon the table). In other words, if a row contains data for multiple NMs with, say, different sizes or surface coatings, but the same core chemical composition, the "Result" column will report a positive overall result (i.e. "+") if at least one positive result was reported for one of the tested NMs described in the current row. On the other hand, we reported a negative overall result (i.e. "-") whenever all the data points included in a single row are negative. We undertook this approach considering that in the majority of the publications analysed in this review, the metal oxide (or silica) nanoparticles of the same core chemical composition did not show different genotoxicity study calls (i.e. positive or negative) in the same test. For instance, Balasubramanyam et al tested two aluminium oxide NMs with nominal diameters of 30 nm and 40 nm. The results from the comet assay showed a statistically significant increase in percentage tail DNA in comparison to the control group, i.e. a positive result, at 1000 and 2000 mg/kg dose levels after 4, 24 and 48 hours with both aluminium oxide NMs studied [81].

In a few cases, the data were not clear, so the "Result" column reports "+/-". For instance, Downs et al. [82] tested two amorphous silica NMs with different sizes in an *in vitro* micronucleus assay for 24 hours of exposure, at four concentration levels: 31.6, 100, 316, 1000 μg/mL. In this publication, no increase was observed in the percentage of *micronuclei* at the lowest concentrations, for both of the NMs described above. This outcome was also observed for the larger silica NM when tested at the highest concentration. However, for the highest concentration tested (i.e. 1000 μg/mL), the author was unable to score the percentage of *micronuclei* for the smallest silica nanomaterial reported in the paper, since the test material excessively precipitated on the slides. In such a case, we labelled the results for the corresponding set of nanomaterials as equivocal i.e. the "Result" column reports "+/-".

Here it should be noted that, in addition to *in vitro* tests, *in vivo* versions of the comet assay and micronucleus tests also exist [37]. *In vivo* data are also available [51, 59, 60, 63, 81, 83-89], but they are quite limited and where available, they were reported in table 1. Below, we give some general information on the genotoxicity tests which are the focus of this review as well as a brief overview of the chromosome aberration test. This test is not the focus of the review and therefore not further discussed.

3.1. The Comet Assay

The comet assay (also known as the single-cell gel electrophoresis assay) is a method for measuring deoxyribonucleic acid (DNA) strand breaks in eukaryotic cells [90, 91]. Cells are embedded in agarose on a microscope slide and lysed with detergent, containing a high concentration of salt, to form nucleoids which contain supercoiled loops of DNA linked to the nuclear matrix. Electrophoresis at high pH gives rise to structures resembling comets, as observed by fluorescence microscopy; the number of DNA breaks is reflected in the intensity of the comet tail relative to the head. The probable basis for this phenomenon is that DNA loops lose their supercoiling upon breaking and are able to extend toward the anode [58]. One way of quantifying DNA damage using this assay is via the so-called "Olive Tail Moment (OTM)" which is equal to the percentage of DNA in the comet tail multiplied by the length of the tail [92]. The assay has found a number of applications: assessing novel chemicals for genotoxicity, monitoring genotoxin contamination of the environment, human biomonitoring and molecular epidemiology, and fundamental research in DNA damage and repair [90, 91]. The specificity and sensitivity of the assay are considerably increased if the nucleoids are incubated with bacterial repair endonucleases which recognize specific kinds of DNA damage and convert DNA lesions to breaks, increasing the DNA content of the comet tail. As well as detecting DNA strand breaks caused by a chemical of interest (for example, a NM), the repair activity in a cell extract can be determined via either incubating cells after treatment with damaging agent and measuring the damage remaining at intervals or by incubating the cell extract with nucleoids containing specific damage [58]. Tice and colleagues reported that modifications to the traditional comet assay can be suitable to investigate specific categories of DNA damage. In greater detail, oxidized pyrimidines can be detected using the endonuclease III enzyme, whereas 8-OH guanine as well as other damaged purines can be detected by using the formamidopyrimidine DNA glycosylase (Fpg) enzyme [91].

3.2. The Micronucleus Test

Micronucleus (MN) assays are one of the preferred methods for assessing chromosome damage for conventional chemicals, as they enable both chromosome breakage and chromosome loss to be measured reliably [93]. Since micronuclei can only be expressed in cells which undergo complete nuclear division, a version of the micronucleus test was developed that identifies cells which have undergone nuclear division by their binucleate appearance when blocked from performing cytokinesis (cell division) by cytochalasin-B, a microfilament-assembly inhibitor [93, 94]. The cytokinesis-block micronucleus (CBMN) assay enables better precision because it prevents the data obtained from being confounded by altered cell division kinetics due to, possible, cytotoxicity of tested agents or suboptimal cell culture conditions [95].

As discussed above, the standard MN assay (OECD Test Guideline No. 487) [96] often (but not always) employs cytochalasin B (CB) to detect micronucleus frequency in binucleate cells formed after mitosis. However, it is known that CB also inhibits endocytosis, and thus might prevent NM cellular uptake. Hence, a modified protocol needs to be used for testing NMs: incubating with NM before adding CB.

This example illustrates that, with certain precautions, standard tests for DNA and chromosome damage may be applied to NM [37, 62].

3.3. The Ames Test

This is a test for identifying mutagens by studying the frequency with which they cause mutations inducing production of an essential amino acid in bacterial colonies initially lacking the ability to synthesize this amino acid [64, 97]. Those bacterial colonies for which mutations occur, giving rise to the ability to produce the essential amino acid, are termed "revertant colonies" [97]. Typically, as recommended in OECD Test Guideline No. 471 [97], one or more strains of *Salmonella* (*S. typhimurium*) and/or *Escherichia coli* are used e.g. the *S. typhimurium* strains TA97a, TA98, TA100, TA102, TA1535 and TA1537 or the *E. coli* strain WP2u-vrA$^-$referred to in Table 3. It can also be used with or without metabolic activation i.e. typically with or without "S9- mix" [97]. OECD Test Guideline No. 471 [97] recommends that a "positive" result for a single strain, with or without metabolic activation, should be identified based on identifying a concentration related increase in the number of revertant colonies and/or a reproducible increase at a single concentration. A "positive" Ames test result would then be assigned if a "positive" result was observed with any strain with or without metabolic activation. It is widely used for the assessment of organic molecules, such as prospective pharmaceutical active ingredients [98], and there are considerable Ames test data for these chemicals in the public domain [99, 100]. However, it has been suggested that the Ames test is one of the least appropriate genotoxicity tests for NMs due to poor uptake of NMs by bacterial cells [37, 101].

3.4. Chromosome aberration

Chromosome aberrations result from failures in repair processes such that breaks either do not rejoin or rejoin in abnormal configurations [102]. The purpose of the *in vitro* chromosomal aberration test is to identify agents that cause structural chromosome aberrations in cultured mammalian cells.

However, it is considered sub-optimal, compared to the micronucleus test, as it substantially slower to perform and cannot detect the same kinds of chromosomal abnormalities i.e. it cannot detect aneugens as well as clastogens [37].

Table 1. Current review of comet assay results on metal oxide/silica NMs (+positive; -negative; +/-equivocal). As explained in section 3, each row in this table summarizes all genotoxicity data found for this test for all nanomaterials with a given core chemical composition reported in a given publication.

Nanomaterial core chemical composition	Physical characteristics (size and etc)	Cells	Exposure	Results	Summary	Reference
Al_2O_3	Two aluminium oxide NMs were studied. Nominal diameters: 30 nm and 40 nm. TEM analysis: 39.85 ± 31.33 nm and 47.33 ± 36.13nm. DLS analysis: average diameters 212.0 and 226.1 nm in water.	*In vivo* female Wistar rat peripherial blood cells	Three dose levels (via gavage): 500, 1000 and 2000 mg/kg body weight. Whole blood was collected at 4, 24, 48 and 72 h	Results showed statistically significant increase in % Tail DNA at 1000 and 2000 mg/kg dose levels after 4, 24 and 48 h with both aluminium oxide NMs studied in comparison to the control group.	+	[81]
Al_2O_3	Nominal size: 16.7 nm. DLS analysis: hydrodynamic diameter 16.7 ± 1.3 nm.	*In vitro* human embryonic kidney (HEK293) and peripheral blood lymphocytes cells	Three concentration levels: 1, 10, and 100 µg/ml. Exposure duration: 3 h	Results showed that all concentration levels of Al_2O_3 did not induce any marked genotoxicity	-	[103]
Al_2O_3	Nominal size < 50 nm.	*In vitro* mouse lymphoma (L5178Y) cells and human bronchial epithelial (BEAS-	Three concentration levels for L5178Y cells: 1250, 2500, 5000 µg/mL. Three concentration levels for	Al_2O_3 NM induced DNA damage in L5178Y at 1250 to 5000 µg/ml with S9 mix (+S9) and induced DNA damage at 2500	+	[104]

		2B) cells	BEAS-2B cells: 68.36, 136.72, 273.44 µg/mL (+S-9); 97.66, 195.32, 390.63 µg/ml (-S-9). Exposure duration: 2 h	µg/mL without S9 mix (-S9). A significant increase in DNA tail was observed in BEAS-2B cells at all concentrations tested under both +S9 and -S9 conditions.		
Bi_2O_3	Nominal size between 90 and 210 nm.	*In vitro Allium cepa* root cells	Five concentration levels: 12.5, 25, 50, 75, and 100 ppm. Exposure duration: 4 h	Results showed a dose-dependent increase in the DNA damage at all concentrations except 12.5 ppm compared to negative control.	+	[105]
CeO_2	Nominal size < 25 nm. TEM analysis: 25 ± 1.512 nm. DLS analysis: hydrodynamic diameter 269.7 ± 27.398 nm	*In vitro* human neuroblastoma (IMR32) cells	Five concentration levels: 10, 20, 50, 100, and 200 mg/ml. Exposure duration: 24 h	A significant increase in the percentage of tail DNA was observed only at the highest dose of 200 mg/ml	+	[106]
CeO_2	Nominal size: 7 nm. DLS analysis: hydrodynamic diameter 15 nm	*In vitro* human dermal fibroblasts	Seven concentration levels: 0.006, 0.06, 0.6, 6, 60, 600, 1200 mg/l. Exposure duration: 2 h	A dose-response increase in the olive tail moment at very low doses (0.006 mg/l) was observed	+	[107]
CeO_2	TEM analysis: average size 5.5 nm. XRD analysis: 6.3 nm	*In vitro* human lens epithelial cells	Two concentration levels: 5 and 10 µg/ml. Exposure duration: 24 h	Results showed that nano-CeO_2, at either tested dose, did not cause any damage to the DNA in cultured eye lens	-	[108]

				epithelial cells.		
CeO_2	Nominal size < 25 nm. TEM analysis: longest dimension between 4 and 25 nm. DLS analysis: 225 nm.	*In vitro* human alveolar Type II-like epithelial (A549) and bronchial epithelium (BEAS-2B) cells	Two concentration levels: 40 and 80 µg/ml. Exposure duration: 4 h	In A549 cells, CeO_2 significantly increased the amounts of DNA breaks compared to control group at both tested concentrations in a dose-dependent manner. In BEAS-2B cells, CeO_2 caused significantly increased levels of DNA breaks only at 80 µg/ml.	+	[109]
CeO_2	SEM analysis: average diameter between 16 and 22 nm.	*In vitro* human alveolar adenocarcinoma (A549), colorectal adenocarcinoma (CaCo2) and hepatic carcinoma ($HepG_2$) cells	Three concentration levels: 0.5, 50, 500 µg/ml. Exposure duration: 24 h		+	[110]
CeO_2	Two different types of CeO_2 were studied. Nominal size: 30 and 15 nm	*In vivo Daphnia magna* and *Chironomus riparius*	Single dose level: 1 mg/l. Exposure duration: 24 h	Tail and olive tail moments increased in both tested species	+	[111]
CeO_2	Nominal size: 3 nm. DLS analysis: hydrodynamic diameter 350 nm	*In vitro* female mice oocytes and follicular cells	Four concentration levels: 2, 5, 10 and 100 mg/l. Exposure duration: 2 h	A significant and dose-dependent increase in DNA damage was shown in follicular cells exposed to CeO_2 NMs at all concentration levels. In oocytes surrounded by	+	[92]

				zona pellucida, DNA damage was observed only at 10 and 100 mg/l		
Co_3O_4	TEM analysis: 21 nm. DLS analysis: average hydrodynamic size 264.8 nm (water)	*In vitro* human hepatocarcinoma (HepG2) cells	Three concentration levels: 5, 10 and 15 µg/ml. Cells were treated for 24 and 48 h	Cells exhibited a significant increase in DNA damage at almost all concentration levels, after 24 and 48 h, except for 5 µg/ml after 24 h.	+	[112]
Co_3O_4	Nominal size < 50 nm. TEM analysis: longest dimension between 9 and 62 nm. DLS analysis: 222 nm.	*In vitro* human alveolar Type II-like epithelial (A549) and bronchial epithelium (BEAS-2B) cells	Two concentration levels: 40 and 80 µg/ml. Exposure duration: 4 h	In A549 cells, Co_3O_4 significantly increased the amounts of DNA breaks compared to control group only at 40 µg/ml. In BEAS-2B cells, Co_3O_4 caused significantly increased levels of DNA breaks only at 80 µg/ml.	+	[109]
CuO	Nominal size: 28 nm. SEM analysis: primary particle size 50 nm	*In vitro* human lung type II epithelial (A549) cells	One concentration level: 80 µg/ml. Exposure duration: 4 h	CuO NM showed significant levels of DNA damage at test conditions	+	[113]
CuO	Nominal size: 42 nm. TEM analysis: average size between 20 and 40 nm. DLS analysis: 220 nm	*In vitro* human lung type II epithelial (A549) cells	Three concentration levels: 2, 40 and 80 µg/ml. Exposure duration: 4 h	A significant increase in DNA damage was observed at concentrations of 40 and 80 µg/ml	+	[114]
CuO	Nominal size: 42 nm. TEM	*In vitro* human lung type II	Two concentration levels: 40 and 80 µg/ml.	A significant damage was found at 80 µg/ml.	+	[31]

	analysis: average size between 20 and 40 nm. DLS analysis: 200 nm	epithelial (A549) cells	Exposure duration: 4 h	However, an increased (non-significant) DNA damage was also observed at 40 µg/ml		
CuO	Four different CuO nanoparticles were studied, with the following size measurements and shapes determined by TEM: (1) 10-100 nm (unspecified shape); (2) 7±1 nm (spheres); (3) 7±1×40±10 nm (rods); (4) 1200±250×270±50×30±10 nm (spindles)	*In vitro* human murine macrophages RAW 264.7 cells and peripheral blood lymphocytes (PBL).	Three concentration levels: 0.1, 1 and 10 µg/ml. Exposure duration: 2 and 24 h	For RAW264.7 cells, all four tested nanoparticles caused statistically significant increase in primary DNA damage after 2 and 24h treatments at all concentrations. For PBL cells, statistically significant primary DNA damage was also detected for all tested CuO samples except for the following results: spheres (0.1 µg/mL , 24h; 1 µg/mL, 2h) and spindles (0.1 µg/mL , 24h; 0.1 µg/mL, 2h).	+	[115]
CuO	Nominal size: 10 nm. TEM analysis: size between 20 and 40 nm. DLS analysis: hydrodynamic diameter 276.4 nm (water)	*In vitro* human lung epithelial (A549) cells	Two concentration levels: 5 and 15 mg/l. Exposure duration: 2, 4, 8, 16 and 24 h	A time-dependent increase in DNA damage was observed for the 15 mg/l concentration level at 8, 16 and 24 h of exposure. For the 5 mg/l concentration level, a significant increase in DNA damage was shown only at 24 h of exposure	+	[116]

CuO	SEM analysis: diameter ranging from 20 to 200 nm. DLS analysis: average size 500 ± 20 nm after sonication	*In vitro* rainbow trout *(O. mykiss)* red blood cells; *in vivo* rainbow trout *(O. mykiss)* erythrocytes	*In vitro*: One concentration level = 7.5 µg/ml; Exposure duration: 1 h. *In vivo* (intraperitoneal injection): One dose level of CuO NM expressed in terms of the equivalent mass of Cu = 1 µg/g body weight. Exposure duration: 38 h	The percentage of tail DNA significantly increased in the presence of Cu compared to the control only in the *in vitro* study	+	[117]
CuO	Nominal size < 50 nm. TEM analysis: 31 ± 10 nm. DLS analysis: 284.0 ± 21.2 nm	*In vivo Mytilus galloprovincialis* hemolymph cells	One dose level: 10 µg/l. Exposure duration: 3, 7 and 15 days	An increase both in the olive tail moment and in the percentage of tail DNA was observed following 7 days of exposure.	+	[118]
CuO	Nominal size < 100 nm. Hydrodynamic size of 204 nm	*In vivo Macoma balthica* soft tissue cells	One concentration level of CuO expressed in terms of the equivalent mass of Cu = 10 mg/l. Exposure duration: 35 days	No significant genotoxic effects were observed	-	[119]
CuO	Nominal size: 10−100 nm. TEM analysis: 29.5 nm. Hydrodynamic size: 197 nm (deionized water) and 810	*In vivo* worms *H. diversicolor* coelomocytes cells and clams *S. plana* hemocytes cells	One dose level: 10 µg/l. Exposure duration: 21 days	In both species, percentages of tail DNA were significantly increased	+	[120]

	nm (seawater)					
CuO	Nominal size: < 50 nm. DLS analysis: 1511 ± 468 nm (water) 3475 ± 357 nm (medium)	*In vitro S. cerevisiae* cells	One concentration level: 31.25 mg/l. No information about exposure duration	Cells exposed to CuO NMs showed a significant amount of DNA damage compared to control.	+	[121]
CuO	Nominal average particle size: 50 nm. TEM analysis: 55.80 ± 8.70 nm. DLS analysis: 68.5 ± 5 nm	*In vitro* human skin epidermal (HaCaT) cells	Three concentration levels: 5, 10 and 20 mg/ml. Cells were treated for 24 and 48 h	A significantly high DNA damage in treated cells was observed	+	[122]
Fe_2O_3	TEM analysis: 35 ± 14 nm. DLS analysis: Z-average hydrodynamic diameter 900 nm	*In vitro* Syrian hamster embryo (SHE) cells	Three concentration levels: 10, 25 and 50 $\mu g/cm^2$. Cells were treated for 24 h	No significant DNA damage was found with Fe_2O_3 particles, at any of the tested concentrations	-	[123]
Fe_2O_3	Nominal size: 90 nm. TEM analysis: average particle diameter 93 nm. DLS analysis:	*In vitro* human lung epithelial cells (A549) and murine alveolar macrophages (MH-S)	One concentration level: 40 $\mu g/cm^2$. Exposure duration: 24 h	Tail DNA was not modified following incubation with Fe_2O_3 NM	-	[124]

	average particle hydrodynamic diameter 68 nm					
Fe_2O_3	Nominal size < 100 nm. DLS analysis: hydrodynamic diameter 50 nm	*In vitro* human lung fibroblasts (IMR-90) and human bronchial epithelial cells (BEAS-2B)	Four concentration levels: 2, 5, 10, 50 $\mu g/cm^2$. Exposure duration: 24 h	DNA damage was showed at concentrations of 10 and 50 $\mu g/cm^2$ in IMR-90 cells and at 50 $\mu g/cm^2$ in BEAS-2B cells	+	[125]
Fe_2O_3	Nominal size: 29 nm. TEM analysis: average size between 30 and 60 nm. DLS analysis: 1580 nm.	*In vitro* human lung type II epithelial (A549) cells	Three concentration levels: 2, 40 and 80 µg/ml. Exposure duration: 4 h	No significant DNA damage was observed at tested concentration levels	-	[114]
Fe_2O_3	Nominal size: 29 nm. TEM analysis: average size between 30 and 60 nm. DLS analysis: 1.6 µm.	*In vitro* human lung type II epithelial (A549) cells	Two concentration levels: 40 and 80 µg/ml. Exposure duration: 4 h	No significant DNA damage was showed at tested concentration levels	-	[31]
Fe_2O_3	Nominal size < 50 nm. TEM analysis: mean size 29.75 ± 1.87 nm. DLS analysis: hydrodynamic	*In vivo* albino Wistar female rat peripherial blood cells	Three dose levels (oral administration): 500, 1000 and 2000 mg/kg body weight. Exposure duration: 6, 24, 48 and 72 h	No statistically significant damage was observed at any sampling time in comparison to control.	-	[126]

	diameter 363 nm (water)					
Fe_2O_3	Nominal mean size: 6 nm. TEM and XRD mean analysis coherent diameter: 6 nm.	*In vitro* human fibroblast cells	Six concentration levels: 0.001, 0.01, 0.1, 1, 10 and 100 µg/ml. Exposure duration: 2 and 24 h	No DNA damage was observed at any tested concentration levels	-	[127]
Fe_2O_3	Nominal size < 50 nm. TEM analysis: 29.75 ± 1.87 nm. DLS analysis: 363 nm	*In vivo* female Wistar rats peripheral blood leucocytes	Three dose levels (oral administration): 500, 1000 and 2000 mg/kg body weight. Exposure duration: 6, 24, 48 and 72 h	No statistically significant damage was observed at 6, 24, 48, 72 h sampling time in comparison to control	-	[128]
Fe_3O_4	TEM analysis: average diameter 10 nm (naked particles) increased up to 150 nm upon surface modifications	*In vitro* murine fibroblast cell line (L-929 cells from mouse subcutaneous connective tissue)	Three concentration levels: 100, 200 and 1000 ppm. Exposure duration: 24 h	NMs tested showed dose-dependent genotoxic effects on the cells, which varied with surface modifications, although not all surface variations gave statistically significant results versus the non-treated control	+	[129]
Fe_3O_4	TEM analysis: 27 ± 8 nm. DLS analysis: hydrodynamic diameter between 700 and 800 nm	*In vitro* Syrian hamster embryo (SHE) cells	Three concentration levels: 10, 25 and 50 µg/cm^2. Cells were treated for 24h	No significant DNA damage was found with iron oxide particles at any concentration level.	-	[123]
Fe_3O_4	TEM analysis: 24.83 nm. DLS analysis:	*In vitro* human skin epithelial	Three concentration levels: 25, 50 and 100 µg/ml. Cells were	The cells exposed to different concentrations, exhibited significantly	+	[130]

	average hydrodynamic size was 247 nm (water) and 213 nm (cell culture medium)	(A431) cells	treated for 24h	higher DNA damage in cells than those of the controls.		
Fe_3O_4	TEM analysis: 24.83 nm. DLS analysis: average hydrodynamic size was 247 nm (water) and 213 nm (cell culture medium)	*In vitro* human lung epithelial (A549) cells	Three concentration levels: 25, 50 and 100 µg/ml. Cells were treated for 24h	The cells exposed to different concentrations, exhibited significantly higher DNA damage in cells than those of the controls.	+	[130]
Fe_3O_4	Nominal size: from 20 nm to 60 nm. Photon correlation spectroscopy (PCS) analysis: mean diameter of 311 nm	*In vitro* human lung adenocarcinoma type-II alveolar epithelial cells A549	Four dose levels: 1, 10, 50 and 100 µg/cm^2. Cells were exposed for 4 h	DNA damage was observed in a concentration-dependent manner	+	[131]
Fe_3O_4	Nominal size: 29 nm. TEM analysis: average sire between 30 and 60 nm. DLS analysis: 1.6 µm	*In vitro* human lung type II epithelial (A549) cells	Two concentration levels: 40 and 80 µg/ml. Exposure duration: 4 h	No DNA damage was showed at the two tested concentration levels	-	[31]
Fe_3O_4	Nominal size between 20 and 30 nm. TEM	*In vitro* human lung type II epithelial (A549)	Three concentration levels: 2, 40 and 80 µg/ml. Exposure	No DNA damage was observed at the tested concentration levels	-	[114]

	analysis: average size between 20 and 40 nm. DLS analysis: 200 nm	cells	duration: 4 h			
Fe_3O_4	TEM analysis: average size 8.0 ± 2.0 nm	*In vitro* human embryonic kidney (HEK-293) and peripheral blood lymphocytes (HPL) cells	Three concentration levels: 10, 30 and 70 µg/ml. Exposure duration: 30 min and 1 h	A significant increase in DNA damage was observed at all tested concentrations after 1 h exposure with both types of cells	+	[132]
Fe_3O_4	Nominal size: 30 nm. TEM analysis: : longest dimension between 20 and 40 nm. DLS: 200 nm	*In vitro* human alveolar Type II-like epithelial (A549) and bronchial epithelium (BEAS-2B) cells	Two concentration levels: 40 and 80 µg/ml. Exposure duration: 4 h	Fe_3O_4 NM caused significant DNA damage only In BEAS-2B cells, at 40 µg/ml	+	[109]
MgO	Nominal size: 8 nm	*In vitro* human colon epithelium (CaCo-2) cells	One concentration level: 20 mg/cm^2. Exposure duration: 4 h	No significant change compared to the control was observed.	-	[133]
MnO_2	Nominal size: 45 nm. TEM analysis: 45 ± 17 nm. DLS analysis: 334.4 nm.	*In vivo* female albino Wistar rat peripherial blood leucocytes (PBL)	Three dose levels: 100, 500 and 1000 mg/kg body weight. Exposure duration: 6, 24, 48 and 72 h	A significant increase in the percentage of tail DNA was observed in the at the highest dose of 1000 mg/kg body weight at 24 and 48 h sampling times; however, no significant DNA damage was observed at 6 and 72 h. An increase in the percentage of tail DNA was observed after	+	[128]

				treatment with lower doses of 100 mg/kg body weight and 500 mg/kg body weight, but these results were not statistically significant at all-time intervals compared with the control groups.		
MnO_2	TEM average mean size diameter: 42.63 ± 23 nm. DLS size in water: 324.8nm. (The result of DLS showed larger values than NPs size measured by TEM, indicating NPs formed larger agglomerates in water suspension. Surface area: 52.21 m^2/g.)	*In vivo* wistar rat leucocytes and bone marrow cells	After 28-day repeated oral dosing in male and female Wistar rats at various doses (30, 300, 1000 mg/kg/body weight per day) for 28 days.	A statistically significant ($P < 0.01$) increase in the DNA damage (percentage oftail DNA) with the highest and medium doses. No significant increase was found with the lowest dose.	+	[134]
NiO	Nominal size: <50 nm. TEM analysis: 2-67 nm. DLS: 167 nm.	*In vitro* human alveolar type II like epithelial A549 and bronchial	40-80 µg/mL for 4h	In A549 cells DNA in tail 31.6% at 40 µg/mL increased amounts of DNA breaks, significantly increased at 80 µg/mL. In	+	[109]

		epithelium BEAS-2B cells		BEAS-2B cells NiO (29.0%) at the low dose and 28.5% at the higher dose.		
SiO_2	Nominal size: 15 nm. TEM analysis: 11-27 nm. DLS: 8.7 nm. The particle size was calculated from the Brownian motion of the particles using the Stokes–Einstein equation.	*In vitro* human alveolar type II like epithelial A549 and bronchial epithelium BEAS-2B cells	40-80 µg/mL for 4h	No significant change compared to the control was observed	-	[109]
SiO_2	Two different types of SiO_2 were used; Nominal size: 10 and 7 nm. BET surface area: 644.44 and 349.71 m^2/g.	*In vivo* in the freshwater crustacean Daphnia magna and the larva of the aquatic midge Chironomus riparius	The fish were collected 24 h from the control and experimental tanks after exposure to 1 mg/L of NPs.	No genotoxic effect on either species as no significant increase both in the tail and in the Olive Tail Moment was observed	-	[111]
SiO_2 (amorphous)	Two silica NMs were tested. Nominal sizes: 15 nm and 55 nm. DLS analysis: z-average particle	*In vivo* Wistar rat peripheral blood cells	Single dose for 15 nm SiO_2: 50 mg/kg; two dose levels for 55 nm SiO_2: 25 mg/kg and 125 mg/kg. Rats injected i.v. at 48h, 24h, and 4h prior to tissue collection	The percentage of DNA damage was increased compared to vehicle-treated rats by 1.4–1.6-fold in all three tissues at the maximum tolerated dose (50 mg/kg)	+	[82]

	diameters (pH 7.5): 31.6 nm and 105.1 nm			of the 15 nm silica NPs, which was significant in the liver.		
SiO_2 (with three types of functionalization: unmodified, vinyl and aminopropyl groups	SEM average diameter: 10 to 50 nm. DLS average hydrodynamic diameter: 4 ± 4.6, 176.7 ± 5.1 and 256.3 ± 7.2 nm respectively.	*In vitro* human peripheral blood lymphocytes	10, 25, 50 and 100 µg/mL after 2 and 24 h	Results revealed no significant increase of basal DNA strand breaks in cells treated with all three types of silica.	-	[135]
SiO_2 (amorphous, fumed)	Nominal size: 14 nm. BET surface area: 200 m^2/g.	*In vitro* human colon epithelium cell line (CaCo-2)	Cells were treated 4h with 20 mg/cm^2 particles (in MEM without serum)	FPG comet assay results found no significant effect in DNA strand breakage and slight effects in oxidative DNA damage study.	-	[133]
SiO_2	Nominal diameter: 50 nm 50 ± 3 nm. TMR- and RuBpy-doped luminescent silica NP (laboratory synthesised)	*In vitro* A549 cells	0.1–500 µg/mL in DMEM with serum for 48 and 72 h	Low genotoxicity was found in alkaline comet assay. Tail length was not significantly different from the control after 48h. Results showed a slight increase in DNA single-strand breaks after 72 h. The comet assay result was further verified using PFGE indicating no additional DNA damage as compared to the untreated control.	-	[136]

SiO_2	Size distribution measured with High Performance Particle Sizer (HPPS): by volume 7.21 nm (100%); by intensity 9.08 nm (71.4%) and 123.21 (28.6%).	*In vitro* WIL2-NS human B-cell lymphoblastoid cells	60 and 120 µg/mL for 24 h	No significant levels of DNA tail percentage in alkaline comet assay	-	[137]
SiO_2	TEM analysis: 20.2 ± 6.4 nm	*In vitro* primary mouse embryo fibroblasts (PMEF)	5 and 10 µg/mL particles in DMEM for 24 h	There were significant increases in tail length, percentage of DNA in tail, tail moment and Olive Tail Moment after PMEF cells were treated with at both examined concentrations (6.8% tail DNA, $p < 0.05$) in alkaline comet assay.	+	[55]
SiO_2	Particle size distribution in the suspension as measured by the high performance particle sizer (Z-Average size): 12.2 nm.	*in vitro* WIL2-NS human B cell lymphoblastoid cell line	0, 60, 120 µg/mL in 10h	There is no significant increment in DNA damage observed when measured by the comet assay.	-	[138]
SiO_2 (amorphous, alumina-coated	Five different samples of nominal size:	*In vitro* human lymphoblastoid fibroblasts (T3T-	4 and 40 µg/mL for 3, 6, and 24h	In the comet assay, DNA damage of human cells was assessed via	-	[139]

with a positive charge)	30–400 nm	L1)		measuring tail length, percentage of tail DNA, and Olive Tail Moment. There were no significant differences between the control and tested NM		
SiO_2	Nominal powder diameter: 10 nm	*In vitro* mouse lymphoma cell line (L5178Y thymidine kinase (tk)+/--3.7.2C cells) and human bronchial epithelial cells (BEAS-2B)	Concentrations from 629.88 µg/mL to 2,519.53 µg/mL with S-9 and from 610.36 µg/mL to 2,441.41 µg/mL without S-9 in L5178Y cells	Nano-silica significantly induced DNA damage at all concentrations compared to control ($P < 0.05$)	+	[140]
SiO_2	TEM analysis: 16.4 ± 2.5 nm and 60.4 ± 8.3 nm	*In vitro* human lung carcinoma (A549) cells	Two concentration levels: 46 and 60 µg/ml. Exposure duration: 15 min and 4h	Treatment with 16 nm or 60 nm SiO_2 showed no increase of DNA strand breaks after 15 min or 4 h as compared to the controls.	-	[141]
SiO_2	Nominal size: 15, 30, 100 nm. Hydrodynamic sizes in MEM suspension after 24 hour were 14.6 ± 0.3, 20.4 ± 1.7, 169.2 ± 3.1 nm	*In vitro* human epidermal keratinocyte (HaCaT) cells	Three concentration levels: 2.5, 5 and 10 µg/ml. Cells were treated for 24h	Three SiO_2 NMs caused more DNA damage and more percentage of DNA in the tail than untreated groups	+	[142]

SiO_2	Nominal size: 12 nm and 40 nm. TEM analysis: "12-nmNPs" ranged between 16 and 40 nm; "40-nm NPs" varied between 50 and 100 nm. DLS analysis (water): 165 nm (12-nm NP); 271 nm (40-nm NP)	*In vitro* human colon carcinoma cells (HT29)	Seven concentration levels: 0.03, 0.3, 3.1, 15.6, 31.3, 93.8, 156.3 mg/cm^2. Exposure duration: 3 and 24h	After 3h as well as after 24h of incubation, none of the tested particles really affected the integrity of the DNA of HT29 cells in the investigated concentration range. However, for some scattered concentration steps, significant differences compared with the medium control were apparent. The appearance of these significances seems to be more random and did not follow a recognisable trend	-	[143]
SiO_2	Nominal size: 2-5 nm. Agglomeration: 1-5-µ granules. No further characterization reported in the paper	*In vivo* F1(CBA×C57Bl/6) mice bone marrow and brain cells	Two dose levels: 5 and 50 mg/kg Exposure duration: 3, 24h and 7 days	A significant increase in the levels of DNA damage in the bone marrow cells of animals injected with 5 mg/kg nc-Si was observed after 24h exposure.	+	[144]
SnO_2	No characterization of the NM is reported in the paper	*In vitro* lymphocyte cells	Two concentration levels: 50 and 100 µg/mL. No exposure duration information	No significant changes in the tail length were showed at both tested concentration levels	-	[145]
TiO_2	Nominal size: 25	*In vitro* murine	Five dose levels: 10, 20,	Results showed that TiO_2	-	[146]

	nm. DLS analysis: mean particle size 300 nm Manufacturer data: SEM analysis: aggregates. DLS analysis: 220 nm. Ramon spectroscopy: a mixture of rutile and anastase forms. BET specific surface area: 27.1 m^2/g.	fibroblasts BALB/3T3 clone A31	60, 100 and 250 µg/mL. Cells were exposed for 3 and 24h	NM caused only a slight (however with a clear concentration-effect relationship) genotoxic effect in BALB/3T3 fibroblasts at the highest concentrations used.		
TiO_2	Nominal size: 21 nm. DLS hydrodynamic diameter: 129.50 ± 2.6 nm	*In vivo* Adult male Wistar rats bone marrow cells	Single dose of 5 mg/kg body weight. Animals were sacrificed at 24h, 1 week and 4 weeks after the injections	The values for exposed animals were sometimes slightly enhanced as compared to control, but results were not statistically significant	-	[147]
TiO_2	Nominal size < 25 nm. DLS hydrodynamic size (Z-average): 1611 ± 21 nm after 24h	*In vivo* P. mesopotamicus (pacu caranha) erythrocytes cells	The fish were exposed (with visible light or ultraviolet and visible light) to the following concentrations of nano-TiO2 during a 96 h period: 0 (control), 1, 10, and 100 mg/l.	No statistically significant differences between the groups were observed.	-	[148]
TiO_2	Nominal average size: 75 ± 15 nm. ZetaSizer Nano	*In vitro* chinese hamster lung fibroblasts (V79 cells)	Three dose levels: 5, 20 and 100 µg/mL. Exposure duration: 6h and 24h	However, TiO_2 NPs exposure only increased the percentage of DNA in the tail (% Tail DNA) at	-	[149]

	ZS90 hydrodynamic diameter: 473.6 nm and 486.8 nm size when suspended in H2O and FBS-free DMEM			the concentration of 100 µg/mL and at the time point 24h.		
TiO_2	Nominal size: 2.3 nm. TEM analysis: average diameter 2.3 ± 0.5 nm	*In vitro* human embryonic kidney (HEK293) cells and human peripheral blood lymphocytes	Concentrations of 1, 10, or 100 µg/mL	Results demonstrated that at all concentration NP did not induce any marked genotoxicity, except for 100 µg/mL. Produced significant genotoxicity and appeared more effective in the comet assay with and without the FPG and Endo III enzymes in both human peripheral blood lymphocytes and HEK293 cell. In contrast ionic type did not show any positive result in the cells	+	[103]
TiO_2	Nominal size: <25 nm	*In vitro* leukocytes from dolphins	20, 50, and 100 µg/mL for 4, 24, and 48 h in RPMI with serum	Positive in alkaline comet assay at 24 and 48 h	+	[150]
TiO_2	Nominal size: <100 nm. BET surface area: 49.71 ± 0.19 m2/g. DLS average particle	Human lung fibroblasts (IMR-90) and human bronchial epithelial cells (BEAS-2B)	Concentrations of 2, 5, 10, 50 µg/cm^2 for 24 h in MEM with serum and in keratinocyte serum-free medium, respectively.	TiO_2-NPs did not induce DNA-breakage measured by the comet-assay in both human cell lines.	+	[125]

	hydrodynamic diameter: 91 nm.					
TiO_2	Nominal size: 20-50 nm. Particles were extracted from sunscreens. The precise composition of the samples (particle size, surface area per unit weight, presence/absence of coatings).	*In vitro* MRC-5 fibroblasts with or without irradiation from a solar simulator	0.025% w/v particles	Positive in alkaline comet assay after combined treatment with sunscreen extract and irradiation.	+	[151]
TiO_2	Two crystalline forms (phases) of TiO_2. Nominal size: nanosized rutile (>95%, <5% amorphous SiO_2 coating; 10 × 40 nm), nanosized anatase (99.7%; size <25 nm). BET analysis: rutile 132 and anastase 222 m^2/g. The particles were also characterized by	*In vitro* human bronchial epithelial cell line (BEAS-2B)	Eight doses of 3.8-380 µg/mL for 24, 48, or 72 h	In alkaline comet assay results showed induction of DNA damage by all the TiO_2 forms examined, with SiO_2-coated nanosized rutile having the lowest effects. Anatase was more active than (coated) rutile.	+	[152]

	TEM and XRD.					
TiO_2	TEM analysis: TiO_2 particles consisted of agglomerates of 10–60 nm crystallites with an average primary particle size of 21 nm. XRD analyses: the particles comprised of two phases of TiO_2, anatase (74%, v/v) and brookite (26%, v/v), with respective crystallite sizes of 41 nm and 7 nm.	*In vivo* alveolar type II/Clara cells collected immediately after the last exposure of male C57BL/6J mice.	The mice were exposed repeatedly, 4 h per day during 5 consecutive days, to three different concentrations of nanosized TiO_2 (0.8, 7.2 and 28.5 mg/m^3).	No significant induction of DNA damage was seen in the comet assay at any of the three doses of nanosized TiO_2, when the exposed mice were compared with the corresponding negative controls. However, the ethylene oxide-treated mice (the positive control group) showed a statistically significant 1.7-fold increase in the mean percentage of DNA in tail in comparison with the concurrent negative control group, despite the high inter-individual variation in DNA damage levels seen in the concurrent control animals.	-	[153]
TiO_2	Nominal diameter: 5 nm. TEM primary particle size:4.9 nm. BET surface area: 316 m^2/g. DLS analysis: 19.0 (13.5–31.3) (Anastase form)	*In vivo* lung cells of rat (after a single or repeated intratracheal instillation in rats)	The NPs were instilled intratracheally at a dosage of 1.0 or 5.0mg/kg body weight (single instillation group) and 0.2 or 1.0 mg/kg body weight once a week for 5weeks (repeated instillation group) into male	In the comet assay, there was no increase in % tail DNA in any of the TiO_2 groups. In the EMS group, there was a significant increase in % tail DNA compared with the negative control group. TiO_2 NPs in the anatase crystal phase are not	-	[85]

			Sprague-Dawley rats. A positive control, ethyl methanesulfonate (EMS) at 500mg/kg, was administered orally 3h prior to dissection.	genotoxic following intratracheal instillation in rats.		
TiO_2	The UV-Titan L181 (NanoTiO_2) was a rutile coated with Si, Al, Zr and polyalcohol. The average crystallite size was determined to be 20.6 nm and the powder had a specific surface area of 107.7 m^2/g.	*In vivo* broncheoalveolar lavage cells of mice	Mice received a single intratracheal instillation of 18, 54 and 162 µg of NanoTiO 2or 54, 162 and 486 µg of the sanding dust from paint with and without NanoTiO 2 (evaluated 1, 3 and 28 days after intratracheal instillation).	Pulmonary inflammation and DNA damage and hepatic histopathology were not changed in mice instilled with sanding dust from Nano TiO_2 paint compared to paint without Nano TiO_2.	-	[154]
TiO_2	Nominal size: 20-80 nm. BET surface area: 50 m^2/g (mixture of anatase and rutile)	*In vitro* human colon epithelium cell line (CaCo-2)	Cells were treated 4h with 20 mg/cm^2 particles (in MEM without serum)	No significant change comparing to the control in FPG-modified comet assay was observed.	+	[133]
TiO_2	SEM analysis: 40–70 nm. (anastase form)	*In vitro* lymphocytes and sperm cells	4concentration levels: 3.73, 14.92, 29.85 and 59.7 µg/ml in PBS for 30 min in the dark, preirradiated and simultaneous irradiation with UV	Positive in alkaline comet assay with both cell types. The ZnO particles are capable of inducing genotoxic effects on human sperm and	+	[155]

				lymphocytes Stronger effects with TiO_2 in lymphocytes with UV treatment.		
TiO_2	Nominal size: 7 nm (NM 101), 10 nm (NRCWE 001, NRCWE 002, NRCWE 003) and 94 nm (NRCWE 004). TEM analysis: 4-8/50-100 nm, 80-400 nm and 1-4/10-100/100-200/1000-2000 nm. DLS analysis (MEM): 185, 742 nm; 203-1487 nm; 339 nm	*In vitro* human hepatoblastoma C3A cells	Three concentration levels: 5, 10 and 20 µg/cm^2 or 2.5, 5 and 10 µg/cm^2.Exposure duration: 4h	DNA damage was most evident following exposure to NM 101 (TiO2 - 7 nm) and NRCWE 002 (TiO2 - 10 nm positively charged). NRCWE 003 – negatively charged TiO_2 10 nm is the only exception.	+	[156]
TiO_2	Nominal size: 12 nm, 20 nm, 25 nm. TEM analysis: 12 nm, 21 nm, 24 nm	*In vitro* A549 human lung carcinoma cells (CCL-185)	One concentration level: 100 µg/ml. Exposure duration: 4h, 24h, 48h	After 4h of exposure a significant increase in the level of DNA breaks was observed. This increase in the level of breaks further increased after 24h of exposure.	+	[157]
TiO_2	Nominal size: 17 nm. No further characterization reported in the	*In vivo* nulliparous time-mated mice (C57BL/6BomTac) bronchoalveolar	One dose level (inhalation during the gestational period): 42 mg UV-Titan/m^3.	Inhalation of UV-Titan did not affect the levels of DNA strand breaks in BAL or liver cells in the non-	-	[158]

	paper	lavage (BAL) and liver cells	Exposure duration: 1h/day X 11 days	pregnant females and dams compared with their controls. Prenatal exposure to UV-titan did not affect the levels of DNA strand breaks in the livers of newborn or weaned offspring compared with their controls		
TiO_2	Nominal size: 10-20 nm. No further characterization reported in the paper	*In vivo* earthworm *Eisenia fetida* (Savigny, 1826)	Four dose levels: 0.1, 0.5, 1.0, 5.0 g/kg dry soil. Exposure duration: 7 days	Earthworms exhibited DNA damage when exposed to ZnO at 1 and 5 g/kg. At 5 g/kg the degrees of DNA damage were significant when compared to controls.	+	[159]
TiO_2	Nominal size: 5.9 nm, 34.1 nm, 15.5 nm, 1-10 nm. DLS analysis: 460 nm, 400 nm, 420 nm, 600 nm	*In vitro* Chinese hamster lung fibroblast (V79) cells	One concentration level: 100 mg/l. Exposure duration: 24h	The % Tail DNA and the OTM were increased by twofold in cells treated with 100 mg/l of non-coated nano-TiO_2 after 24h. Cell viability was more than 40% after exposure to 100 mg/L of nano-TiO_2 after 24h.	+	[160]
TiO_2	Nominal size: 25 nm. TEM analysis: 15–30 nm; agglomeration size: 285 ± 52	*In vitro* primary human nasal epithelial cells	Four concentration levels: 10, 25, 50 and 100 µg/ml. Exposure duration: 24h	No genotoxic effect could be shown for any of the tested concentrations of TiO_2-NPs.	-	[161]

	nm					
TiO_2	Nominal size < 25 nm. TEM analysis: 285 ± 52 nm	*In vitro* human peripheral blood lymphocytes	Four concentration levels: 20, 50, 100, and 200 µg/ml. Exposure duration: 24h	No evidence for genotoxicity could be shown for any of the tested concentrations of TiO_2-NPs.	-	[162]
TiO_2	TEM analysis: 14 ± 4 nm and 25 ± 6 nm. DLS analysis was carried out (see reference)	*In vitro* Syrian hamster embryo (SHE) cells	Three concentration levels: 10, 25 and 50 µg/cm^2. Cells were treated for 24h	At the highest particle concentration (50 µg/cm^2), all TiO2 particles except rutile NPs caused increased DNA damage after 24 h of exposure.	+	[123]
TiO_2	Nominal size: 100 nm. AFM analysis: 90–110 nm	*In vitro Allium cepa, Nicotiana tabacum* root or leaf nuclei and human lymphocyte cells	(Plants) five concentration levels: 2, 4, 6, 8 and 10 mM. Exposure duration: 3, 6 and 24 h. (Lymphocytes) eight concentration levels: 0.25, 0.50, 0.75, 1, 1.25, 1.50, 1.75, 2 mM. Exposure duration: 3 h	A uniform pattern of dose response was observed in A. cepa at all treatment schedules, no particular time dependent effect was noticed. Similarly TiO_2 NPs treated (24h) N. tabacum leaf nuclei showed an initial increase in extent of DNA damage followed by a gradual decrease up to the highest dose. The value was statistically significant at 2 mM. The percentage of tail DNA (% tail DNA) in lymphocytes treated with different concentrations of NPs revealed a distinct	+	[163]

				pattern of genotoxicity. These NPs showed signs of significant DNA damage only at lower concentration (0.25 mM) followed by gradual decrease		
TiO_2	Nominal size: ~100 nm. TEM analysis: 50.93 ± 7.08 nm. DLS analysis: average hydrodynamic diameter 6180.73 nm	*In vitro* human lymphocyte cells	Three concentration levels: 25, 50 and 100 µg/ml. Exposure duration: 3 h	DNA fragmentation induced by TiO_2 NPs in human lymphocytes was statistically significant at a treatment dose of 25 mg/ml. Treatment doses of 50 and 100 mg/ml induced DNA damage, but was not significant compared with the control set	+	[164]
TiO_2	Nominal size: 21 nm and 50 nm. DLS analysis: 21 ± 0.8 nm for nano-TiO2 (21 nm) and 50 ± 0.5 nm for nano-TiO2 (50 nm)	*In vitro Allium cepa* root meristem cells	Three concentration levels: 10,100 and 1000 µg/ml. Exposure duration: 1h	The results obtained from root meristem cells of A. cepa demonstrated that only the highest concentration (1000 µg/mL) of TiO_2 NPs (21 nm) was statistically significant in comparison to the control, while all concentrations of TiO2 NPs (50 nm) were significant for % DNA tail. On the other hand, TiO2 NPs tested did show a dose-dependent	+	[165]

				increment for tail moment.		
TiO_2	Nominal average diameter 21 nm. TEM analysis 24 ± 4.6 nm (fresh); aged nTiO2 formed aggregates of particles with average diameters ranging from 27.60 ± 6.9 to 108.40 ± 5.2 nm	*In vivo* marine mussels (*Mytilus galloprovincialis*) haemocytes	One dose level: 10 mg/l. Exposure duration: 4 days	All treatments showed significantly higher DNA damage than controls. Interestingly all TiO_2 treatments resulted in approximately 40% tail DNA and there were no significant differences between the treatments.	+	[166]
TiO_2	Nominal size: 21 nm and <25 nm. DLS analysis: mean hydrodynamic diameter 160.5 nm and 420.7 nm	*In vitro* human gastric epithelial cancer (AGS)	One concentration level: 150 µg/ml. Exposure duration: 3h	In the comet assay, there was a 1.88-fold significant increase in %Tail DNA when the cells were treated with TiO_2 NPs.	+	[167]
TiO_2	Nominal size: 1–3 nm. DLS analysis: 99.20 ± 6.2 nm (water) 337e5 ± 190e5	*In vitro S. cerevisiae* cells	One concentration level: 31.25 mg/l. No information about time exposure	A significant amount of DNA damage was detected in NP-exposed cells when compared with controls.	+	[121]

	nm (medium)					
TiO_2	TEM analysis: 12 ±3 nm. BET analysis: 17 nm	*In vitro* NRK-52E rat kidney proximal cells	Four concentration levels: 50, 75, 100, 200 µg/ml. Exposure duration: 24h	DNA damage induced by TiO_2-CEA increased with exposure concentration and was statistically significant for exposure concentrations equal or higher than 100 µg/ml.	+	[168]
TiO_2	TiO2 at 10 nm (Hombikat UV100) and 20 nm (Millenium PC500) in diameter. No further investigations are reported in the paper. (Anatase form)	*In vitro* human bronchial epithelial cells, BEAS-2B (ATCC CRL-9609)	Cells were treated with 10 µg/mL of TiO2 for 24 h	The results showed that apparent DNA damage was detected in treatment with 10 µg/mL anatase 10 nm particles	+	[169]
TiO_2	Nominal size: 25 nm. X-ray diffraction analysis (XPD) analysis specific surface area: 50 m2/g, mean powder size approximately 30 nm. (A mixture of	*In vitro* human peripheral blood lymphocytes	20, 50, or 100 µg/mL for 6, 12, or 24 h	Positive in alkaline comet assay. Reduced effect was found when cells were pretreated with N-acetylcysteine. The dose- and time-dependent effect on DNA fragmentation was found. Lymphocytes exposed had a significantly greater OTM than those not exposed ($P < 0.05$).	+	[170]

	anatase (70–85%) and rutile (30–15%))					
TiO_2	Nanopowder nominal size: 63 nm. TEM analysis: 20-100 nm. DLS analysis: 300 nm.	*In vitro* A549 cells	1 μg/cm^2 (2 μg/mL), 20 μg/cm^2 (40 μg/mL), and 40 μg/cm^2 (80 μg/mL) for 4 h. FPG sensitive sites were measured at 20 μg/cm2, and 40 μg/cm^2 after 4h.	A dose-response trend in induced DNA damage could be seen in cells treated with TiO_2. Positive in alkaline comet assay. In FPG particles caused a slight increase, although this was not statistically significant (19% tail, $p < 0.001$).	+	[114]
TiO_2	Nominal average size: 5 nm. (anatase form)	Fish skin cells	1, 10, and 100 μg/mL for 2 or 24 h in cell medium with serum	A modified comet assay using bacterial lesion-specific repair endonucleases (Endo-III, FPG) was employed to specifically target oxidative DNA damage. Negative with endonuclease III. For the comet assay, doses of 1, 10 and 100 g/mL in the absence of UVA caused elevated levels of FPG-sensitive sites, indicating the oxidation of purine DNA bases (i.e. guanine) by TiO_2. UVA irradiation of TiO_2-treated cells caused further increases in DNA	+	[171]

				damage.		
TiO_2	Mixture of anatase (25%) and rutile (75%). TEM cross sectional diameter Mean size: 24.4 ± 0.5 nm, minimum = 11.8 nm, maximum = 38.5 nm). Though ENPs (sonicated in H2O) aggregated while preparing for TEM studies, the NPs could still be characterised as less than <100 nm in diameter.	*In vivo* rainbow trout gonad (RTG-2) cells (fibroblastic cell line)	5 and 50 µg/mL in MEM or PBS for 4 or 24 h with or without 30 min exposure to UV light	Positive in alkaline and FPG comet assay in combination with UV.	+	[172]
TiO_2	Nominal size powder: 63 nm. TEM analysis: 20-100 nm. DLS analysis: 300 nm.	*In vitro* A549 cells	40 to 80 µg/mL for 4h	In alkaline comet assay significantly higher levels of DNA damage were found compared to control (24% tail, $p < 0.001$). In FPG-modified comet assay, no significant levels of oxidative DNA damage at 80 µg/mL was found compared to control	+	[31]

				were observed. None of the particles caused a significant increase in oxidative DNA damage when cells were exposed to 40 μg/mL.		
TiO_2	HPPS size: by volume 6.57 nm (100%); by intensity: 8.2 nm (80.4%) and 196.52 nm (19.4%)	*In vitro* WIL2-NS human B-cell lympho- blastoid cells	WIL2-NS cells were incubated for 6, 24 and 48 h with 0, 26, 65 and 130 μg/mL. Results of comet assay were reported for 65 μg/mL for 24 h.	There was a 3-fold significant ($P < 0.05$) increase in %Tail DNA when the cells were treated with UF-TiO2 at a dose of 65g/mL for 24 h exposure (16±3% tail).	+	[173]
TiO_2	TEM dry size distribution: 10x30 nm (They were heavily aggregated not only in dry powder but also in solutions (the aggregated sizes was approximately 130–170 nm); (anastase form)	*In vitro* TK6 human lymphoblastoid cells	50, 100, 150, 200 μg/mL for 24 h	The standard comet assay and endonucleases enzyme-modified comet assay were performed. None of the TiO2-NPs treatments increased DNA damage in either of the assays.	-	[174]
TiO_2	TEM primary particle size: 21 nm. BET specific surface area: 50 ± 15 m^2/g. DLS agglomerates range: 21-1446	*In vivo* mice peripheral blood was collected by submandibular vein puncture	60, 120, 300, and 600 μg/mL concentrations in drinking water for 5 days	Tail moment significantly increased after TiO_2 NPs treatment. The average tail moment was 0.0102 ± 0.001 before treatment and 0.0137 ± 0.0011 after TiO_2 NPs treatment.	+	[89]

	nm and mean size: 160 ± 5 nm. (A mixture of 75% anatase and 25% rutile TiO_2, purity was at least 99.5% TiO_2)					
TiO_2	TEM mean size: 33.2 ± 16.7 nm. DLS analysis: (anastase form)	*In vivo* CBAB6F1 mice, brain, liver and bone marrow	40, 200 mg/kg body weight, daily oral for seven days	Increased DNA strand breaks in bone marrow cells was found. The % tail DNA in the comet tail significantly increased after treatment, from 3.66 in the control group to 7.99 ± 1.21 and 6.8 ± 1.13 in the treated groups ($p < 0.05$). No statistically significant changes have been found in the cells of liver and brain.	+	[87]
TiO_2	Nominal mean diameter: 28nm. DLS size of particles and agglomerates in cell culture medium analysis: 280 nm.	*In vitro* human lung epithelial A549 cells	0, 5, and 15 µg/mL for 12 h	Alkaline comet assay, no change has been found comparing to the control.	-	[175]
TiO_2	TEM size: 50 nm. DLS mean hydrodynamic	*In vitro* human epidermal cells (A431)	Concentrations ranging form 80 to 0.008 µg/mL (0.008, 0.08, 0.8, 8, 80	A statistically significant ($p < 0.05$) induction in the DNA damage was	+	[176]

	size (in water): 124.9 nm.		µg/mL)	observed by the FPG-modified comet assay in cells exposed to 0.8 µg/mL NPs (2.20 ± 0.26 vs. control 1.24 ± 0.04) and higher concentrations for 6 h.		
TiO_2	TEM size: 30-70 nm. DLS mean hydrodynamic size (in water and medium respectively): 124.9-192.5 nm	*In vitro* human liver cells (HepG2)	1, 10, 20, 40 and 80 µg/mL after 6h	The FPG-modified comet assay revealed a significant ($p < 0.05$) concentration-dependent increase in oxidative DNA damage in response to TiO_2 NP exposure as analysed using qualitative and quantitative parameters of the comet assay viz. OTM and % Tail DNA respectively. FPG elicited a significantly greater response at all the concentrations of TiO_2 NPs	+	[177]
TiO_2	Two samples of TiO_2: A1 and A2. XRD crystal form analysis: respectively anastase and mixture anastase:rutile 2:8 ratio. SEM diameter:	*In vitro* Erythrocytes	4.8 µg/mL for 1h	To investigate the presence of DNA damage due to oxidation of pyrimidine and purine bases, Endo III and FPG enzymes were used, respectively. A statistically significant increase in the % tail DNA was observed in the	+	[178]

	spherical 10-20 nm, spherical 20-150 nm			presence of A1 and A2 TiO2 NPs when the slides were incubated with both enzymes. TiO_2 NPs (4.8 µg/mL) induce DNA damage and the entity of the damage is independent from the type (A1 or A2) of TiO_2 NPs used.		
TiO_2	TEM average particle size: 15 nm. DLS average hydrodynamic radius: 820 nm. BET surface area: 190-290 m^2/g	*In vitro* and *in vivo* Tetrahymena thermophila cells	Two different concentrations (1 - 0.1 µg/mL and 2 - 100 µg/mL). Three different exposure scenarios (acellular, in vitro, in vivo) were applied and two different protocols of comet assay (alkaline lysis and neutral lysis)	After alkaline lysis indicated significant damage of DNA in T. thermophila in both *in vivo* and *in vitro* treatments. This was independent of the concentration of particles. Statistical analysis of comet assays by neutral lysis showed that in cells treated, the average DNA tail length does not significantly differ from that in control cells	+	[179]
TiO_2	XRD average size: 30.6 nm. DLS diameter in medium and water respectively: aggregates and	*In vitro* human amnion epithelial (WISH) cells	0.625, 1.25, 2.5, 5.0, 10, 20 µg/kg for 6 h	A significant induction ($p < 0.05$) in DNA damage (% DNA tail: 23.94 ± 0.66) at a concentration of 20 µg/mL in neutral comet assay was observed	+	[180]

	particles of 13 and 152 nm and in water aggregates of 380 nm. (Crystalline polyhedral rutile synthesized for this study)					
TiO_2	Listed by the manufacturer: Primary particle size: 27.5 nm. Specific surface area: 49 m^2/g.. DLS analysis of the NPs in different media is also reported. (Crystal form 86% anastase and 14% rutile)	*In vitro* human lung cells (BEAS-2B) in three different dispersion media (KF, KB, and DM)	Different concentrations from 0 to 100 µg/mL for 24 h	There was a concentration-dependent increase in DNA damage after TiO_2 NP exposure in all three treatment media that was genotoxic but statistically significant. All concentrations in all treatment media induced DNA damage that was significantly greater than the concurrent negative control except for two points: 10 µg/mL in KF and 50 µg/mL in DM	+	[181]
TiO_2	Listed by the manufacturer: Primary particle size: 27.5 nm. Specific surface area: 49 m^2/g. DLS analysis of the NPs in different media is also reported.	*In vitro* human liver cells (HepG2)	Different concentrations from 0 to 100 µg/mL for 24h	DNA damage increased significantly with increasing concentrations of nano-TiO_2 in both treatment media, indicating a genotoxic effect. The responses at the two highest concentrations were significantly greater than	+	[182]

	(Crystal form 86% anastase and 14% rutile.)			the control; however, the type of medium used did not influence the level of DNA damage		
TiO_2	Listed by the manufacturer: Field-emission-gun scanning electron microscopy (FEG-SEM) particle size within the agglomerates and aggregates TiO2-An and TiO2-Ru: <25 and <100 nm. XRD analysis of crystal: TiO_2-An anastase and TiO_2-Ru rutile form. BET specific surface area: 129.3 and 116.7 m^2/g	*In vitro* human hepatic carcinoma cells (HepG2)	Four concentration levels: 0, 1, 10, 100, 250 µg/mL for 2, 4 and 24 h	TiO2-An, but not TiO_2-Ru, caused a persistent increase in DNA strand breaks (comet assay) and oxidized purines (FPG-comet). In HepG2 cells exposed to TiO_2-An NPs we detected slight, however statistically significant ($P < 0.05$) greater amount of DNA strand breaks than in the control	+	[183]
TiO_2	Nominal size: <25 nm. BET specific surface area: 129.3 m^2/g. XRD analysis: 18 nm. FEG-SEM: 1	HepG2 cells	0, 1, 10, 100, 250 µg/mL for 2, 4 and 24 h	UV pre-irradiated TiO2-B induced significant ($p < 0.05$) increases in FPG-sensitive sites after 2 h and 4 h exposure at all of the concentrations tested.	+	[184]

TiO_2	Nanopowder nominal size: <25 nm. DLS mean hydrodynamic diameter: 92±3.6 at 0h in the dispersion of 12.5 µg/mL.	Allium cepa Root Tip	When the roots reached 2 to 3 cm in length they were treated with different concentrations (12.5, 25, 50, 100 µg/mL) of TiO2 NP suspensions for 4 h	The lowest reported exposure concentration of TiO_2 NPs to exert a significant damage to DNA was 20 µg/mL. Olive Tail Moments of about 2.3460.74 and 8.662.81% was observed at the test concentrations of 12.5 µg/mL and 100 µg/mL respectively indicating damaged DNA structure	+	[185]
TiO_2	XRD analysis of different samples: 9, 10 and 10 nm. (NM101, NRCWE001, NRCWE002, NRCWE003 that are in anatase form, respectively with no coating, no coating, positive charged and negative charged). TEM analysis respectively: 4-8/50-100, 80-400, 80-400 and 80-400 nm) A sample of	*In vitro* HK-2 cells	0.8, 40, 20, 60, and 40 µg/cm^2 after a 4h treatment	Significant tail increase in FPG-modified comet for one of the samples of TiO_2, others small but significant	+	[186]

	XRD size: approximately 100 nm (NRCWE004). In this sample five different particle types were identified.					
TiO_2	Two different types of TiO_2 were used; Nominal size: 20 and 7 nm. BET surface area: 66.604 and 300.81 m^2/g	*In vivo* in the freshwater crustacean Daphnia magna and the larva of the aquatic midge Chironomus riparius	The fish were collected 24 h from the control and experimental tanks after exposure to 1 µg/L of NPs	No genotoxic effect on either species as no significant increase in the tail/Olive Tail Moments was observed in these species when exposed	-	[111]
V_2O_3	Nominal size of spherical diameter: approximately 70 nm. TEM average diameter: 25 nm. TEM length: 100 – 1.000 nm. (Needle-like structure)	*In vitro* human epithelial lung cell line (A549)	Concentrations: 1 and 2 µg/cm^2, time: 24, 36, 48 h via inhalation	Positive	+	[52]
V_2O_5	Nominal size of spherical diameter: 170 – 180 nm.	*In vitro* human epithelial lung cell line (A549)	Concentrations: 1 and 2 µg/cm^2, time: 24, 36, 48 h via inhalation	Negative	-	[52]

	They are up to several hundred nanometer in length and usually have a diameter of less than 50 nm. (Rod-shaped)					
ZnO	XRD analysis of different samples: 70 to > 100 an 58-93 nm. (NM110 and NM111, with no coating,). TEM size: 20-200/10-450 and 20-200/10-450 nm. BET surface area: 14 and 18 m^2/g. Mainly 2 euhedral morphologies: 1) aspect ratio close to 1; 2) ratio 2 to 7.5. Minor amounts of particles with irregular morphologies observed.	*In vitro* HK-2 cells	0.8, 40, 20, 60, and 40 μg/cm^2 after a 4h treatment	No significant tail increase in % tail in FPG-modified comet for one of the samples of ZnO, others small but significant	+	[186]

	M111 as M110 but with different size distributions. 1) particles with aspect ratio close to 1; 2) particles with aspect ratio 2 to 8.					
ZnO	Two NPs of ZnO have been evaluated. EZ-1 (coated) and EZ-2 (uncoated) with the following characterization results respectively: TEM primary size: 30±20, 40±20 nm. XRD powder hydrodynamic diameter in water: 70-150 and 90-160 nm.	*In vitro* A549, HT29, HaCaT cells	0, 0.1, 1, 10 µg/mL for	The results show a small, but significant increase in DNA damage compared to that of controls at concentrations of 10 µg/mL ZnO for HT29 cells for the polymer coated NPs. For The HaCaT cells, only the polymer coated NPs (EZ-1) show an increase in DNA damage at 1 µg/mL, while the A549 cells are not significantly affected by any of the NPs.	+	[187]
ZnO	Respectively Nominal size and BET surface area: 10 nm, 70 m^2/g	*In vitro* human colon epithelium cell line (CaCo-2)	Cells were treated 4h with 20 µg/cm^2 particles (in MEM without serum)	Significant effects found in FPG-modified comet assay.	+	[133]

	(nanoactive aggregates) and 20 nm, 50 m^2/g (nanoscale particles).					
ZnO	TEM mean size 30 nm. DLS: 165 nm.	*In vitro* human epidermal cell line (A431)	0.001, 0.008, 0.08, 0.8, 5 µg/mL for 6h	A significant induction ($p < 0.05$) in DNA damage was observed in cells exposed to ZnO NPs for 6 h at 5 and 0.8 µg/mL concentrations compared to control.	+	[188]
ZnO	TEM analysis: 30, 50 and 70 nm. DLS size in water: 272 nm.	*In vivo* liver and kidney cells of mice after oral exposure	50 and 300 mg/kg of NPs for 14 days	In both alkaline and FPG-modified comet assay, at the highest concentration DNA % tail was significantly increased (16.15±1.56)	+	[189]
ZnO	TEM analysis: 30 nm. DLS hydrodynamic size in water: 165 nm.	*In vitro* A431 cells	Cells were exposed to 0.001, 0.008, 0.08, 0.8, 5 µg/mL for 6 h	A significant induction ($p < 0.05$) in DNA damage was observed in cells exposed to ZnO NPs for 6 h at 5 and 0.8 µg/mL concentrations compared to control respectively % DNA tail were 10.6 ± 0.76 and 13 ± 1.5.	+	[188]
ZnO	Respectively Nominal size and BET: 50 and 70 nm. TEM average size: 30 nm. DLS mean hydrodynamic	*In vivo* mice liver and kidney cells	50 and 300 mg/kg mice oral exposure for 14 consecutive days	A statistically significant ($p < 0.05$) qualitative and quantitative increase in the oxidative DNA damage was observed in the liver of mice exposed to the	+/-	[189]

	diameter (water): 272 nm.			higher dose (300 mg/kg) in the presence of FPG. However, no significant DNA damage was observed in the mice administered with the lower dose (50 mg/kg). There was no significant difference in the comet parameters in the kidney cells of control and ZnO NPs exposed mice.		
ZnO	TEM analysis: 20.2 ± 6.4 nm	*In vitro* primary mouse embryo fibroblasts *(PMEF)*	5 and 10 µg/mL particles in DMEM for 24 h	There were significant increases in tail length, percentage of DNA in tail, tail moment and Olive Tail Moment after PMEF cells were treated with at both examined concentrations (18.8% tail DNA , $p < 0.01$) in alkaline comet assay.	+	[55]
ZnO	Nanopowder nominal size: 71 nm. TEM analysis: 20-200 nm. DLS analysis: 320 nm.	*In vitro* A549 cells	1 µg/cm^2 (2 µg/mL), 20 µg/cm^2 (40 µg/mL), and 40 µg/cm^2 (80 µg/mL) for 4 h. FPG sensitive sites were measured at 20 µg/cm2, and 40 µg/cm^2 after 4h.	DNA damage was induced when cells were exposed for 4 h to 40 µg/cm^2 (12% tail, $p < 0.05$). ZnO showed statistically significant ($p < 0.05$) increased levels of oxidative DNA lesions compared to those of the control in the highest dose.	+	[114]
ZnO	DLS analysis	*In vitro* human	20-30-40 µg/mL for 3h	These increases were	+	[190]

	hydrodynamic diameter: 243.7 nm (in water), 273.4 (medium). Nominal size (BET analysis): 100 nm. Surface area: 15-25 mg(Provided by the supplier)	neuroblastoma SHSY5Y cell line	and 6h	statistically significant in all the conditions tested in the comet assay, except for the highest concentration after the 6 h exposure.		
ZnO	Nominal size: 20 and 70 nm. SEM analysis: 35 ± 5, 28 ± 8, 70 ± 19, and 72 ± 11 nm. DLS hydrodynamic size ranges from 200 to 400 nm, 180 to 300 nm, 300 to 900 nm, and 200to 500 nm [20 nm (+) charge, 20 nm (−) charge, 70 nm (+) charge,and 70 nm (−) charge NPs, respectively	*In vivo* male Crl: CD (SD) rats liver and stomach single cells	Three dose levels: 500, 1000, and 2000 mg/kg body weight. Test substance was administered three times by gavage at 0, 24, and 45h	Tail intensity of liver and stomach single cells treated with ZnO NPs with 20 nm (+) and (−) charge had no significant increase in comparison with solvent control group. The results of 70 nm (+) and (−) charged ZnO NPs also revealed no significant increase in tail intensity.	-	[191]
ZnO	DLS particle size: 45-150 nm. TEM: Spherical, triangolare and	*In vitro* human lymphocyte cells	0, 125, 500, and 1000 µg/mL for 3h	Significant ($p < 0.05$) increase in DNA fragmentation at 1000 µg/mL which is much	-	[192]

	hexagonal structures size 45-150 nm and average diameter: 75 ± 5 nm.			higher than predicted concentrations. These NPs are safe up to 500 µg/mL.		
ZnO	Nominal size: 100 nm (NM 110). TEM analysis: 20-250/50-350 nm. DLS analysis (MEM): 306 nm	*In vitro* human hepatoblastoma C3A cells	Three concentration levels: 0.62, 1.25 and 2.5 µg/cm^2.Exposure duration: 4h	A small but significant increase in percentage tail DNA following exposure was observed	+	[156]
ZnO	Nominal size: 10-20 nm. No further characterization reported in the paper	*In vivo* earthworm *Eisenia fetida* (Savigny, 1826)	Four dose levels: 0.1, 0.5, 1.0, 5.0 g/kg dry soil. Exposure duration: 7 days	Earthworms exhibited DNA damage when exposed to ZnO at 1 and 5 g/kg. At 5 g/kg the degrees of DNA damage were significant when compared to controls.	+	[159]
ZnO	Nominal size < 100 nm. TEM analysis: rod shaped 86 ± 41 nm X 42 ± 21 nm; mean diameter was 353 nm	*In vitro* primary human nasal mucosa cells	Five concentration levels: 0.01, 0.1, 5, 10 and 50 µg/ml. Exposure duration: 24h	A ZnO-NP concentration-dependent increase in the Olive Tail Moment (OTM) as an indicator for genotoxic effects could be seen. The enhanced DNA migration was significant at 10 µg/ml and 50 µg/ml.	+	[193]
ZnO	Nominal size: 50–80 nm size and average	*In vitro Allium cepa* root	Three concentration levels: 10,100 and 1000 µg/ml. Exposure	The results obtained in the comet assay show that both tested ZnO NPs	+	[165]

	particle size ≤ 35 nm. DLS analysis: 50 ± 0.3 nm for ZnO 50 nm NPs and 35 ± 1.1 nm for ZnO NPs (≤ 35 nm)	meristem cells	duration: 1h	are genotoxic in the root meristem cells of A. cepa in terms of both the percentage of DNA in tail and tail moment.		
ZnO	Nominal size: 50–80 nm size and average particle size ≤35 nm. DLS analysis: 50.75 ± 0.0 nm for ZnO 50–80 nm) NPsand 36.42 ± 0.1 nm for ZnO (≤35 nm) NPs	*In vitro* human embryonic kidney (HEK293) and mouse embryonic fibroblast (NIH/3T3) cells	Three concentration levels: 10,100 and 1000 µg/ml. Exposure duration: 1h	The results show that both tested ZnO NPs are genotoxic in the two cell lines used. The significance of the genotoxicity results were independently of using the percent-age of DNA in tail or the tail moment. The induced genotoxicity followed a direct dose–response effect with positive induction at 100 and 1000 µg/mL concentrations	+	[194]
ZnO	TEM analysis: 17 nm. DLS analysis: average hydrodynamic size 263.0 nm (in medium)	*In vitro* human skin melanoma (A375) cells	Three concentration levels: 5, 10 and 20 µg/ml. Cells were treated for 24 and 48h	Cells exposed to different concentrations of ZnO NPs showed significantly more DNA damage than did the control cells.	+	[195]

ZnO	Nominal average particle size: 50 nm. TEM analysis: 22 nm. DLS analysis: average hydrodynamic size 264.8 nm (in water)	*In vivo* freshwater snail *Lymnaea luteola* digestive gland cells	Three dose levels: 10, 21 and 32 µg/ml. Isolation of digestive gland cells was done at intervals of 24 and 96h	The cells exposed to different concentrations of ZnO NPs exhibited significantly higher DNA damage in cells than those of the control groups.	+	[196]
ZnO	Nominal size: <100 nm. DLS analysis: 612 ± 10.9 nm (water) 5294 ± 3184 nm (medium)	*In vitro* *S. cerevisiae* cells	One concentration level: 31.25 mg/l. No information about time exposure	A significant amount of DNA damage was detected in NP-exposed cells when compared with controls.	+	[121]
ZnO	SEM analysis: 40-70 nm.	*In vitro* lymphocytes and sperm cells	Approximately 4–93 µg/mL in PBS for 30 min in the dark, preirradiated and simultaneous irradiation with UV	The ZnO particles are capable of inducing genotoxic effects on human sperm and lymphocytes and that the effect of ZnO is enhanced by UV both in case of lymphocytes and sperm, but effects are only statistically significantly different from responses in the dark at the highest	+	[155]

				does after pre-irradiation and simultaneous irradiation.		
ZrO_2	Nominal size: 6 nm. TEM analysis: average hydrodynamic diameter 6 ± 0.8nm.	*In vitro* human embryonic kidney (HEK293) cells and human peripheral blood lymphocytes	Concentrations of 1, 10, or 100 µg/mL	Results demonstrated that at all concentration NP did not induce any marked genotoxicity.	-	[103]

Table 2. Current review of genotoxicity studies (Micronucleus test) on metal oxide NPs (+ positive; - negative; +/- equivocal; bw = body weight). As explained in section 3, each row in this table summarizes all genotoxicity data found for this test for all nanomaterials with a given core chemical composition reported in a given publication.

Nanomaterial core chemical composition	Characteristics (Size)	Cell type and assay	Exposure	Results	Summary	Ref.
Al_2O_3	Two aluminium oxide NMs were studied. Nominal diameter: 30 nm and 40 nm. TEM analysis: 39.85±31.33 nm and 47.33±36.13 nm	*In vivo* inbred female albino Wistar rats bone marrow cells	Three dose levels (oral administration): 500, 1000 and 2000 mg/kg body weight. The study was performed at 30 and 48 h of sampling times	Significantly increased frequency of MN was observed with 1000 and 2000 mg/kg body weight dose levels of Aluminum oxide 30 nm and Aluminum oxide 40 nm over control at 30 h. Likewise, at 48 h sampling time a significant increase in frequency of MN was evident at 1000 and 2000 mg/kg body weight dose levels of Aluminum oxide 30 nm and Aluminum oxide 40 nm	+	[197]

				compared to control.		
Al_2O_3	Two aluminium oxide NMs were studied. Nominal diameters: 30 nm and 40 nm. TEM analysis: 39.85 ± 31.33 nm and 47.33 ± 36.13nm. DLS analysis: average diameters 212.0 and 226.1 nm in water.	*In vivo* female Wistar rat peripherial blood cells	Three dose levels (via gavage): 500, 1000 and 2000 mg/kg body weight. Whole blood was collected at 48 and 72 h	Data indicated statistically significant effects on micronuclei frequency after treatment with both NMs compared to the control group at 1000 and 2000 mg/kg dose levels after 48 and 72 h.	+	[81]
CeO_2	Nominal size < 25 nm. TEM analysis: 25 ± 1.512 nm. DLS analysis: hydrodynamic diameter 269.7 ± 27.398 nm	*In vitro* human neuroblastoma (IMR32) cells	Five concentration levels: 10, 20, 50, 100, and 200 mg/ml. Exposure duration: 24 h	At concentration levels of 100 and 200 mg/ml the frequency of micronucleus in binucleated cells was increased significantly.	+	[106]
CeO_2	Nominal size: 7 nm. DLS analysis: hydrodynamic diameter 15 nm	*In vitro* human dermal fibroblasts	Four concentration levels: 0.06, 0.6, 6 and 60 mg/l. Exposure duration: 48 h	Binucleated micronucleated fibroblast frequencies were significantly increased in a dose-dependence manner from the lowest tested concentrations (0.06 mg/l)	+	[107]
CuO	Four different CuO nanoparticles were studied, with the following size measurements and shapes determined by	*In vitro* human murine macrophages RAW 264.7 cells and peripheral blood	Three concentration levels: 0.1, 1 and 10 µg/ml. Exposure duration: 48 h	In all tested NMs, macrophages showed a higher number of micronucleated cells than lymphocytes, except for the NM (1). Spheres and spindles showed a dose-dependent increase in the	+	[115]

	TEM: (1) 10-100 nm (unspecified shape); (2) 7±1 nm (spheres); (3) 7±1×40±10 nm (rods); (4) 1200±250×270±50×30±10 nm (spindles)	lymphocytes (PBL).		micronuclei frequency in macrophages.		
CuO	Two different CuO NMs were studied. Nominal average size between 30 and 40 nm. SEM analysis: diameter between 70 and 100 nm. TEM analysis: protein–NPs complex had a total average size of 356 ± 70 nm	*In vitro* mouse neuroblastoma (Neuro-2A) cells	Four concentration levels: 12.5, 25, 50 and 100. Exposure duration: 24 h	Treated cells showed a significant increase in the frequency of micronuclei at the lowest concentration level	+	[198]
CuO	Nominal size between 27.2 and 95.3 nm	*In vivo* female ICR mice peripheral blood cells	Two dose levels (intraperitoneal injection): 1 mg/mouse and 3 mg/mouse. Exposure time: 24, 48 and 72 h	A significant differences was observed between control and 3 mg doses treated cells	+	[86]
Fe_2O_3	Nominal size < 50 nm. TEM analysis: mean size 29.75 ± 1.87 nm. DLS analysis: hydrodynamic diameter 363 nm (water)	*In vivo* albino Wistar female rat peripheral blood and bone marrow cells	Three dose levels (oral administration): 500, 1000 and 2000 mg/kg body weight. Peripheral blood cells exposure duration: 48 and 72 h. Bone marrow cells exposure duration: 24 and 48 h	The frequencies of micronuclei were statistically insignificant at all doses in both cell lines and at every exposure duration	-	[126]
Fe_2O_3	Nominal size between 60 and 100 nm	*In vivo* female ICR mice peripheral	Two dose levels: 1 mg/mouse and 3 mg/mouse. Exposure	A significant increase in micronucleated reticulocytes cells was observed	+	[86]

		blood cells	time: 72 h			
Fe_3O_4	Nominal size between 20 nm and 60 nm. Photon correlation spectroscopy (PCS) analysis: mean diameter 311 nm	*In vitro* human lung adenocarcinoma type-II alveolar epithelial cells A549	Four concentration levels: 1, 10, 50 and 100 µg/cm^2. Exposure duration: 24 h	A significantly enhanced MN induction was already observed at 10 µg/cm^2, reaching a maximum at 100 µg/cm^2	+	[131]
Fe_3O_4	TEM analysis: primary diameter of 26.1 ± 5.2 nm	*In vivo* kunming mice bone marrow cells	Four dose levels: 5, 2.5, 1.25, and 0.625 g/kg. The 30 h injection method was used, ie, a 24 h interval between two injections with a 6-hour wait after the second injection	No significant difference was found between the test animals and the negative controls	-	[199]
Fe_3O_4	Nominal size: 80 nm	*In vivo* female ICR mice peripheral blood cells	Two dose levels: 1 mg/mouse and 3 mg/mouse. Exposure time: 72 h	Significant increases in micronucleated reticulocytes cells was observed	+	[86]
MnO_2	MnO2 nanopowder nominal size of <30 nm. TEM analysis: mean size distribution 45 ± 17 nm. DLS size in the Milli Q water suspension was 334.4 nm	*In vivo* bone marrow cells extracted from the femurs of female albino Wistar rats	Three dose levels: 100, 500 and 1000 mg/kg body weight. The study was performed at 24 and 48 h after treatment	The data revealed statistically significant enhancement in the MN frequency in the groups treated with 1000 mg/kg body weight of MnO2-45 nm at 24 and 48 h of sampling times	+	[128]
SiO_2 (amorphous)	Nominal size: 15 nm and 55 nm. DLS analysis: z-average particle diameter (pH 7.5) 31.6 nm and 105.1 nm	*In vitro* human peripheral blood lymphocytes (HPBLs); *In vivo* Wistar rat	(*In vitro*) Four concentration levels: 31.6, 100, 316, 1000 µg/mL. Exposure duration 24h. (*In vivo*) Single concentration	For both the 15 nm and 55 nm silica NPs, no increase in the % MN was observed with any of these particles at any dose tested in this *in vitro* system in HPBLs. (*In vivo*) Injection of silica NPs resulted in a	+/-	[82]

		peripheral blood cells	for 15 nm SiO_2: 50 mg/kg; two concentration levels for 55 nm SiO_2: 25 mg/kg and 125 mg/kg. Rats injected i.v. at 48h, 24h, and 4h prior to tissue collection	dose-dependent increase in DNA damage in liver and lung tissue and in white blood cells		
SiO_2 (amorphous)	DLS analysis: hydrodynamic diameter 12 nm in DMEM and 75 nm in DMEM + 10%FBS	*In vitro* A549 human lung carcinoma cells	Three concentration levels: 1.5, 2.5, 5 µg/mL. Cells were treated for 40h	No induction of MN was observed compared to the untreated control both in 10% serum and in 0% serum	-	[200]
SiO_2 (amorphous)	DLS hydrodynamic diameter: ranging from 12 nm to 174 nm without foetal calf serum (FCS) and from 52 nm to 258 nm in FCS	*In vitro* A549 human lung carcinoma cells	Concentrations range between 0 µg/mL and 1056 µg/mL. Cells were treated for 40h with different doses of the SNPs either in presence or absence of 10% FCS	A statistically significant increase in MN frequencies was observed after treatment with L-40 in the absence of serum as well as with L-40 and S-174 in the presence of serum and after treatment with L-40, S-59 and S-139 in the absence of serum. No dose dependency was observed	+	[201]
SiO_2 (amorphous)	Nominal size: ranging from 5 nm to 80 nm. DLS analysis: mean particle diameter between 17.42 ± 0.16 and 185.1 ± 7.51 in ultrapure water; between 16.08 ± 0.81 and 332.6 ± 11.42 in serum-free cell culture medium	*In vitro* Balb/3T3 mouse fibroblasts	Cells were treated at the fixed concentration of 100 µg/mL for 24h	SiO_2 NPs did not trigger the formation of micronuclei, suggesting that neither the size diameter nor the particles' synthesis procedure induces genotoxicity	-	[202]
SiO_2 (quartz)	Nominal size: diameter <5 µm.	*In vitro* WIL2-NS (ATCC, CRL	Two concentration levels: 60, and 120	The results show that the frequency of	+	[138]

	High-performance particle sizer (HPPS) analysis after filtration: Z-Average size 12.2 nm	8155) human lymphoblastoid B-cell	µg/mL. Cyt-B was added and the cultures were incubated for 26h	MNed BNCs increased significantly with the increase of particle dose, from 5 MN per 1000 BNed cells at untreated control to 12 at 120 µg/mL of particles		
TiO_2	TEM analysis: 12.1 ± 3.2 nm. Agglomerates in the treatment solution was found to be around 130 nm and around 170 nm in cell culture medium	*In vivo* male B6C3F1 mice blood cells	Three dose level: 0.5, 5.0 and 50 mg/kg for three consecutive days	No difference in %MN-RET frequencies between TiO2-NP treated and control animals was observed	-	[203]
TiO_2	X-ray diffraction (XRD) analysis: diameter ranging from 7 nm to 10 nm. DLS analysis: hydrodynamic diameter ranging from 139 nm to 211 nm in DMEM and from 109 nm to 233 nm in DMEM + 10%FBS	*In vitro* A549 human lung carcinoma cells	Four concentration levels: 50, 75, 125, 250 µg/mL. Cells were treated for 40h	Results are not available as the MN were obscured by NM agglomerates over the cells and thus could not be scored	+/-	[200]
TiO_2	Nominal size: 25 nm. DLS analysis: mean particle size 300 nm	*In vitro* human lymphocytes and hamster lung fibroblasts V79 cells	Four concentration levels: 20, 60, 100 and 250 µg/mL. Cells were exposed without metabolic activation system for 24h	Weak mutagenic effect on human lymphocytes at 60–250 µg/mL	+	[146]
TiO_2	Nominal size: 40 ± 5 nm. SEM analysis: average size distribution 42.30 ± 4.60 nm	*In vivo* ICR mice bone marrow cells	Four dose levels: 140, 300, 645, and 1387 mg/kg body weight. Blood samples were collected 14 days after treatment	Micronucleus test result 14 days after a single intravenous injection of different doses of TiO2 NPs shows no significant increase in micronucleus cell number	-	[204]
TiO_2	Nominal size < 25 nm.	*In vivo* P.	The fish were exposed	Micronuclei were not detected, but	-	[148]

	DLS hydrodynamic size (Z-average): 1611 ± 21 nm after 24h	mesopotamicus (pacu caranha) erythrocytes cells	(with visible light or ultraviolet and visible light) to the following concentrations of nano-TiO2 during a 96 h period: 0 (control), 1, 10, and 100 mg/l.	the extent of morphological alterations in the erythrocyte nuclei revealed an influence of the type of illumination, since the alterations were more prevalent in groups exposed to UV light		
TiO_2	Nominal size: 21 nm. DLS hydrodynamic diameter: 129.50 ± 2.6 nm	*In vivo* Adult male Wistar rats bone marrow cells	Single dose of 5 mg/kg body weight. Animals were sacrificed at 24h, 1 week and 4 weeks after the injections	A significantly elevated frequency of MN was observed for TiO2NPs after 24h. The frequencies of micronuclei were statistically insignificant after 1 and 4 weeks.	+	[147]
TiO_2	Nominal average size: 75 ± 15 nm. ZetaSizer Nano ZS90 hydrodynamic diameter: 473.6 nm and 486.8 nm size when suspended in H2O and FBS-free DMEM	*In vivo* Sprague-Dawley male rat bone marrow cells	Three dose levels: 10, 50 and 200 mg/kg body weight every day for 30 days	These results showed that TiO2NPs could induce DNA double strand breaks in bone marrow cells after oral administration, but no significant chromosomes or mitotic apparatus damage and toxicity were found in bone marrow cells.	+	[149]
TiO_2	UF-TiO_2 particle size ≤ 20 nm. No further investigations are reported in the paper	*In vitro* Syrian hamster embryo (SHE) cells.	Cells were treated with different concentrations: 0.5, 1.0, 5, and 10 μg/cm^2, for different periods: 12, 24, 48, 66, and 72 h	UF-TiO_2 induced MN, which significantly increased at concentrations between 0.5 and 5.0 μg/cm^2	+	[205]
TiO_2	TiO2 anatase at 10 nm (Hombikat UV100) and 20 nm (Millenium PC500) in diameter. No further investigations are reported in the paper	*In vitro* human bronchial epithelial cells, BEAS-2B (ATCC CRL-9609)	Cells were treated with 10 g/mL of TiO_2 for 24 h	The results indicated that treatment with anatase-sized (10 and 200 nm) TiO_2 increased micronuclei	+	[169]
TiO_2	No characterization of the NM is reported in the	*In vitro* Chinese hamster ovary-	Cells were treated with various	Results show that TiO_2 significantly induced MN in CHO-K1 cells using	+	[206]

	paper	K1 (CHO-K1) cells	concentrations of TiO_2 (0 to 20 µM) for 18h	cytokinesis block technique. Furthermore, the frequency of MN was slightly enhanced by TiO_2 in the conventional MN assay system, i.e., without cytokinesis block		
TiO_2	Ultrafine TiO_2 (UF1 - uncoated anatase) average crystal sizes: 20 nm. No further investigations are reported in the paper	*In vitro* rat liver epithelial cell (RLE)	Three concentrations: 5, 10 and 20 µg/cm^2. All the cultures were treated with cytochalasin B and incubated for 20 h. A duplicate series of experiments was carried out by irradiating the TiO2 exposed cells with near-UV light	No observed increase of the number of micronucleated cells. Exposure of the cells to UV light gave a slight but not statistically significant effect, Interestingly, TiO_2 appeared to have a slight decreasing effect on the frequency of micronuclei at the lowest treatment concentrations both in the presence and in the absence of UV irradiation.	-	[207]
TiO_2	Particle size distribution measured by high-performance particle sizer (HPPS): by volume 6.57 nm (100%); by intensity: 8.2 nm (80.4%) and 196.52 nm (19.4%)	*In vitro* WIL2-NS human lymphoblastoid cells	Cells were treated with 26, 65 and 130 µg/mL of UF-TiO2. Cyt-B was added and the cultures were incubated for 26h	Exposure to UF-TiO_2 resulted in significant increases in MNBNCs compared to untreated control.	+	[173]
TiO_2	Nominal size: 19.7–101.0 nm. No further investigations are reported in the paper	*In vivo* female ICR mice peripheral blood cells	Two dose levels: 1 mg/mouse and 3 mg/mouse. Exposure time: 72h	Significant increases in micronucleated reticulocytes (MNRETs) observed	+	[86]
TiO_2	TEM analysis: cross sectional diameter 24.4 ± 0.5 nm	*In vitro* RTG-2 gonadal tissue fish cell line from rainbow trout	Two concentration levels: 5 and 50 µg/mL. 48h time exposure before adding the	No significant difference in micronuclei induction over the control. Decreases in frequencies of MN were observed with the ENP treatments, which in	-	[172]

			cyto-B for 48 h	addition, had little effect on cell division or cytotoxicity		
V_2O_3	Nominal size of spherical diameter: approximately 70 nm. TEM average diameter: 25 nm. TEM length: 100 – 1.000 nm. (Needle-like structure)	*In vitro* human epithelial lung cell line (A549)	Two exposure levels: 1 and 2 µg/cm^2. 24 hours time of exposure via inhalation	No induction of micronuclei was observed in the micronucleus test but morphological changes in cell nuclei.	-	[52]
V_2O_5	Nominal size of spherical diameter: 170 –180 nm. They are up to several hundred nanometer in length and usually have a diameter of less than 50 nm. (Rod-shaped)	*In vitro* human epithelial lung cell line (A549)	Two exposure levels: 1 and 2 µg/cm^2. 24 hours time of exposure via inhalation	No induction of micronuclei was observed in the micronucleus test but morphological changes in cell nuclei.	-	[52]
WO_3	No characterization of the NM is reported in the paper	*In vivo* bone marrow cells of male Sprague-Dawley rats	Three dose levels: 25, 50 and 100 mg/kg body weight. Animals received daily intraperitoneal injections of WO_3 for 30 days.	No statistically significant difference was found between 25 mg WO_3 applied and control group. On the contrary, the higher doses of WO_3 (50 and 100 mg) caused increases of MN rates	+	[83]
ZnO	Nominal size: 20 and 70 nm. SEM analysis: 35 ± 5, 28 ± 8, 70 ± 19, and 72 ± 11 nm. DLS hydrodynamic size ranges from 200 to 400 nm, 180 to 300 nm, 300 to 900 nm, and 200to 500 nm [20 nm (+) charge, 20 nm (−) charge,	*In vivo* Out-bred mice of strain ICR, 6–7 bone marrow cells	Three dose levels: 500, 1000, and 2000 mg/kg body weight. The test substance was given twice with a 24h interval	The frequencies of MNPCE (micronucleated polychromatic erythrocyte) were not represented statistical significance and dose-dependent response at any dose on four kinds of ZnO NPs	-	[191]

	70 nm (+) charge,and 70 nm (−) charge NPs, respectively					
ZnO	X-ray diffraction (XRD) analysis: diameter ranging from 71 to >100. DLS analysis: hydrodynamic diameter 250 (±100) in DMEM and 258 (±93) in DMEM + 10%FBS	*In vitro* A549 human lung carcinoma cells	Three concentration levels: 10, 25, 50 µg/mL. Cells were treated for 40h	No significant increase in MN was shown for ZnO NM, except at the highest dose tested (50 µg/mL) in the presence of 10% serum, where high toxicity was observed	-	[200]
ZnO	Nominal size < 100 nm. DLS analysis: effective diameter 120 ± 2.6 nm	*In vitro A. cepa* root cells	Four concentration levels: 25, 50, 75 and 100 µg/mL. Exposure duration: 4h	Dose dependent increase of MN was observed.	+	[208]
ZnO	TEM analysis: particle size 29 ± 10 nm	*In vitro* WIL2-NS human lymphoblastoid cells	Cells were cultured with 10 mg/l NPs for 24h	The assessment of DNA damage indicated significant increases in the frequency of MNi in cells exposed to OA-coated and PMAA-coated NPs, respectively, whereas there was no significant elevation of MNi found in cells exposed to uncoated or medium-coated NPs	+/-	[209]

Table 3. Current review of genotoxicity studies (Ames test) on metal oxide NMs. As discussed in section 3.3, in the Ames test one or more strains of *Salmonella* (*S. typhimurium*) and/or *E. coli* are used e.g. the *S. typhimurium* strains (TA) TA97a, TA98, TA100, TA102, TA1535 and TA1537 or the *E. coli* strain WP2u-vrA^{-} referred to in Table 3. It can also be used with or without metabolic activation i.e. typically with or without "S9- mix". Typically, a single "positive" result in any one of these combinations results in the outcome of the Ames test being "positive" [97]. As explained in section 3, each row in this table summarizes all genotoxicity data found for this test for all nanomaterials with a given core chemical composition reported in a given publication.

Nanomaterial core chemical composition	size (nm)	Ames outcome	TA97a	TA97a +S9	TA98	TA98 +S9	TA100	TA100 +S9	TA102	TA102 +S9	TA1535	TA1535 +S9	TA1537	TA1537 +S9	E. coli WP2u -vrA⁻	E. coli WP2u -vrA⁻ +S9	publications
Al_2O_3	<50	-	-	-			-	-							-	-	[210]
Al_2O_3	30-40	-	-	-	-	-	-	-	-	-	-	-					[81, 197]
Co_3O_4	<50	-	-	-			-	-							-	-	[210]
CuO	<50	+	-	+			+	+							+	colony inhibition	[210]
Fe_3O_4	8.0 ±2 (10-30ppm)	-			-	-	-	-	-	-							[132]
Fe_3O_4	8.0 ±2 (70ppm)	+			-	-	-	+	-	-							[132]
TiO_2	50	+			+	+	-	-			-	-	+	+	+	+	[211]
TiO_2	<100	+	-				-								+	+	[210]
TiO_2	10	-			-		-		-		-		-				[174]
TiO_2	<100	+			+	+	-	+									[213]
ZnO	5.4	-			-	-	-	-					-	-	-	-	[214]
ZnO	30	+			-	+	-	-			-	-	-	+	-	+	[211]
ZnO	<100	+	-				-								+	+	[210]
ZnO	100	-			-		-						-		-		[215]

ZnO	20 and 70	-			-	-	-	-			-	-	-	-	-	-	[191]
WO_3	<100	+			+		-				-				-		[216]
In_2O_3	<100	+			+		-				-				-		[216]
Dy_2O_3	<100	+			+		+				+				+		[216]

4. Survey of available genotoxicity data for metal oxide NMs in the literature

In order to estimate an overall situation with genotoxicity tests for NPs, we have performed a literature search in the Scopus online database, searching articles published from January 1997 until July 2014 using the keywords: “genotoxicity” and “nanomaterial” or “nanoparticle”. The results of literature search were last updated in July 2014. The search identified more than 600 publications which contained the keywords mentioned above; the distribution of years of publication is shown in Figure 2. From these publications, 165 reporting experimental data relating only to metal oxide/silica NMs’ genotoxicity were selected. The data presented in these publications are summarized in Tables 1-3.

Furthermore, the selected publications were analyzed, identifying the particular genotoxicity test used, with Figure 3 showing the trend in the number of publications per year for each test type. Interestingly, the comet assay appears to be the most popular genotoxicity test for NMs at the current time. Furthermore, the number of publications reporting NM studies using the comet assay increases year on year, while the number of publications reporting use of the, currently second most popular, micronucleus test appears to be declining. Among the other two tests considered, the Ames and chromosome aberration tests, the use of the chromosome aberration test would appear to be declining whilst the Ames test is becoming increasingly popular for NMs, in spite of warnings regarding its suitability for NMs [37, 101].

From the 165 articles with genotoxicity data (Tables 1-3), 137 genotoxicity studies describe the use of the comet assay, 38 the micronucleus assay, 20 the Ames test and 6 the chromosome aberrations test (some papers include two or three tests), (Figure 4).

Based on Table 4 we can see that TiO_2, SiO_2 and ZnO NMs are the most assessed NMs, out of the group of metal oxides/silica considered in this review, in genotoxicity studies (Table 4). The other types of NMs evaluated in these studies, out of the group of metal oxides/silica considered in this review, are, in descending order of number of publications presenting genotoxicity studies of NMs, as follows: Fe_3O_4, Fe_2O_3, CuO, Al_2O_3, CeO_2, Co_3O_4, NiO, MnO_2, WO_3, V_2O_5, Dy_2O_3, In_2O_3, ZrO_2, MgO, V_2O_3, Bi_2O_3 NMs.

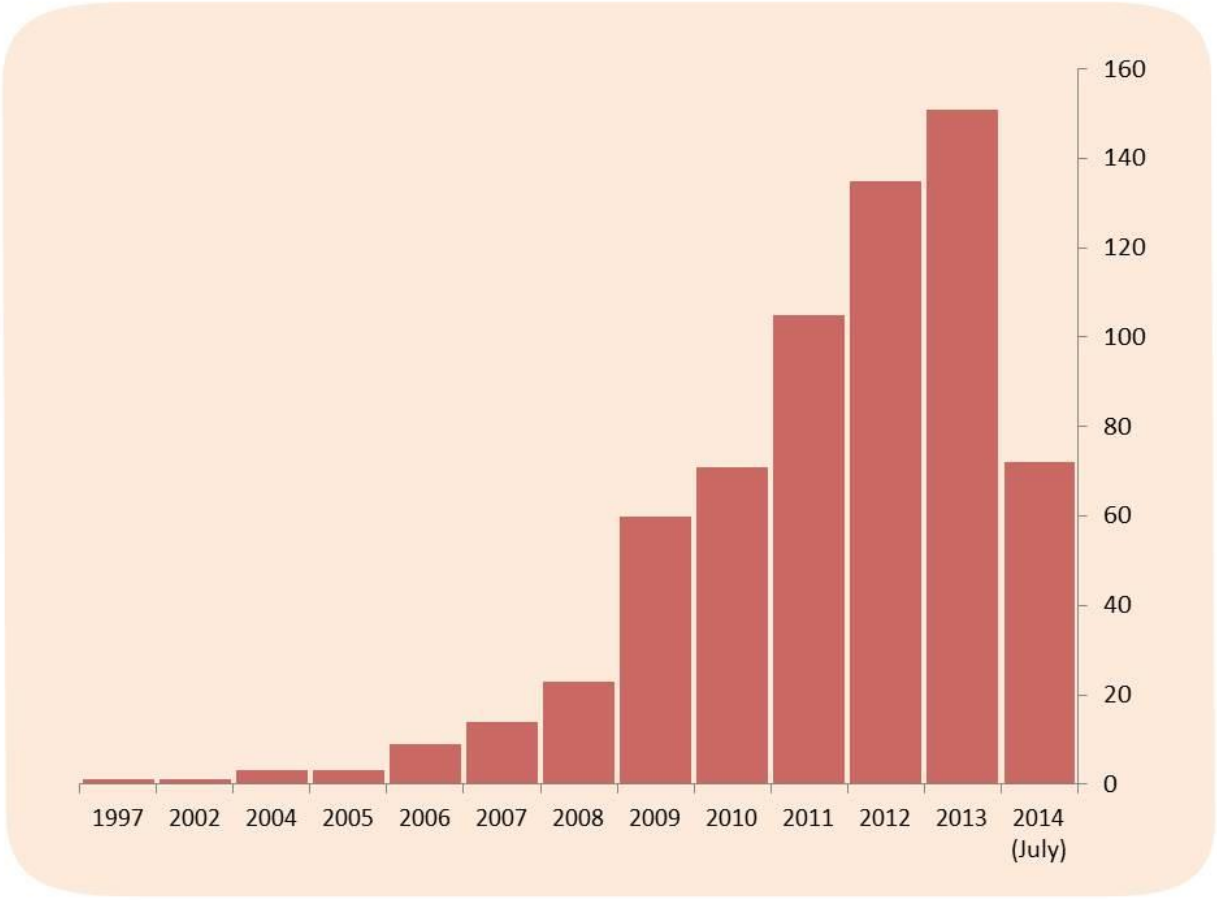

Figure 2. Literature results in terms of number of papers per year on genotoxicity of NMs performed in the Scopus online database from year 1997 using “nanoparticle”or “nanomaterial” and “genotoxicity” as key words.

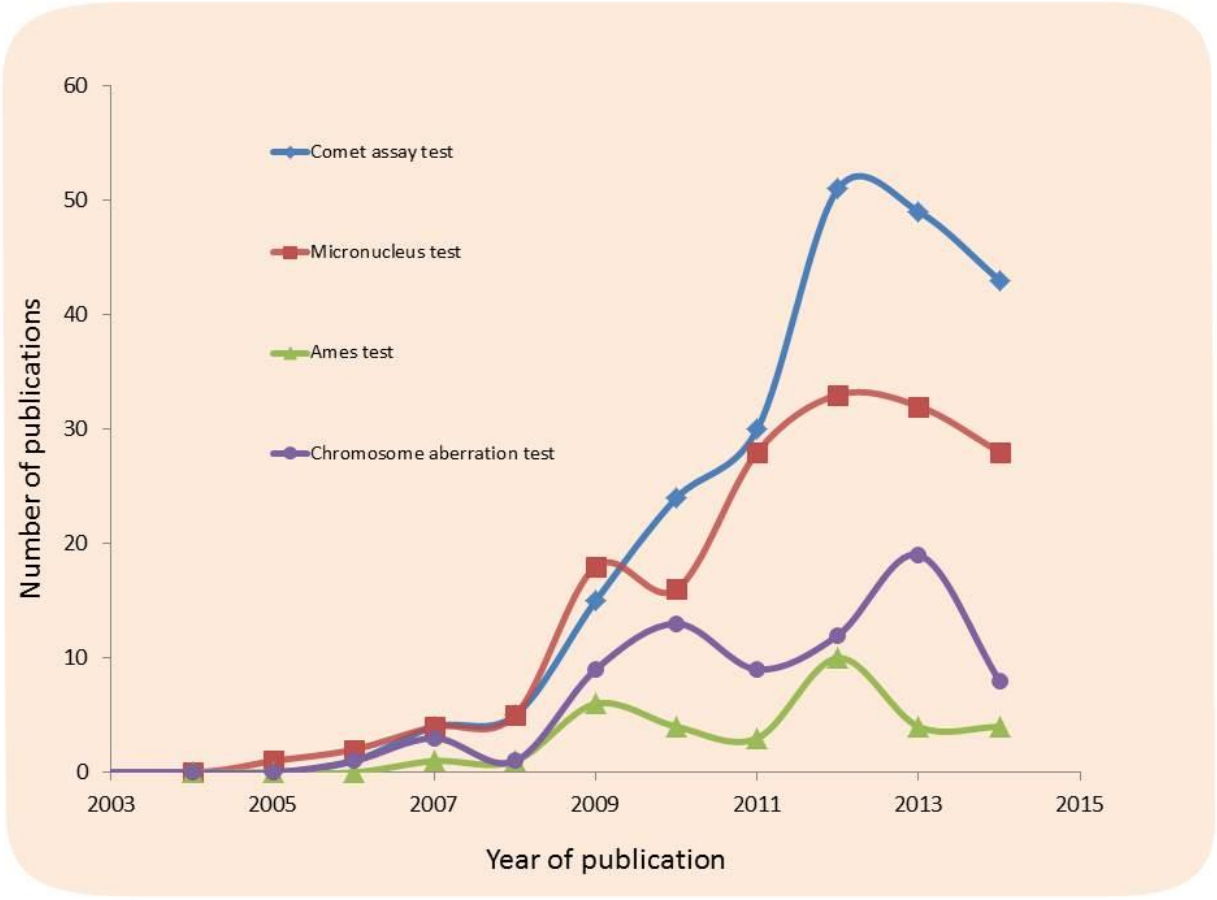

Figure 3. Number of publications per each genotoxicity test in a range from 1997 to 2014 (July).

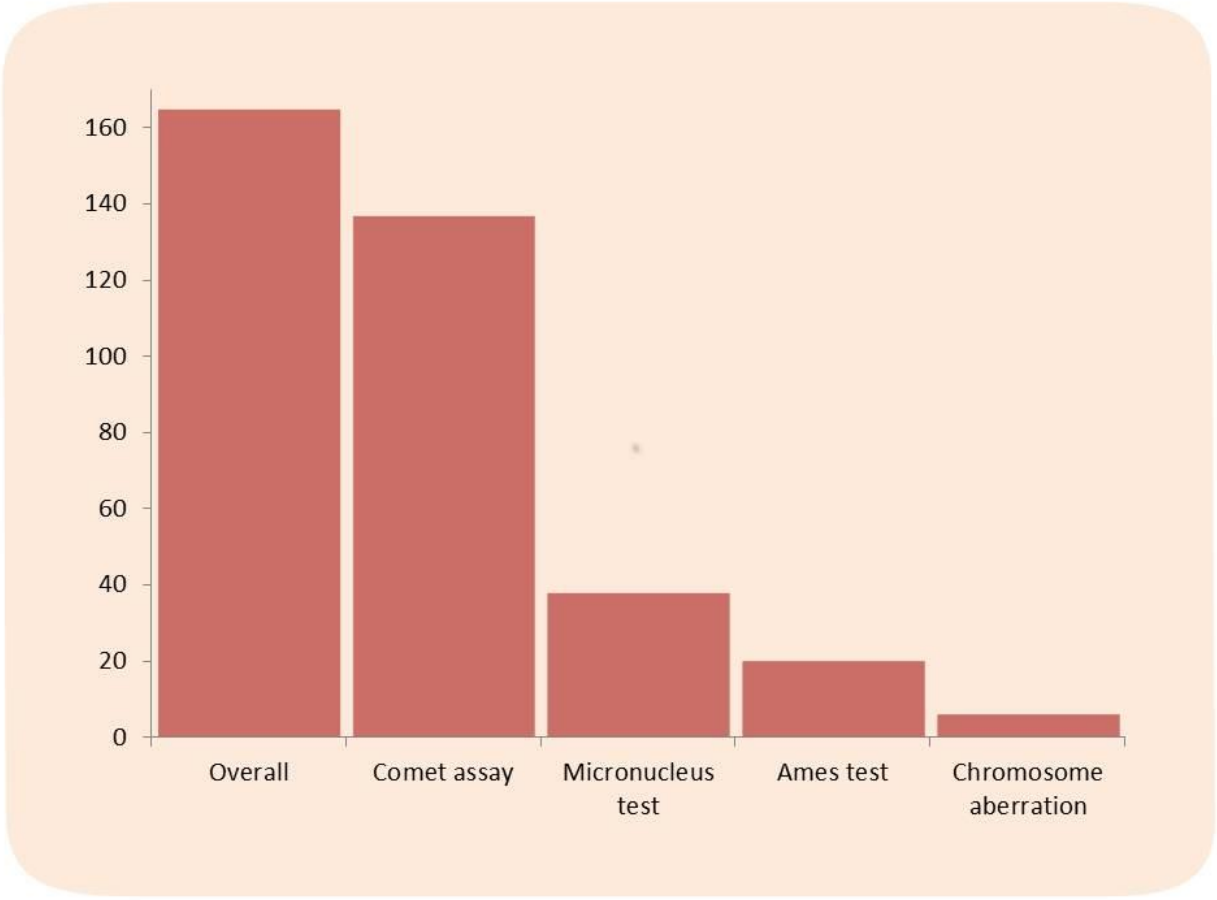

Figure 4. Ranking of genotoxicity tests by the number of publications reporting their use for evaluating - the tests that are more frequently used for evaluation of MeOx and silica NMs genotoxicity. N.B. This figure reflects the information on total number of publications, given in Table 4.

Table 4. Ranking of different kinds of metal oxide/silica NMs by: a) Number of publications reporting genotoxicity evaluations by different tests, b) Datum point for each assay performed for each type of nano metal oxide/silica.

Nano metal oxides	Number of publications [a]	Comet[b]	Micronucleus[b]	Ames[b]	Chromosome aberration[b]
Total	165	137	39	20	6
TiO_2	63	53	14	5	2
ZnO	25	21	4	5	1
SiO_2	18	15	5		
CuO	14	11	3	2	
Fe_3O_4	10	9	3	2	

Fe_2O_3	9	8	2		
CeO_2	7	7	2		
Al_2O_3	5	3	2	2	1
Co_3O_4	3	2		1	
MnO_2	2	2	1		1
V_2O_5	1	1	1		
Bi_2O_3	1	1			
Dy_2O_3	1			1	
In_2O_3	1			1	
MgO	1	1			
NiO	1	1			
V_2O_3	1	1	1		
WO_3	1		1	1	1
ZrO_2	1	1			

5. Mechanisms of metal oxide/silica NM-induced genotoxicity

The knowledge of the various possible mechanisms of NMs' toxicity and genotoxicity, in particular, is critically important in order to assess the level of hazard posed by NMs towards the environment and living organisms. Inorganic materials can interfere with the delicate balance of cellular homeostasis and hereby alter intracellular signaling pathways, resulting in cascade of possible effects. As for all NMs, the detailed mechanisms of genotoxicity for metal oxide/silica NMs are still not well understood, and as was discussed in [26, 60] it is often not clear if an effect on DNA is "nano-specific". By "nano-specific effect", we mean that the mechanism of toxic action is specific to particles with initial dimensions within the size range 1-100 nm as opposed to also being associated with particles of different size but with the same chemical composition. In general, particle induced genotoxicity may be classified as either "primary genotoxicity" or "secondary genotoxicity", where "secondary genotoxicity" refers to the induction of genotoxicity via reactive oxygen species (ROS) generated during particle-elicited inflammation and "primary genotoxicity" refers to genotoxicity induced in the absence of inflammation [217] . There are studies that suggest primary genotoxicity could be the result of direct interaction of NMs with DNA, as well as studies that confirm indirect damage from NM-induced reactive oxygen species (ROS) formation, or by toxic ions released from soluble or even from low soluble NMs [57, 107, 116, 139, 172, 189, 218-220]. At the same time, secondary genotoxicity may result from DNA attack by ROS generated via activated phagocytes (neutrophils, macrophages) during NM-elicited inflammation [60, 221]. A more detailed discussion regarding possible metal oxide/silica NM genotoxicity mechanisms of action is given below.

5.1. Direct primary genotoxicity

As soon as particles enter the nucleus, they have the potential to interact directly with DNA molecules. During these interactions, the metal oxide/silica NMs might bind and influence DNA replication or disturb other DNA processes, for example, transcription to RNA [222].

Several studies support the hypothesis of direct primary genotoxicity of NMs indicating binding with DNA [223-236], although many of them are computational studies [228-230, 232-235]. Palchoudhury et al [224], using gel electrophoresis, studied platinum-attached iron oxide NMs' interaction with DNA and showed that DNA has strong interaction with iron oxide NMs' attached to platinum. Tang et al [225] investigated the interaction of cadmium quantum dots with DNA and, using circular dichroism spectroscopy, indicated that the Cd-MAA complex might interact with DNA fragments. Rice et at [226] studied the interactions of TiO_2-NMs with DNA and, using adsorption studies, showed that terminal phosphate groups influence binding of DNA to TiO_2. In another study, Wahab et al [227] investigated ZnO-NMs by various spectroscopy methods and observed the interaction of zinc oxide NMs with DNA by UV-vis and atomic force microscopy (AFM) spectroscopy. The dissociation of double-stranded DNA (dsDNA) by small metal NMs (5nm Au) was observed through a series of DNA melting transition measurements by Yang et al [236], which confirms the strong non-specific interaction between DNA and metal NMs. In addition to the experimental studies discussed, a number of computational studies support the scarce experimental evidence that metal oxide NMs can interact with DNA bases and DNA fragments [228-230, 232-235]. For example, Shewale et al [234], applying first-principles calculations, identified possible interactions of ZnO clusters with DNA nucleobases. Fahrenkopf et al [228], using density functional theory (DFT) calculations, showed the interaction between hafnium dioxide NMs and DNA, suggesting that the interactions were predominantly mediated by the terminal phosphate in an oriented manner. Jin et al [229] used DFT calculations to indicate strong interactions between $Al_{12}X$ (X=Al, C, N and P) NMs and DNA base pairs, suggesting that Al-based NMs might affect structural stability of DNA and cause structural damage. In another computational study, Paillusson et al [232] investigated interactions between model NMs and DNA. They investigated the influence on the effective interaction of the following conditions: the shape of the NP, the magnitude of the nanoparticle charge and its distribution, the value of the pH of the solution, the magnitude of Van der Waals interactions, depending on the nature of the constitutive material of the NM (metal vs. dielectric), and showed that, for positively charged concave NPs, the effective interaction is repulsive at short distances i.e. the interaction energy shows a minimum at a finite distance from the DNA.

5.2. Indirect primary genotoxicity

The indirect mechanisms of nanoparticle primary genotoxicity were recently reviewed systematically [60]. Here we discuss only those mechanisms applicable to metal oxide NPs. In fact, to cause damage, metal oxide NPs do not need to be in direct contact with DNA. Some possible indirect genotoxicity mechanisms for metal oxide NPs include: interaction with nuclear proteins (involved in replication, transcription, and repair), disturbance of cell cycle checkpoint functions, ROS arising from the NP surface, release of toxic metal ions from the NP surface, ROS produced by cell components, and inhibition of antioxidant defense [54, 110, 237]. Several experimental studies have shown that indirect DNA damage might be caused by oxidative stress initiated by ROS species generated by metal oxide NPs [92, 109, 114, 116, 238-246].

5.3. Secondary genotoxicity

Metal oxide/silica NMs interactions may cause secondary genotoxicity via the following pathway: NMs trigger ROS production by inflammatory cells (neutrophils and macrophages), i.e. in this case ROS are not generated by the NM itself or by ions leaching from the NM surface, but by inflammatory cells via an inflammation signaling pathway. Several publications confirmed the genotoxicity of metal oxide NMs being associated with inflammation processes [59, 87, 89, 186, 247-252].

6. Brief overview of experimental data identified and comparative analysis of genotoxicity for metal oxide/silica NMs

This section provides a brief overview of the experimental data identified generalizing the data represented in Tables 1-3 and discussing the main findings.

6.1. Toxicity of NMs compared to their micrometer-sized and bulk counterparts

Karlsson et al [31] compared the ability of nano-sized (<100 nm) and micrometer-sized (<5 μm) particles of some metal oxides (Fe_2O_3, Fe_3O_4, TiO_2 and CuO) to cause cell death, mitochondrial damage, DNA damage and oxidative DNA lesions after exposure to the human cell line A549. This publication reported that NPs of CuO were much more toxic compared to CuO micrometer-sized particles. One key mechanism may be the ability of CuO NPs to damage the mitochondria. In contrast, micrometer-sized particles of TiO_2 caused more DNA damage compared to the NPs, although this may be explained by differences in their crystal structures. The iron oxides showed low toxicity and no clear difference between the different particle sizes.

Singh et al [126] studied Fe_2O_3 (< 50 nm) - and Fe_2O_3-bulk (< 5 μm) particles in female Wistar rats. The genotoxicity was evaluated at 6, 24, 48 and 72 hours by the comet assay in leucocytes, at 48 and 72 hours by the micronucleus test in peripheral blood cells, at 18 and 24 hours by the chromosomal aberration assay in bone marrow cells and at 24 and 48 hours by the micronucleus test in bone marrow cells. The tail DNA (comet), frequencies of micronuclei (micronucleus test) and chromosome aberrations were statistically insignificant ($p>0.05$) at all doses. These results suggested that 30nm and bulk Fe_2O_3 were not genotoxic at the doses tested.

In a similar study, Singh et al [128] assessed MnO_2 nano- (45 nm) and micrometer-sized particles (< 5 μm). Nano-MnO_2 elicited genotoxicity in rats as determined using the micronucleus test, comet and chromosomal aberration assays at 1000 mg/kg but bulk particles did not. A significant ($p < 0.05$) increase in the percentage tail DNA was observed in the peripheral blood leukocytes (PBLs) of rats exposed to MnO_2-45 nm at the highest dose of 1000 mg/kg body weight at 24 and 48 h sampling times; however, no significant DNA damage was observed at 6 and 72 h. In rats treated orally with 100, 500 and 1000 mg/kg body weight of MnO_2-bulk particles at 6, 24, 48, and 72 h, no significant DNA damage was observed. Moreover, there was a clear size dependent biodistribution as well as toxicity. These findings support the view that NMs may have both higher toxicity and distribution rates compared to their bulk counterparts.

Midander et al [113] assessed the toxic aspects of nano-sized (50 nm) and micrometer-sized (<10 μm) particles of copper(II) oxide in contact with cultivated lung cells. The nano-sized particles caused a higher degree of DNA damage (single-strand breaks) and caused a significantly higher percentage of cell death than micrometer-sized particles. Since these authors also observed higher release of copper for the nano-sized particles, under similar conditions to the toxicity assays, their results suggest that both the observed genotoxicity and cytotoxicity were caused by the release of copper from the particles.

In another comparative study by Guichard et al [253], commercially available nanosized (<90 nm) and microsized (<0.75 μm) anatase TiO_2, rutile TiO_2, Fe_3O_4, and Fe_2O_3 particles were compared in Syrian hamster embryo (SHE) cells. Similar levels of DNA damage were observed in the comet assay after 24 h of exposure to anatase NPs and microparticles. Rutile microparticles were found to induce more DNA damage than the nanosized particles. However, no significant increase in DNA damage was detected from nanosized and microsized iron oxides. None of the samples tested showed significant induction of micronuclei formation after 24 h of exposure.

Balasubramanyam et al. stated that [81], Al_2O_3-bulk particles (50–200 μm) did not induce statistically significant changes over control values when assessed via the comet assay. The nanosized Al_2O_3 however, produced a genotoxic effect in the comet assay.

The studies highlighted above suggest that (at least in terms of their genotoxic effects) NPs do not always have higher toxicity than micrometer-sized particles or their bulk counterparts of the same chemical composition. However, the higher toxicity of some NPs compared to their micrometer-sized counterparts arguably justifies caution when moving from the micrometer to nanometer scale.

One important issue needs to be appreciated. Although the number of studies on the genotoxicity of metal oxide/silica NMs is increasing, many results are inconsistent and need to be confirmed by additional experiments. In previoous sections we have discussed the results that may be conflicting, but overall, show some trends in metal oxides NMs' genotoxicity. We assume that experimental data for NMs of the same core chemical composition may vary to some extent because of the following reasons, along with other possible variations: 1) various average sizes of NMs used; 2) various size distributions; 3) various purity of NMs; 4) various surface areas of NMs with the same average size; 5) different coatings; 6) differences in crystal structures of the same types of NMs; 7) different sizes of aggregates in different media; 8) differences in assays; 9) different concentrations of NMs in assay tests; 10) variation in concentration of analytes in assays. The situation of conflicting reports (experimental data) and inherent problems with nanotoxiclogy studies was discussed in the following publications [254-259]. For example, in a recent research article [255], the authors evaluated publications related to engineered NMs' safety assessments where evaluation was spurred by conflicting reports demonstrating different degrees of toxicity with the same NMs. They found that that ca. 95% of papers from 2010 using biochemical techniques to assess nanotoxicity did not account for potential interference of NMs (i.e. interference of NMs properties with analytical techniques), and this number had not substantially improved in 2012. Based on these findings, they provided recommendations for authors of future nanotoxicology studies [255].

6.2. Discussion of results from the experimental studies for each type of metal oxide/silica NM

The 165 publications obtained from the literature search refer to nano oxides of different metals (cerium oxide, copper oxide, iron oxides, titanium oxide, nickel oxide, manganese oxide, magnesium oxide, cobalt oxide, bismuth oxide, and zirconium oxide) as well as silica (silicon dioxide). The data obtained using the comet and micronucleus assay are summarized in Table 1 and Table 2 respectively. The experimental protocols clearly differ in many respects. The main differences between the different studies are the heterogeneity of cell types and methods used. In addition, the nano-sized metal oxides/silica were of varying sizes etc. Nonetheless, in spite of this inconsistency, it is possible to draw some general findings in some cases. The Ames

test results are reported in Table 3. The number of studies concerning this test on NMs is low. Furthermore, a few studies consider Ames test not appropriate for NMs [52].

Overall genotoxicity of each nano metal oxide/silica considering the data gathered in this review:

Comet assay results were as following for each compound (Table 1):

Al_2O_3

Results from the comet assay are reported in three publications [81, 103, 104]. In two *in vitro* studies [103, 104] this nano metal oxide gave different outcomes; it increased the DNA damage significantly comparing to control in mouse lymphoma (L5178Y) cells and human bronchial epithelial (BEAS-2B) cells and had no significant effect on human embryonic kidney (HEK293) cells and peripheral blood lymphocytes. The third publication reported an increase in DNA damage in an *in vivo* test [81].

Bi_2O_3

One publication [105] reports that DNA damage in the root cells of *Allium cepa* for different concentrations of the NM (25, 50, 75, 100 ppm) exhibit statistically significant differences compared to the control.

CeO_2

Reports are provided in seven publications of the comet assay being employed to assess NMs of CeO_2. The type of cells and duration of exposure varied. Each study was performed on a different cell type and exposure criteria. This might explain the contrasting results: five publications [92, 106, 107, 109, 111] reported a positive comet assay outcome and two [108, 110] did not report significant genotoxic effects. However, another possible explanation for the contrasting results could be differences in size or surface functionalization etc.

Co_3O_4

Two publications have reported genotoxic effects observed in comet assay for NMs of this cobalt oxide [109, 112].

CuO

In ten publications (on human lung epithelial cells (A549) cells and human murine macrophages cells (RAW)) the CuO NMs ranging in size from 10-100nm, induced DNA strand breakages as assessed by the alkaline comet assay [31, 113-118, 120-122]. A publication reported no

genotoxicity observed following exposure to the metal oxide in aquatic organism (*Macoma balthica*) [119].

Fe_2O_3

Reports in seven publications stated that Fe_2O_3 of different dimensions and preparations elicited no significant genotoxic effect as determined with the alkaline comet assay [31, 114, 123, 124, 126, 127]. However, in one publication [31], these kinds of particles were found to be genotoxic according to the comet assay.

Fe_3O_4

Six publications conducted on A549 and BEAS-2B cells and human lymphocytes reported that these kinds of nano particles induced DNA breakages as detected by the comet assay [109, 129-132, 260]. Three publications reported no genotoxic effect of which one study conducted on peripherial blood lymphocytes HEK293 and HPL cells showed no significant genotoxicity at all concentrations after 1 h incubation with both types of cells [123] and no DNA damage was observed at the tested concentration levels on *in vitro* human lung type II epithelial (A549) cells in two studies [31, 114].

MnO_2

Two publications report the *in vivo* genotoxic effects of the MnO_2 nano metal oxides: A statistically significant ($p < 0.05$) increase in the percentage of tail DNA was observed in the PBLs of rats exposed to MnO_2-45 nm at the highest dose of 1000 mg/kg body weight at 24 and 48 h sampling times; however, no significant DNA damage was observed at 6 and 72 h [128]. Singh et al [134] reported a statistically significant ($P < 0.01$) increase in the DNA damage (percentage of tail DNA) with the highest and medium doses. No significant increase was found with the lowest dose.

NiO

One publication has reported genotoxic effects observed in comet assay for NPs of NiO [109].

MgO

Particle-induced DNA strand breakage and oxidative DNA damage in Caco-2 cells was detected using the FPG variant of the comet assay. DNA strand breakage and oxidative DNA damage was determined in Caco-2 cells by the FPG-modified comet assay following 4 h treatment at 20 mg/cm^2. After treatment, all samples were processed in the comet assay. MgO produced no significant change compared to the control [133] .

SiO_2

Fifteen publications were obtained for silica, with different crystalline structures (amorphous and quartz forms) as well as differences in surface functionalization. These studies showed the genotoxic [55, 82, 140, 142, 144] or non- genotoxic behavior of this NM [109, 111, 133, 135-144].

TiO_2

Fifty three publications were retrieved for titanium dioxide NMs [31, 85, 87, 89, 103, 111, 114, 121, 123, 125, 133, 146-168, 170-176, 178-180, 182-186, 249, 261-263]. These studies included data on different forms of TiO_2, such as anastase, rutile and the mixture of both forms. Genotoxic effects, as determined with the alkaline comet assay, were observed in forty of these publications - whilst the other thirteen detected no significant genotoxic effect for this kind of NMs.

V_2O_3 and V_2O_5

One study has reported genotoxic effects observed in comet assay for NPs of V_2O_3 and no genotoxic effects of V_2O_5 [52].

ZnO

Twenty one comet publications were found for these nano metal oxides [55, 114, 121, 133, 152, 155, 156, 159, 165, 186-196]. Genotoxic effects were observed in CaCo-2 cells [133], lymphocytes and sperm cells [155], A549 [114, 152], human epidermal cell line [189], primary mouse embryo fibroblasts [55], HK2 cells [186]. Among all the studies, two reported non-genotoxic results from the comet assay, where the size of agglomerates was about 200nm [191, 192]. The large size (over 100nm) of NPs studied is one possible reason of non-genotoxic results and therefore it is questionable if these results are truly relevant for most NPs.

ZrO_2

In a single publication performed on nano metal oxides of ZrO_2, no significant induction in DNA damage by the comet assay was observed with or without the Endo III and FPG enzymes at all concentrations.

Micronucleous test results for each compound (Table 2):

Al_2O_3

Two publications reported positive results in the *in vivo* micronucleous assays on the same type of Al_2O_3 NMs (30-40 nm Nominal size). One publication reported results of the test performed after oral administration in bone marrow cells [197]. The other publication reported resultson peripherial blood cells after gavage administration [81].

CeO_2

In two publications [106, 107] genotoxic effects of these NMs were observed for the micronucleous assay on *in vitro* human cells (dermal fibroblasts and neuroblastoma).

CuO

In two publications *in vitro* micronucleous test results reported genotoxic effects of these NMs [115, 198]. Song et al [86] reported an *in vivo* micronucleous test genotoxic outcome.

Fe_2O_3

Two publications reported results of *in vivo* micronucleous assay for this compound; whereas one paper reported statistically insignificant results [126], the other publication reported genotoxic effects for these NMs [86]. The studies were conducted on albino Wistar female rat peripheral blood and bone marrow cells and female ICR mice peripheral blood cells.

Fe_3O_4

Three publications reported results of the micornucleous assay, a study conducted *in vivo* on female ICR mice peripheral blood cells identified significant increases in micronucleated reticulocytes cells [131]. Chen et al. found no significant difference between the test animals and the negative controls in the *In vivo* kunming mice bone marrow cells [199]. Song et al. observed a significantly enhanced MN induction on human lung adenocarcinoma type-II alveolar epithelial cells A549 (*in vitro*) at 10 μg/cm^2 [86].

MnO_2

In a study performed by Singh et al [128] the micronucleous assay conducted on bone marrow cells extracted from the femurs of female albino Wistar rats (*in vivo*) the data revealed statistically significant enhancement in the MN frequency in the groups treated with 1000 mg/kg body weight of MnO2-45 nm at 24 and 48 h of sampling times.

SiO_2

Micronucleous assay was reported in five publications on different crystalline structures. These studies reported genotoxic [201, 202] and non genotoxic [138] [200] effects of these NMs. One publication showed equivocal results [82].

TiO_2

Micronucleous assay was reported in fourteen publications. Among these, in five non-genotoxic effects were observed [148, 172, 203, 204, 207] and genotoxic effects in the remaining studies [86, 137, 146, 147, 169, 199, 200, 205, 206].

For a detailed report on genotoxicity of these nanoparticles see reviews [264, 265].

V_2O_3 and V_2O_5

No induction of the micronuclei has been observed for NPs of V_2O_3 and V_2O_5 [52].

ZnO

Four publications reported micronucleous test results for these NMs: An *in vivo* study, described in [191], on mice bone marrow cells reported non-genotoxic micronucleous test results. In three publications [16, 200, 209] *in vitro* studies on different cells (A549 human lung carcinoma cells 199, A549 human lung carcinoma cells, and A. cepa root cells) showed negative, positive and equivocal results. In one of these *in vitro* studies [209] coated and uncoated nano ZnO were tested. The uncoated ZnO NMs were not genotoxic in the micronuclei assay. The coated ZnO was, however, genotoxic.

WO_3

One publication [83] reported micronucleous test conducted on the nanoparticles of WO_3. No statistically significant difference was found between 25 mg WO3 applied and control group. On the contrary, the higher doses of WO_3 (50 and 100 mg) caused increases of MN rates. No characterization of the NMs was reported in the paper.

Ames test results; an overall view (Table 3):

Mutagenicity assessed by the Ames test is reported in Table 3. Al_2O_3, Co_3O_4, Fe_3O_4 tested on various strains of *S. typhimurium* and *E. coli*, with and without metabolic activation gave negative results in Ames test. Fe_3O_4 was reported in one publication to be positive in the Ames test. Nano TiO_2 in four publications gathered in this review, showed at least one positive result in Ames test. Woodruff et al [174] reported negative mutagenicity of the nano TiO_2. Hasegawa et al [216] reported positive Ames results for nano WO_3, In_2O_3, and Dy_2O_3. In two publications ZnO was found to have positive Ames test data results and to be negative in three other publications.

7. Conclusions

The number of published genotoxicity studies on metal oxide/silica NMs is still limited, although this endpoint has recently received more attention for NMs and the number of related publications has increased. However, more, well designed, genotoxicity studies are required, with a particular need for more *in vivo* experiments. We can expect an increasing number of genotoxicity studies of NMs, with our literature analysis showing an increasing number of genotoxicity publications every year. In particular, we can see that the number of papers reporting comet assay studies for NMs is increasing year on year, although this is not true for the micronucleus test which was the second most popular test amongst those considered in this review. Among the other two tests considered in this review, the Ames and chromosome aberration tests, the former is much more popular for NMs analysis and its use is increasing, in spite of concerns raised about the validity of the Ames test for NMs, whilst the use of the latter would seem to be decreasing in popularity for nanomaterials. Although the number of studies of the genotoxicity of metal oxide/silica NMs is increasing, many results, for the same core chemical composition, are inconsistent: these may need to be confirmed by additional experiments or they may reflect genuine differences due to differences in particles sizes, functionalization etc. In this review, we have discussed the results that may be conflicting. We assume that experimental data for genotoxicity, for NMs with the same core chemical composition, may vary to some extent because of the following reasons: 1) various sizes of NPs used; 2) various size distribution; 3) various purity of NMs; 4) various surface areas for NMs with the same average size; 5) different coatings; 6) differences in crystal structures of the same types of NMs; 7) different sizes of aggregates in solution/media; 8) differences in assays; 9) different concentrations of NMs in assay tests; 10) variation in concentration of analytes in assays etc. The experimental data in the public domain are still quite scarce and exhibit considerable heterogenity. Ideally, all experimental studies would need to be performed using the same protocol to be able to properly compare these data. As a result of these issues, the genotoxicity data for NMs are quite difficult to compare and make robust conclusions.

As can be seen from the above discussion, different kinds of metal-oxide/silica NMs exhibited varying degrees of genotoxicity. In the majority of the literature references analysed, the NMs considered caused DNA strand breaks or oxidative DNA lesions. Our analysis of these data shows that NMs based on ZnO, NiO, CuO, V_2O_3, Al_2O_3, TiO_2 exhibited at least one positive genotoxic response in most of the references analyzed, while Fe_2O_3 and SiO_2 based NMs mainly showed non-genotoxic responses in these references. Nonetheless, caution is advised regarding these generalizations as considerable inconsistency in the experimental protocols was observed as well as variation in the characteristics of the studied NMs, of any given chemical composition, such as particle size, functionalization etc. In addition to considering the outcome of the tests (i.e. “positive” or “negative” study calls), it should be noted that metal oxide/silica

NMs may induce genotoxicity via various mechanisms. For example, metal oxide NMs may induce genotoxicity via primary or secondary ROS generation pathways. There is a great need for careful scrutiny of the genotoxicity of metal oxide/silica NMs at the molecular level.

This review should help to improve genotoxicity testing of metal oxide/silica NMs, as well as help in understanding of mechanisms and, crucially, provides a valuable summary of genotoxicity data for these NMs reported in the literature up until July 2014.

Acknowledgements

We thank the support of the Interdisciplinary Center for Nanotoxicity, NSF-CREST grant no. 0833178; NSF EPSCoR Grant no. 362492 190200-01\NSFEPS-0903787 and NSF-RISE no. HRD-1137763 and NSF-PREM # DMR-0611539.

The research leading to these results has received funding from the European Union Seventh Framework Programme (FP7/2007-2013) under grant agreement n° 309837 (NanoPUZZLES project).

References

1. Oberdörster, G., E. Oberdörster, and J. Oberdörster, *Nanotoxicology: An emerging discipline evolving from studies of ultrafine particles.* Environmental Health Perspectives, 2005. **113**(7): p. 823-839.
2. Magdolenova, Z., et al., *Can standard genotoxicity tests be applied to nanoparticles?* Journal of Toxicology and Environmental Health - Part A: Current Issues, 2012. **75**(13-15): p. 800-806.
3. Göran Lövestam, H.R., Gert Roebben, and N.G. Birgit Sokull Klüttgen, Jean-Philippe Putaud and Hermann Stamm. *Considerations on a Definition of Nanomaterial for Regulatory Purposes*. Joint Research Center (JRC) reference reports 2010; Available from: http://ihcp.jrc.ec.europa.eu/our_activities/nanotechnology/report-definition-nanomaterial.
4. 2011, E., *Commission Recommendation of 18 October 2011 on the Definition of Nanomaterial*. O. J. L 275: 38–40. Brussels: European Union.
5. Warheit, D.B., et al., *Testing Strategies to Establish the Safety of Nanomaterials: Conclusions of an ECETOC Workshop.* Inhalation Toxicology, 2007. **19**(8): p. 631-643.
6. Barreto, J.A., et al., *Nanomaterials: Applications in cancer imaging and therapy.* Advanced Materials, 2011. **23**(12): p. H18-H40.
7. Chen, X. and S.S. Mao, *Titanium dioxide nanomaterials: Synthesis, properties, modifications and applications.* Chemical Reviews, 2007. **107**(7): p. 2891-2959.
8. Guo, S. and E. Wang, *Noble metal nanomaterials: Controllable synthesis and application in fuel cells and analytical sensors.* Nano Today, 2011. **6**(3): p. 240-264.
9. Jang, J., *Conducting polymer nanomaterials and their applications*. 2006. p. 189-259.
10. Lu, X., C. Wang, and Y. Wei, *One-dimensional composite nanomaterials: Synthesis by electrospinning and their applications.* Small, 2009. **5**(21): p. 2349-2370.
11. Mauter, M.S. and M. Elimelech, *Environmental applications of carbon-based nanomaterials.* Environmental Science and Technology, 2008. **42**(16): p. 5843-5859.
12. West, J.L. and N.J. Halas, *Engineered nanomaterials for biophotonics applications: Improving sensing, imaging, and therapeutics*. 2003. p. 285-292.
13. Karlsson, H.L., *The comet assay in nanotoxicology research.* Analytical and Bioanalytical Chemistry, 2010. **398**(2): p. 651-666.
14. Foltête, A.S., et al., *Environmental impact of sunscreen nanomaterials: Ecotoxicity and genotoxicity of altered TiO 2 nanocomposites on Vicia faba.* Environmental Pollution, 2011. **159**(10): p. 2515-2522.
15. Hubbs, A.F., et al., *Nanotechnology: Toxicologic pathology.* Toxicologic Pathology, 2013. **41**(2): p. 395-409.
16. Kumar, V., et al., *Evaluating the toxicity of selected types of nanochemicals*. 2012. p. 39-121.
17. Singh, N., et al., *NanoGenotoxicology: The DNA damaging potential of engineered nanomaterials.* Biomaterials, 2009. **30**(23-24): p. 3891-3914.
18. Vega-Villa, K.R., et al., *Clinical toxicities of nanocarrier systems.* Adv. Drug Deliv. Rev., 2008. **60**: p. 929–938.
19. Xie, H., M.M. Mason, and J.P. Wise Sr, *Genotoxicity of metal nanoparticles.* Reviews on Environmental Health, 2011. **26**(4): p. 251-268.
20. Zhao, J. and V. Castranova, *Toxicology of nanomaterials used in nanomedicine.* Journal of Toxicology and Environmental Health - Part B: Critical Reviews, 2011. **14**(8): p. 593-632.
21. Gwinn, M.R. and V. Vallyathan, *Nanoparticles: Health effects - Pros and cons.* Environmental Health Perspectives, 2006. **114**(12): p. 1818-1825.
22. Hardman, R., *A toxicologic review of quantum dots: Toxicity depends on physicochemical and environmental factors.* Environmental Health Perspectives, 2006. **114**(2): p. 165-172.

23. Helland, A., et al., *Reviewing the environmental and human health knowledge base of carbon nanotubes.* Environmental Health Perspectives, 2007. **115**(8): p. 1125-1131.
24. Schulte, P., et al., *Occupational risk management of engineered nanoparticles.* Journal of occupational and environmental hygiene, 2008. **5**(4): p. 239-249.
25. Tomalia, D.A., *In quest of a systematic framework for unifying and defining nanoscience.* Journal of Nanoparticle Research, 2009. **11**(6): p. 1251-1310.
26. Donaldson, K. and C.A. Poland, *Nanotoxicity: challenging the myth of nano-specific toxicity.* Curr Opin Biotechnol, 2013. **24**(4): p. 724-34.
27. Limbach, L.K., R.N. Grass, and W.J. Stark, *Physico-chemical differences between particle- and molecule-derived toxicity: Can we make inherently safe nanoparticles?* Chimia, 2009. **63**(1-2): p. 38-43.
28. Moore, M.N., *Do nanoparticles present ecotoxicological risks for the health of the aquatic environment?* Environment International, 2006. **32**(8): p. 967-976.
29. Shvedova, A.A., et al., *Mechanisms of pulmonary toxicity and medical applications of carbon nanotubes: Two faces of Janus?* Pharmacology and Therapeutics, 2009. **121**(2): p. 192-204.
30. Wörle-Knirsch, J.M., K. Pulskamp, and H.F. Krug, *Oops they did it again! Carbon nanotubes hoax scientists in viability assays.* Nano Letters, 2006. **6**(6): p. 1261-1268.
31. Karlsson, H.L., et al., *Size-dependent toxicity of metal oxide particles-A comparison between nano- and micrometer size.* Toxicology Letters, 2009. **188**(2): p. 112-118.
32. Riediker, M., *compendium of projects in the European NanoSafety Cluster*. 2013, Institute for Work and Health, Lausanne, Switzerland.
33. Suter, G., - *Risk assessment of chemicals: An introduction, second edition, edited by C.J. van Leeuwen and T.G. Vermier.* - Integrated Environmental Assessment and Management, (- 3): p. - 380.
34. Gottschalk, F., T. Sun, and B. Nowack, *Environmental concentrations of engineered nanomaterials: Review of modeling and analytical studies.* Environmental Pollution, 2013. **181**(0): p. 287-300.
35. OECD. *No 36. Guidance on sample preparation and doismetry for the safety testing of manufactured nanomaterials*. Safety of manufactured nanomaterials.
36. Warheit, D.B. and E.M. Donner, *Rationale of genotoxicity testing of nanomaterials: Regulatory requirements and appropriateness of available OECD test guidelines.* Nanotoxicology, 2010. **4**(4): p. 409-413.
37. Doak, S.H., et al., *In vitro genotoxicity testing strategy for nanomaterials and the adaptation of current OECD guidelines.* Mutation Research/Genetic Toxicology and Environmental Mutagenesis, 2012. **745**(1â€“2): p. 104-111.
38. Kühnel, D. and C. Nickel, *The OECD expert meeting on ecotoxicology and environmental fate — Towards the development of improved OECD guidelines for the testing of nanomaterials.* Science of The Total Environment, 2014. **472**(0): p. 347-353.
39. *ECOTOXICOLOGY AND ENVIRONMENTAL FATE OF MANUFACTURED NANOMATERIALS: TEST GUIDELINES*, in *Series on the Safety of Manufactured Nanomaterials*. 2014, OECD Environment, Health and Safety Publications.
40. OECD. *Report of the OECD expert meeting on the physical chemical properties of manufactured nanomaterials and test guidelines*. Safety of manufactured nanomaterials; ENV/JM/MONO(2014)15]. Available from: http://www.oecd.org/officialdocuments/publicdisplaydocumentpdf/?cote=env/jm/mono%282014%2915&doclanguage=en.

41. Stone, V., et al., *Nanomaterials for environmental studies: classification, reference material issues, and strategies for physicochemical characterisation.* Sci. Total. Environ., 2010. **408**: p. 1745–1754.
42. Puzyn, T., et al., *Using nano-QSAR to predict the cytotoxicity of metal oxide nanoparticles.* Nature Nanotechnology, 2011. **6**(3): p. 175-178.
43. OECD. *No.27 List of Manufactured Nanomaterials and List of Endpoints for Phase One of the Sponsorship Programme for the Testing of Manufactured Nanomaterials: Revision*. Safety of manufactured nanomaterials; Available from: http://www.oecd.org/science/nanosafety/publicationsintheseriesonthesafetyofmanufacturednanomaterials.htm.
44. (SCCS), S.C.o.C.S., et al. *Silica (nano) CAS n.l 12945-52-5; Hydrated Silica(nano) CAS n. 112926-00-8; Silica Sylilate CAS n. 68909-20-6; Silica Dimethyl silylate (nano) CAS n. 68611-44-9*. 2 October 2013 [cited 2014 July 29]; Nanomaterial in cosmetic ingredie**nts**

Request for a scientific opinion]. Available from: http://ec.europa.eu/health/scientific_committees/consumer_safety/requests/index_en.htm.
45. Landsiedel, R., et al., *Application of short-term inhalation studies to assess the inhalation toxicity of nanomaterials.* (1743-8977 (Electronic)).
46. Vernon, R.E., *Which Elements Are Metalloids?* Journal of Chemical Education, 2013. **90**(12): p. 1703-1707.
47. *Project on Emerging Nanotechnologies. Consumer Products Inventory*. 2014 [cited 2014 July]; Available from: http://www.nanotechproject.org/cpi.
48. Hendren, C.O., et al., *Estimating production data for five engineered nanomaterials as a basis for exposure assessment.* Environmental science & technology, 2011. **45**(7): p. 2562-2569.
49. Wijnhoven, S., et al., *Exposure to nanomaterials in consumer products.* RIVM Letter report, 2009. **340370001**(2009): p. 2009.
50. Claxton, L.D., V.S. Houk, and T.J. Hughes, *Genotoxicity of industrial wastes and effluents.* Mutation Research/Reviews in Mutation Research, 1998. **410**(3): p. 237-243.
51. Gonzalez, L., D. Lison, and M. Kirsch-Volders, *Genotoxicity of engineered nanomaterials: A critical review.* Nanotoxicology, 2008. **2**(4): p. 252-273.
52. Landsiedel, R., et al., *Genotoxicity investigations on nanomaterials: Methods, preparation and characterization of test material, potential artifacts and limitations-Many questions, some answers.* Mutation Research - Reviews in Mutation Research, 2009. **681**(2-3): p. 241-258.
53. Ng, C.T., et al., *Current studies into the genotoxic effects of nanomaterials.* Journal of Nucleic Acids, 2010. **2010**.
54. Petersen, E.J. and B.C. Nelson, *Mechanisms and measurements of nanomaterial-induced oxidative damage to DNA.* Analytical and Bioanalytical Chemistry, 2010. **398**(2): p. 613-650.
55. Yang, H., et al., *Comparative study of cytotoxicity, oxidative stress and genotoxicity induced by four typical nanomaterials: The role of particle size, shape and composition.* Journal of Applied Toxicology, 2009. **29**(1): p. 69-78.
56. Schins, R.P., *Mechanisms of genotoxicity of particles and fibers.* Inhal Toxicol, 2002. **14**: p. 57-78.
57. Kisin, E.R., et al., *Single-walled carbon nanotubes: genoand cytotoxic effects in lung fibroblast V79 cells.* J. Toxicol. Environ. Health Part A, 2007. **70**: p. 2071–2079.
58. Collins, A.R., *The comet assay for DNA damage and repair: Principles, applications, and limitations.* Applied Biochemistry and Biotechnology - Part B Molecular Biotechnology, 2004. **26**(3): p. 249-261.
59. Magaye, R., et al., *Genotoxicity and carcinogenicity of cobalt-, nickel- and copper-based nanoparticles (Review).* Experimental and Therapeutic Medicine, 2012. **4**(4): p. 551-561.

60. Magdolenova, Z., et al., *Mechanisms of genotoxicity. A review of in vitro and in vivo studies with engineered nanoparticles.* Nanotoxicology, 2014. **8**(3): p. 233-278.
61. Oesch, F. and R. Landsiedel, *Genotoxicity investigations on nanomaterials.* Archives of Toxicology, 2012. **86**(7): p. 985-994.
62. Arora, S., J.M. Rajwade, and K.M. Paknikar, *Nanotoxicology and in vitro studies: The need of the hour.* Toxicology and Applied Pharmacology, 2012. **258**(2): p. 151-165.
63. Krishna, G. and M. Hayashi, *In vivo rodent micronucleus assay: Protocol, conduct and data interpretation.* Mutation Research - Fundamental and Molecular Mechanisms of Mutagenesis, 2000. **455**(1-2): p. 155-166.
64. Ames, B.N., et al., *Carcinogens are mutagens: a simple test combining liver homogenates for activation and bacteria for detection.* Proceedings of the National Academy of Sciences of the United States of America, 1973. **70**(8): p. 2281-2285.
65. Mosesso, P., et al., *In vitro cytogenetic assays: Chromosomal aberrations and micronucleus tests*. 2013. p. 123-146.
66. Greenwood, N.N. and A. Earnshaw, *Chemistry of the Elements*. Second Edition ed. 1997, Oxford, UK: Elsevier Butterworth-Heinemann.
67. Fernandez-Garcia, M., et al., *Nanostructured oxides in chemistry: characterization and properties.* (0009-2665 (Print)).
68. Baresel, D., et al., *Influence of catalytic activity on semiconducting metal oxide sensors I. experimental sensor characteristics and their qualitative interpretation.* Sensors and Actuators, 1984. **6**(1): p. 35-50.
69. Haralambous, K.J., Z. Loizos, and N. Spyrellis, *Catalytic properties of some mixed transition-metal oxides.* Materials Letters, 1991. **11**(3-4): p. 133-141.
70. Fujishima, A., T.N. Rao, and D.A. Tryk, *Titanium dioxide photocatalysis.* Journal of Photochemistry and Photobiology C: Photochemistry Reviews, 2000. **1**(1): p. 1-21.
71. O'Regan, B. and M. Grätzel, *A low-cost, high-efficiency solar cell based on dye-sensitized colloidal TiO2 films.* Nature, 1991. **353**(6346): p. 737-740.
72. Billinge, S.J.L. and I. Levin, *The Problem with Determining Atomic Structure at the Nanoscale.* Science, 2007. **316**(5824): p. 561-565.
73. Samsonov, V.M., N.Y. Sdobnyakov, and A.N. Bazulev, *On thermodynamic stability conditions for nanosized particles.* Surface Science, 2003. **532-535**: p. 526-530.
74. Song, Z., et al., *Molecular level study of the formation and the spread of MoO3 on Au (111) by scanning tunneling microscopy and X-ray photoelectron spectroscopy.* Journal of the American Chemical Society, 2003. **125**(26): p. 8059-8066.
75. Zhang, H. and J.F. Banfield, *Thermodynamic analysis of phase stability of nanocrystalline titania.* Journal of Materials Chemistry, 1998. **8**(9): p. 2073-2076.
76. Rodríguez, J.A. and M. Fernández-García, *Introduction the World of Oxide Nanomaterials*, in *Synthesis, Properties, and Applications of Oxide Nanomaterials*. 2007, John Wiley & Sons, Inc. p. 1-5.
77. Rodriguez, J.A., *Orbital-band interactions and the reactivity of molecules on oxide surfaces: From explanations to predictions.* Theoretical Chemistry Accounts, 2002. **107**(3): p. 117-129.
78. Albright, T.A., J.K. Burdett, and M.H. Whangbo, *Orbital Interactions in Chemistry*. 1985, New York: Wiley-Interscience.
79. Hoffmann, R., *Solids and Surfaces: A Chemist's View of Bonding in Extended Structures*. 1988, New York: VCH.
80. Zhang, H., et al., *Use of Metal Oxide Nanoparticle Band Gap To Develop a Predictive Paradigm for Oxidative Stress and Acute Pulmonary Inflammation.* ACS Nano, 2012. **6**(5): p. 4349-4368.

81. Balasubramanyam, A., et al., *In vivo genotoxicity assessment of aluminium oxide nanomaterials in rat peripheral blood cells using the comet assay and micronucleus test.* Mutagenesis, 2009. **24**(3): p. 245-251.
82. Downs, T.R., et al., *Silica nanoparticles administered at the maximum tolerated dose induce genotoxic effects through an inflammatory reaction while gold nanoparticles do not.* Mutation Research/Genetic Toxicology and Environmental Mutagenesis, 2012. **745**(1–2): p. 38-50.
83. Hasan Turkez, B.C., Kubra Celik, *Evaluation of the Potential In Vivo Genotoxicity of Tungsten (VI) Oxide Nanopowder for Human Health.* Key Engineering Materials, 2013. **543**: p. 89-92.
84. Klien, K. and J. Godnić-Cvar, *Genotoxicity of metal nanoparticles: Focus on in vivo studies.* Arhiv za Higijenu Rada i Toksikologiju, 2012. **63**(2): p. 133-145.
85. Naya, M., et al., *In vivo genotoxicity study of titanium dioxide nanoparticles using comet assay following intratracheal instillation in rats.* Regulatory Toxicology and Pharmacology, 2012. **62**(1): p. 1-6.
86. Song, M.F., et al., *Metal nanoparticle-induced micronuclei and oxidative DNA damage in mice.* Journal of Clinical Biochemistry and Nutrition, 2012. **50**(3): p. 211-216.
87. Sycheva, L.P., et al., *Investigation of genotoxic and cytotoxic effects of micro- and nanosized titanium dioxide in six organs of mice in vivo.* Mutation Research - Genetic Toxicology and Environmental Mutagenesis, 2011. **726**(1): p. 8-14.
88. Totsuka Y, H.T., Imai T, Nishikawa A, Nohmi T, Kato T, Masuda S, Kinae N, Hiyoshi K, Ogo S, Kawanishi M, Yagi T, Ichinose T, Fukumori N, Watanabe M, Sugimura T, Wakabayashi K, *Genotoxicity of nano/microparticles in in vitro micronuclei, in vivo comet and mutation assay systems.* Part Fibre Toxicol., 2009 **6**(23): p. 1-11.
89. Trouiller, B., et al., *Titanium dioxide nanoparticles induce DNA damage and genetic instability in vivo in mice.* Cancer Research, 2009. **69**(22): p. 8784-8789.
90. Fairbairn, D.W., P.L. Olive, and K.L. O'Neill, *The comet assay: A comprehensive review.* Mutation Research - Reviews in Genetic Toxicology, 1995. **339**(1): p. 37-59.
91. Tice, R.R., et al., *Single cell gel/comet assay: Guidelines for in vitro and in vivo genetic toxicology testing.* Environmental and Molecular Mutagenesis, 2000. **35**(3): p. 206-221.
92. Courbiere, B., et al., *Ultrastructural Interactions and Genotoxicity Assay of Cerium Dioxide Nanoparticles on Mouse Oocytes.* International journal of molecular sciences, 2013. **14**(11): p. 21613-21628.
93. Fenech, M., *The in vitro micronucleus technique.* Mutation Research - Fundamental and Molecular Mechanisms of Mutagenesis, 2000. **455**(1-2): p. 81-95.
94. Schmid, W., *The micronucleus test.* Mutation Research, 1975. **31**(1): p. 9-15.
95. Fenech, M., *The micronucleus assay determination of chromosomal level DNA damage.* Methods in molecular biology (Clifton, N.J.), 2008. **410**: p. 185-216.
96. OECD. *Test No. 487: In Vitro Mammalian Cell Micronucleus Test* OECD Guidelines for the Testing of Chemicals, Section 4 2010 23 July 2010 [cited 2014 May 22, 2014]; Available from: http://www.oecd-ilibrary.org/environment/test-no-487-in-vitro-mammalian-cell-micronucleus-test_9789264091016-en.
97. OECD. *Test No. 471: Bacterial Reverse Mutation Test* OECD Guidelines for the Testing of Chemicals, Section 4 1997 21 July 1997 [cited 2014 May 22, 2014].
98. Kramer, J.A., J.E. Sagartz, and D.L. Morris, *The application of discovery toxicology and pathology towards the design of safer pharmaceutical lead candidates.* Nat Rev Drug Discov, 2007. **6**(8): p. 636-49.
99. Hansen, K., et al., *Benchmark data set for in silico prediction of Ames mutagenicity.* J Chem Inf Model, 2009. **49**(9): p. 2077-81.

100. Webb, S.J., et al., *Feature combination networks for the interpretation of statistical machine learning models: application to Ames mutagenicity.* J Cheminform, 2014. **6**(1): p. 8.
101. Handy, R., et al., *Practical considerations for conducting ecotoxicity test methods with manufactured nanomaterials: what have we learnt so far?* Ecotoxicology, 2012. **21**(4): p. 933-972.
102. OECD, *Guidelines 475 genetic toxicology: in vivo mammalian bone marrow cytogenetic test-chromosome analysis.*, OECD, Editor. 1997.
103. Demir, E., et al., *Determination of TiO2, ZrO2, and Al2O3 Nanoparticles on Genotoxic Responses in Human Peripheral Blood Lymphocytes and Cultured Embyronic Kidney Cells.* J Toxicol Environ Health A, 2013. **76**(16): p. 990-1002.
104. Kim, Y.-J., et al., *Genotoxicity of aluminum oxide (Al2O3) nanoparticle in mammalian cell lines.* Molecular & Cellular Toxicology, 2009. **5**(2): p. 172-178.
105. Liman, R., *Genotoxic effects of Bismuth (III) oxide nanoparticles by Allium and Comet assay.* Chemosphere, 2013. **93**(2): p. 269-73.
106. Kumari, M., et al., *Toxicity Study of Cerium Oxide Nanoparticles in Human Neuroblastoma Cells.* International journal of toxicology, 2014: p. 1091581814522305.
107. Auffan, M., et al., *CeO2 nanoparticles induce DNA damage towards human dermal fibroblasts in vitro.* Nanotoxicology, 2009. **3**(2): p. 161-171.
108. Pierscionek, B.K., et al., *Nanoceria have no genotoxic effect on human lens epithelial cells.* Nanotechnology, 2010. **21**(3).
109. Kain, J., H.L. Karlsson, and L. Möller, *DNA damage induced by micro- and nanoparticles - interaction with FPG influences the detection of DNA oxidation in the comet assay.* Mutagenesis, 2012. **27**(4): p. 491-500.
110. De Marzi, L., et al., *Cytotoxicity and genotoxicity of ceria nanoparticles on different cell lines in vitro.* International Journal of Molecular Sciences, 2013. **14**(2): p. 3065-3077.
111. Lee, S.W., S.M. Kim, and J. Choi, *Genotoxicity and ecotoxicity assays using the freshwater crustacean Daphnia magna and the larva of the aquatic midge Chironomus riparius to screen the ecological risks of nanoparticle exposure.* Environ Toxicol Pharmacol, 2009. **28**(1): p. 86-91.
112. Alarifi, S., et al., *Oxidative stress contributes to cobalt oxide nanoparticles-induced cytotoxicity and DNA damage in human hepatocarcinoma cells.* International journal of nanomedicine, 2013. **8**: p. 189.
113. Midander, K., et al., *Surface characteristics, copper release, and toxicity of nano- and micrometer-sized copper and copper(II) oxide particles: A cross-disciplinary study.* Small, 2009. **5**(3): p. 389-399.
114. Karlsson, H.L., et al., *Copper oxide nanoparticles are highly toxic: A comparison between metal oxide nanoparticles and carbon nanotubes.* Chemical Research in Toxicology, 2008. **21**(9): p. 1726-1732.
115. Di Bucchianico, S., et al., *Multiple cytotoxic and genotoxic effects induced in vitro by differently shaped copper oxide nanomaterials.* Mutagenesis, 2013. **28**(3): p. 287-299.
116. Wang, Z., et al., *CuO nanoparticle interaction with human epithelial cells: Cellular uptake, location, export, and genotoxicity.* Chemical Research in Toxicology, 2012. **25**(7): p. 1512-1521.
117. Isani, G., et al., *Comparative toxicity of CuO nanoparticles and CuSO4 in rainbow trout.* Ecotoxicology and Environmental Safety, 2013. **97**(0): p. 40-46.
118. Gomes, T., et al., *Genotoxicity of copper oxide and silver nanoparticles in the mussel< i> Mytilus galloprovincialis</i>.* Marine environmental research, 2013. **84**: p. 51-59.
119. Dai, L., et al., *Effects, Uptake, and Depuration Kinetics of Silver Oxide and Copper Oxide Nanoparticles in a Marine Deposit Feeder, Macoma balthica.* ACS Sustainable Chemistry & Engineering, 2013. **1**(7): p. 760-767.

120. Buffet, P.-E., et al., *A mesocosm study of fate and effects of CuO nanoparticles on endobenthic species (Scrobicularia plana, Hediste diversicolor).* Environmental science & technology, 2013. **47**(3): p. 1620-1628.
121. Bayat, N., et al., *The effects of engineered nanoparticles on the cellular structure and growth of Saccharomyces cerevisiae.* Nanotoxicology, 2014. **8**(4): p. 363-373.
122. Alarifi, S., et al., *Cytotoxicity and genotoxicity of copper oxide nanoparticles in human skin keratinocytes cells.* International journal of toxicology, 2013: p. 1091581813487563.
123. Guichard, Y., et al., *Cytotoxicity and genotoxicity of nanosized and microsized titanium dioxide and iron oxide particles in Syrian hamster embryo cells.* annals of occupational Hygiene, 2012. **56**(5): p. 631-644.
124. Freyria, F.S., et al., *Hematite nanoparticles larger than 90 nm show no sign of toxicity in terms of lactate dehydrogenase release, nitric oxide generation, apoptosis, and comet assay in murine alveolar macrophages and human lung epithelial cells.* Chemical research in toxicology, 2012. **25**(4): p. 850-861.
125. Bhattacharya, K., et al., *Titanium dioxide nanoparticles induce oxidative stress and DNA-adduct formation but not DNA-breakage in human lung cells.* Particle and Fibre Toxicology, 2009. **6**.
126. Singh, S.P., et al., *Comparative study of genotoxicity and tissue distribution of nano and micron sized iron oxide in rats after acute oral treatment.* Toxicology and Applied Pharmacology, 2013. **266**(1): p. 56-66.
127. Auffan, M., et al., *In vitro interactions between DMSA-coated maghemite nanoparticles and human fibroblasts: A physicochemical and cyto-genotoxical study.* Environmental Science and Technology, 2006. **40**(14): p. 4367-4373.
128. Singh, S.P., et al., *Genotoxicity of nano- and micron-sized manganese oxide in rats after acute oral treatment.* Mutation Research - Genetic Toxicology and Environmental Mutagenesis, 2013. **754**(1-2): p. 39-50.
129. Hong, S.C., et al., *Subtle cytotoxicity and genotoxicity differences in superparamagnetic iron oxide nanoparticles coated with various functional groups.* International journal of nanomedicine, 2011. **6**: p. 3219.
130. Ahamed, M., et al., *Iron oxide nanoparticle-induced oxidative stress and genotoxicity in human skin epithelial and lung epithelial cell lines.* Current pharmaceutical design, 2013. **19**(37): p. 6681-6690.
131. Könczöl, M., et al., *Cytotoxicity and genotoxicity of size-fractionated iron oxide (magnetite) in A549 human lung epithelial cells: role of ROS, JNK, and NF-κB.* Chem Res Toxicol, 2011. **24**(9).
132. Gomaa, I.O., et al., *Evaluation of in vitro mutagenicity and genotoxicity of magnetite nanoparticles.* Drug discoveries & Therapeutics, 2013. **7**(3): p. 116-123.
133. Gerloff, K., et al., *Cytotoxicity and oxidative DNA damage by nanoparticles in human intestinal Caco-2 cells.* Nanotoxicology, 2009. **3**(4): p. 355-364.
134. Singh, S.P., et al., *Toxicity assessment of manganese oxide micro and nanoparticles in Wistar rats after 28 days of repeated oral exposure.* J Appl Toxicol, 2013. **33**(10): p. 1165-79.
135. Lankoff, A., et al., *Effect of surface modification of silica nanoparticles on toxicity and cellular uptake by human peripheral blood lymphocytes in vitro.* Nanotoxicology, 2013. **7**(3): p. 235-50.
136. Jin, Y., et al., *Toxicity of luminescent silica nanoparticles to living cells.* Chemical Research in Toxicology, 2007. **20**(8): p. 1126-1133.
137. Wang, J.J., B.J.S. Sanderson, and H. Wang, *Cytotoxicity and genotoxicity of ultrafine crystalline SiO2 participate in cultured human lymphoblastoid cells.* Environmental and Molecular Mutagenesis, 2007. **48**(2): p. 151-157.

138. Wang, J.J., H. Wang, and B.J.S. Sanderson, *Ultrafine quartz-induced damage in human lymphoblastoid cells in vitro using three genetic damage end-points.* Toxicology Mechanisms and Methods, 2007. **17**(4): p. 223-232.
139. Barnes, C.A., et al., *Reproducible cornet assay of amorphous silica nanoparticles detects no genotoxicity.* Nano Letters, 2008. **8**(9): p. 3069-3074.
140. Choi, H.S., et al., *Genotoxicity of nano-silica in mammalian cell lines.* Toxicology and Environmental Health Sciences, 2011. **3**(1): p. 7-13.
141. Gonzalez, L., et al., *Exploring the aneugenic and clastogenic potential in the nanosize range: A549 human lung carcinoma cells and amorphous monodisperse silica nanoparticles as models.* Nanotoxicology, 2010. **4**(4): p. 382-395.
142. Gong, C., et al., *The role of reactive oxygen species in silicon dioxide nanoparticle-induced cytotoxicity and DNA damage in HaCaT cells.* Molecular biology reports, 2012. **39**(4): p. 4915-4925.
143. Gehrke, H., et al., *In vitro toxicity of amorphous silica nanoparticles in human colon carcinoma cells.* Nanotoxicology, 2011. **7**(3): p. 274-293.
144. Durnev, A., et al., *Evaluation of genotoxicity and reproductive toxicity of silicon nanocrystals.* Bulletin of experimental biology and medicine, 2010. **149**(4): p. 445-449.
145. Khan, M.J. and Q. Husain, *Influence of pH and temperature on the activity of SnO2-bound α-amylase: A genotoxicity assessment of SnO2 nanoparticles.* Preparative Biochemistry and Biotechnology, 2014. **44**(6): p. 558-571.
146. Roszak, J., et al., *A strategy for in vitro safety testing of nanotitania-modified textile products.* Journal of Hazardous Materials, 2013. **256–257**(0): p. 67-75.
147. Dobrzyńska, M.M., et al., *Genotoxicity of silver and titanium dioxide nanoparticles in bone marrow cells of rats in vivo.* Toxicology, 2014. **315**(0): p. 86-91.
148. Clemente, Z., et al., *Fish exposure to nano-TiO2 under different experimental conditions: Methodological aspects for nanoecotoxicology investigations.* Science of The Total Environment, 2013. **463–464**(0): p. 647-656.
149. Chen, Z., et al., *Genotoxic evaluation of titanium dioxide nanoparticles in vivo and in vitro.* Toxicology Letters, 2014. **226**(3): p. 314-319.
150. Bernardeschi, M., et al., *Genotoxic potential of TiO2 on bottlenose dolphin leukocytes.* Analytical and Bioanalytical Chemistry, 2010. **396**(2): p. 619-623.
151. Dunford, R., et al., *Chemical oxidation and DNA damage catalysed by inorganic sunscreen ingredients.* FEBS Letters, 1997. **418**(1-2): p. 87-90.
152. Falck, G.C., et al., *Genotoxic effects of nanosized and fine TiO2.* Hum Exp Toxicol, 2009. **28**(6-7): p. 339-52.
153. Lindberg, H.K., et al., *Genotoxicity of inhaled nanosized TiO2 in mice.* Mutation Research/Genetic Toxicology and Environmental Mutagenesis, 2012. **745**(1â€“2): p. 58-64.
154. Saber, A.T., et al., *Nanotitanium dioxide toxicity in mouse lung is reduced in sanding dust from paint.* Particle and Fibre Toxicology, 2012. **9**.
155. Gopalan, R.C., et al., *The effect of zinc oxide and titanium dioxide nanoparticles in the Comet assay with UVA photoactivation of human sperm and lymphocytes.* Nanotoxicology, 2009. **3**(1): p. 33-39.
156. Kermanizadeh, A., et al., *An in vitro liver model-assessing oxidative stress and genotoxicity following exposure of hepatocytes to a panel of engineered nanomaterials.* Part Fibre Toxicol, 2012. **9**(1): p. 28.
157. Jugan, M.-L., et al., *Titanium dioxide nanoparticles exhibit genotoxicity and impair DNA repair activity in A549 cells.* Nanotoxicology, 2012. **6**(5): p. 501-513.

158. Jackson, P., et al., *Maternal inhalation of surface-coated nanosized titanium dioxide (UV-Titan) in C57BL/6 mice: Effects in prenatally exposed offspring on hepatic DNA damage and gene expression.* Nanotoxicology, 2013. **7**(1): p. 85-96.
159. Hu, C., et al., *Toxicological effects of TiO< sub> 2</sub> and ZnO nanoparticles in soil on earthworm< i> Eisenia fetida</i>.* Soil Biology and Biochemistry, 2010. **42**(4): p. 586-591.
160. Hamzeh, M. and G.I. Sunahara, *In vitro cytotoxicity and genotoxicity studies of titanium dioxide (TiO2) nanoparticles in Chinese hamster lung fibroblast cells.* Toxicology in Vitro, 2013. **27**(2): p. 864-873.
161. Hackenberg, S., et al., *Intracellular distribution, geno-and cytotoxic effects of nanosized titanium dioxide particles in the anatase crystal phase on human nasal mucosa cells.* Toxicology letters, 2010. **195**(1): p. 9-14.
162. Hackenberg, S., et al., *Nanosized titanium dioxide particles do not induce DNA damage in human peripheral blood lymphocytes.* Environmental and molecular mutagenesis, 2011. **52**(4): p. 264-268.
163. Ghosh, M., M. Bandyopadhyay, and A. Mukherjee, *Genotoxicity of titanium dioxide (TiO< sub> 2</sub>) nanoparticles at two trophic levels: Plant and human lymphocytes.* Chemosphere, 2010. **81**(10): p. 1253-1262.
164. Ghosh, M., A. Chakraborty, and A. Mukherjee, *Cytotoxic, genotoxic and the hemolytic effect of titanium dioxide (TiO2) nanoparticles on human erythrocyte and lymphocyte cells in vitro.* Journal of Applied Toxicology, 2013. **33**(10): p. 1097-1110.
165. DEMİR, E., N. Kaya, and B. KAYA, *Genotoxic effects of zinc oxide and titanium dioxide nanoparticles on root meristem cells of< i> Allium</i> cepa by comet assay.* Turkish Journal of Biology, 2014. **38**(1): p. 31-39.
166. D'Agata, A., et al., *Enhanced toxicity of'bulk'titanium dioxide compared to'fresh'and'aged'nano-TiO2 in marine mussels (Mytilus galloprovincialis).* Nanotoxicology, 2014. **8**(5): p. 549-558.
167. Botelho, M.C., et al., *Effects of titanium dioxide nanoparticles in human gastric epithelial cells in vitro.* Biomedicine & Pharmacotherapy, 2014. **68**(1): p. 59-64.
168. Barillet, S., et al., *Toxicological consequences of TiO2, SiC nanoparticles and multi-walled carbon nanotubes exposure in several mammalian cell types: an in vitro study.* Journal of nanoparticle research, 2010. **12**(1): p. 61-73.
169. Gurr, J.R., et al., *Ultrafine titanium dioxide particles in the absence of photoactivation can induce oxidative damage to human bronchial epithelial cells.* Toxicology, 2005. **213**(1-2): p. 66-73.
170. Kang, S.J., et al., *Titanium dioxide nanoparticles trigger p53-mediated damage response in peripheral blood lymphocytes.* Environ Mol Mutagen, 2008. **49**(5): p. 399-405.
171. Reeves, J.F., et al., *Hydroxyl radicals (*OH) are associated with titanium dioxide (TiO(2)) nanoparticle-induced cytotoxicity and oxidative DNA damage in fish cells.* Mutat Res, 2008. **640**(1-2): p. 113-22.
172. Vevers, W.F. and A.N. Jha, *Genotoxic and cytotoxic potential of titanium dioxide (TiO2) nanoparticles on fish cells in vitro.* Ecotoxicology, 2008. **17**(5): p. 410-420.
173. Wang, J.J., B.J.S. Sanderson, and H. Wang, *Cyto- and genotoxicity of ultrafine TiO2 particles in cultured human lymphoblastoid cells.* Mutation Research - Genetic Toxicology and Environmental Mutagenesis, 2007. **628**(2): p. 99-106.
174. Woodruff, R.S., et al., *Genotoxicity evaluation of titanium dioxide nanoparticles using the Ames test and Comet assay.* Journal of Applied Toxicology, 2012. **32**(11): p. 934-943.
175. Wan, R., et al., *DNA damage caused by metal nanoparticles: involvement of oxidative stress and activation of ATM.* Chem Res Toxicol, 2012. **25**(7): p. 1402-11.
176. Shukla, R.K., et al., *ROS-mediated genotoxicity induced by titanium dioxide nanoparticles in human epidermal cells.* Toxicol In Vitro, 2011. **25**(1): p. 231-41.

177. Shukla, R.K., et al., *TiO2 nanoparticles induce oxidative DNA damage and apoptosis in human liver cells.* Nanotoxicology, 2013. **7**(1): p. 48-60.
178. Sekar, D., et al., *DNA damage and repair following In vitro exposure to two different forms of titanium dioxide nanoparticles on trout erythrocyte.* Environ Toxicol, 2014. **29**(1): p. 117-27.
179. Rajapakse, K., et al., *Experimental evidence of false-positive Comet test results due to TiO2 particle--assay interactions.* Nanotoxicology, 2013. **7**(5): p. 1043-51.
180. Saquib, Q., et al., *Titanium dioxide nanoparticles induced cytotoxicity, oxidative stress and DNA damage in human amnion epithelial (WISH) cells.* Toxicol In Vitro, 2012. **26**(2): p. 351-61.
181. Prasad, R.Y., et al., *Effect of treatment media on the agglomeration of titanium dioxide nanoparticles: impact on genotoxicity, cellular interaction, and cell cycle.* ACS Nano, 2013. **7**(3): p. 1929-42.
182. Prasad, R.Y., et al., *Cellular interactions and biological responses to titanium dioxide nanoparticles in HepG2 and BEAS-2B cells: role of cell culture media.* Environ Mol Mutagen, 2014. **55**(4): p. 336-42.
183. Petković, J., et al., *DNA damage and alterations in expression of DNA damage responsive genes induced by TiO2 nanoparticles in human hepatoma HepG2 cells.* Nanotoxicology, 2011. **5**(3): p. 341-53.
184. Petković, J., et al., *Pre-irradiation of anatase TiO2 particles with UV enhances their cytotoxic and genotoxic potential in human hepatoma HepG2 cells.* J Hazard Mater, 2011. **196**: p. 145-52.
185. Pakrashi, S., et al., *In vivo genotoxicity assessment of titanium dioxide nanoparticles by Allium cepa root tip assay at high exposure concentrations.* PLoS One, 2014. **9**(2): p. e87789.
186. Kermanizadeh, A., et al., *An in vitro assessment of panel of engineered nanomaterials using a human renal cell line: Cytotoxicity, pro-inflammatory response, oxidative stress and genotoxicity.* BMC Nephrology, 2013. **14**(1).
187. Mu, Q., et al., *Systematic investigation of the physicochemical factors that contribute to the toxicity of ZnO nanoparticles.* Chem Res Toxicol, 2014. **27**(4): p. 558-67.
188. Sharma, V., et al., *DNA damaging potential of zinc oxide nanoparticles in human epidermal cells.* Toxicology Letters, 2009. **185**(3): p. 211-218.
189. Sharma, V., et al., *Induction of oxidative stress, DNA damage and apoptosis in mouse liver after sub-acute oral exposure to zinc oxide nanoparticles.* Mutation Research - Genetic Toxicology and Environmental Mutagenesis, 2012. **745**(1-2): p. 84-91.
190. Valdiglesias, V., et al., *Neuronal cytotoxicity and genotoxicity induced by zinc oxide nanoparticles.* Environment International, 2013. **55**: p. 92-100.
191. Kwon, J.Y., et al., *Lack of genotoxic potential of ZnO nanoparticles in in vitro and in vivo tests.* Mutation Research/Genetic Toxicology and Environmental Mutagenesis, 2014. **761**(0): p. 1-9.
192. Sarkar, J., et al., *Biosynthesis and safety evaluation of ZnO nanoparticles.* Bioprocess Biosyst Eng, 2014. **37**(2): p. 165-71.
193. Hackenberg, S., et al., *Cytotoxic, genotoxic and pro-inflammatory effects of zinc oxide nanoparticles in human nasal mucosa cells< i> in vitro</i>.* Toxicology in vitro, 2011. **25**(3): p. 657-663.
194. Demir, E., et al., *Zinc oxide nanoparticles: Genotoxicity, interactions with UV-light and cell-transforming potential.* Journal of hazardous materials, 2014. **264**: p. 420-429.
195. Alarifi, S., et al., *Induction of oxidative stress, DNA damage, and apoptosis in a malignant human skin melanoma cell line after exposure to zinc oxide nanoparticles.* International journal of nanomedicine, 2013. **8**: p. 983.
196. Ali, D., et al., *Oxidative stress and genotoxic effect of zinc oxide nanoparticles in freshwater snail< i> Lymnaea luteola</i> L.* Aquatic Toxicology, 2012. **124**: p. 83-90.

197. Balasubramanyam, A., et al., *Evaluation of genotoxic effects of oral exposure to Aluminum oxide nanomaterials in rat bone marrow.* Mutation Research - Genetic Toxicology and Environmental Mutagenesis, 2009. **676**(1): p. 41-47.
198. Perreault, F.o., et al., *Genotoxic effects of copper oxide nanoparticles in Neuro 2A cell cultures.* Science of The Total Environment, 2012. **441**(0): p. 117-124.
199. Chen, D., et al., *Biocompatibility of magnetic Fe3O4 nanoparticles and their cytotoxic effect on MCF-7 cells.* International journal of nanomedicine, 2012. **7**: p. 4973.
200. Corradi, S., et al., *Influence of serum on< i> in situ</i> proliferation and genotoxicity in A549 human lung cells exposed to nanomaterials.* Mutation Research/Genetic Toxicology and Environmental Mutagenesis, 2012. **745**(1): p. 21-27.
201. Gonzalez, L., et al., *Co-assessment of cell cycle and micronucleus frequencies demonstrates the influence of serum on the in vitro genotoxic response to amorphous monodisperse silica nanoparticles of varying sizes.* Nanotoxicology, 2014. **8**(8): p. 876-884.
202. Uboldi, C., et al., *Amorphous silica nanoparticles do not induce cytotoxicity, cell transformation or genotoxicity in Balb/3T3 mouse fibroblasts.* Mutation Research/Genetic Toxicology and Environmental Mutagenesis, 2012. **745**(1–2): p. 11-20.
203. Sadiq, R., et al., *Genotoxicity of TiO2 anatase nanoparticles in B6C3F1 male mice evaluated using Pig-a and flow cytometric micronucleus assays.* Mutation Research/Genetic Toxicology and Environmental Mutagenesis, 2012. **745**(1–2): p. 65-72.
204. Xu, J., et al., *Acute toxicity of intravenously administered titanium dioxide nanoparticles in mice.* PloS one, 2013. **8**(8): p. e70618.
205. Rahman, Q., et al., *Evidence that ultrafine titanium dioxide induces micronuclei and apoptosis in syrian hamster embryo fibroblasts.* Environmental Health Perspectives, 2002. **110**(8): p. 797-800.
206. Lu, P.J., I.C. Ho, and T.C. Lee, *Induction of sister chromatid exchanges and micronuclei by titanium dioxide in Chinese hamster ovary-K1 cells.* Mutation Research - Genetic Toxicology and Environmental Mutagenesis, 1998. **414**(1-3): p. 15-20.
207. Linnainmaa, K., P. Kivipensas, and H. Vainio, *Toxicity and cytogenetic studies of ultrafine titanium dioxide in cultured rat liver epithelial cells.* Toxicology in Vitro, 1997. **11**(4): p. 329-335.
208. Kumari, M., et al., *Cytogenetic and genotoxic effects of zinc oxide nanoparticles on root cells of Allium cepa.* Journal of Hazardous Materials, 2011. **190**(1–3): p. 613-621.
209. Yin, H., et al., *Effects of surface chemistry on cytotoxicity, genotoxicity, and the generation of reactive oxygen species induced by ZnO nanoparticles.* Langmuir, 2010. **26**(19): p. 15399-15408.
210. Pan, X., et al., *Mutagenicity evaluation of metal oxide nanoparticles by the bacterial reverse mutation assay.* Chemosphere, 2010. **79**(1): p. 113-116.
211. Kumar, A., et al., *Engineered ZnO and TiO(2) nanoparticles induce oxidative stress and DNA damage leading to reduced viability of Escherichia coli.* Free Radic Biol Med, 2011. **51**(10): p. 1872-81.
212. Warheit, D.B., et al., *Development of a base set of toxicity tests using ultrafine TiO2 particles as a component of nanoparticle risk management.* Toxicology Letters, 2007. **171**(3): p. 99-110.
213. Lopes, I., et al., *Toxicity and genotoxicity of organic and inorganic nanoparticles to the bacteria Vibrio fischeri and Salmonella typhimurium.* Ecotoxicology, 2012. **21**(3): p. 637-648.
214. Yoshida, R., D. Kitamura, and S. Maenosono, *Mutagenicity of water-soluble ZnO nanoparticles in Ames test.* Journal of Toxicological Sciences, 2009. **34**(1): p. 119-122.
215. Dufour, E.K., et al., *Clastogenicity, photo-clastogenicity or pseudo-photo-clastogenicity: Genotoxic effects of zinc oxide in the dark, in pre-irradiated or simultaneously irradiated Chinese hamster ovary cells.* Mutation Research - Genetic Toxicology and Environmental Mutagenesis, 2006. **607**(2): p. 215-224.

216. Hasegawa, G., M. Shimonaka, and Y. Ishihara, *Differential genotoxicity of chemical properties and particle size of rare metal and metal oxide nanoparticles.* Journal of Applied Toxicology, 2012. **32**(1): p. 72-80.
217. Schins, R.P. and A.M. Knaapen, *Genotoxicity of poorly soluble particles.* Inhal Toxicol, 2007. **19 Suppl 1**: p. 189-98.
218. AshaRani, P.V., et al., *Cytotoxicity and genotoxicity of silver nanoparticles in human cells.* ACS Nano, 2009. **3**(2): p. 279-290.
219. Chompoosor, A., et al., *The role of surface functionality on acute cytotoxicity, ROS generation and DNA damage by cationic gold nanoparticles.* Small, 2010. **6**(20): p. 2246-2249.
220. Merhi, M., et al., *Study of serum interaction with a cationic nanoparticle: Implications for in vitro endocytosis, cytotoxicity and genotoxicity.* International Journal of Pharmaceutics, 2012. **423**(1): p. 37-44.
221. Stone, V., H. Johnston, and R.P. Schins, *Development of in vitro systems for nanotoxicology: methodological considerations.* Crit. Rev. Toxicol., 2009. **39**(613–626).
222. Storm, A.J., et al., *Insulating behavior for DNA molecules between nanoelectrodes at the 100 nm length scale.* Applied Physics Letters, 2001. **79**(23): p. 3881-3883.
223. Grigor'Eva, A., et al., *Fine mechanisms of the interaction of silver nanoparticles with the cells of Salmonella typhimurium and Staphylococcus aureus.* BioMetals, 2013. **26**(3): p. 479-488.
224. Palchoudhury, S., et al., *DNA interaction of Pt-attached iron oxide nanoparticles.* IEEE Transactions on Magnetics, 2013. **49**(1): p. 373-376.
225. Tang, W., et al., *The cadmium-mercaptoacetic acid complex contributes to the genotoxicity of mercaptoacetic acid-coated CdSe-core quantum dots.* International Journal of Nanomedicine, 2012. **7**: p. 2631-2640.
226. Rice, Z., N.C. Cady, and M. Bergkvist. *Terminal phosphate group influence on DNA - TiO 2 nanoparticle interactions*. 2010.
227. Wahab, R., et al., *A non-aqueous synthesis, characterization of zinc oxide nanoparticles and their interaction with DNA.* Synthetic Metals, 2009. **159**(23-24): p. 2443-2452.
228. Fahrenkopf, N.M., et al., *Immobilization mechanisms of deoxyribonucleic acid (DNA) to hafnium dioxide (HfO 2) surfaces for biosensing applications.* ACS Applied Materials and Interfaces, 2012. **4**(10): p. 5360-5368.
229. Jin, P., et al., *Interactions between Al 12X (X = Al, C, N and P) nanoparticles and DNA nucleobases/base pairs: Implications for nanotoxicity.* Journal of Molecular Modeling, 2012. **18**(2): p. 559-568.
230. Komarov, P.V., L.V. Zherenkova, and P.G. Khalatur, *Computer simulation of the assembly of gold nanoparticles on DNA fragments via electrostatic interaction.* Journal of Chemical Physics, 2008. **128**(12).
231. Liu, J., *Adsorption of DNA onto gold nanoparticles and graphene oxide: Surface science and applications.* Physical Chemistry Chemical Physics, 2012. **14**(30): p. 10485-10496.
232. Paillusson, F., et al., *Effective interaction between charged nanoparticles and DNA.* Physical Chemistry Chemical Physics, 2011. **13**(27): p. 12603-12613.
233. Rubin, Y.V. and L.F. Belous, *Molecular structure and interactions of nucleic acid components in nanoparticles: Ab initio calculations.* Ukrainian Journal of Physics, 2012. **57**(7): p. 723-731.
234. Shewale, V., et al., *First-principles study of nanoparticle-biomolecular interactions: Anchoring of a (ZnO) 12 cluster on nucleobases.* Journal of Physical Chemistry C, 2011. **115**(21): p. 10426-10430.
235. Pong, B.K., J.Y. Lee, and B.L. Trout, *First principles computational study for understanding the interactions between ssDNA and gold nanoparticles: Adsorption of methylamine on gold nanoparticulate surfaces.* Langmuir, 2005. **21**(25): p. 11599-11603.

236. Yang, J., et al., *Dissociation of double-stranded DNA by small metal nanoparticles.* Journal of Inorganic Biochemistry, 2007. **101**(5): p. 824-830.
237. Park, M.V.D.Z., et al., *Genotoxicity evaluation of amorphous silica nanoparticles of different sizes using the micronucleus and the plasmid lacZ gene mutation assay.* Nanotoxicology, 2011. **5**(2): p. 168-181.
238. Semisch, A., et al., *Cytotoxicity and genotoxicity of nano - and microparticulate copper oxide: Role of solubility and intracellular bioavailability.* Particle and Fibre Toxicology, 2014. **11**(1).
239. Alarifi, S., et al., *Oxidative stress contributes to cobalt oxide nanoparticles-induced cytotoxicity and DNA damage in human hepatocarcinoma cells.* International Journal of Nanomedicine, 2013. **8**: p. 189-199.
240. Bazak, R., et al., *Cytotoxicity and DNA cleavage with core-shell nanocomposites functionalized by a KH domain DNA binding peptide.* Nanoscale, 2013. **5**(23): p. 11394-11399.
241. Chibber, S., S.A. Ansari, and R. Satar, *New vision to CuO, ZnO, and TiO2 nanoparticles: Their outcome and effects.* Journal of Nanoparticle Research, 2013. **15**(4).
242. Guichard, Y., et al., *Cytotoxicity and genotoxicity of nanosized and microsized titanium dioxide and iron oxide particles in syrian hamster embryo cells.* Annals of Occupational Hygiene, 2012. **56**(5): p. 631-644.
243. Lin, W., et al., *Toxicity of nano- and micro-sized ZnO particles in human lung epithelial cells.* Journal of Nanoparticle Research, 2009. **11**(1): p. 25-39.
244. Saquib, Q., et al., *Zinc ferrite nanoparticles activate IL-1b, NFKB1, CCL21 and NOS2 signaling to induce mitochondrial dependent intrinsic apoptotic pathway in WISH cells.* Toxicology and Applied Pharmacology, 2013. **273**(2): p. 289-297.
245. Wang, C.C., et al., *Phototoxicity of zinc oxide nanoparticles in HaCaT keratinocytes-generation of oxidative DNA damage during UVA and visible light irradiation.* Journal of Nanoscience and Nanotechnology, 2013. **13**(6): p. 3880-3888.
246. Zhao, X., et al., *Acute ZnO nanoparticles exposure induces developmental toxicity, oxidative stress and DNA damage in embryo-larval zebrafish.* Aquatic Toxicology, 2013. **136-137**: p. 49-59.
247. Jacobsen, N.R., et al., *Lung inflammation and genotoxicity following pulmonary exposure to nanoparticles in ApoE-/-mice.* Particle and Fibre Toxicology, 2009. **6**.
248. Park, M.V.D.Z., et al., *The effect of particle size on the cytotoxicity, inflammation, developmental toxicity and genotoxicity of silver nanoparticles.* Biomaterials, 2011. **32**(36): p. 9810-9817.
249. Patil, G., et al., *Evaluation of cytotoxic, oxidative stress, proinflammatory and genotoxic responses of micro- and nano-particles of dolomite on human lung epithelial cells A549.* Environmental Toxicology and Pharmacology, 2012. **34**(2): p. 436-445.
250. Reeves, J.F., et al., *Hydroxyl radicals ({radical dot}OH) are associated with titanium dioxide (TiO2) nanoparticle-induced cytotoxicity and oxidative DNA damage in fish cells.* Mutation Research - Fundamental and Molecular Mechanisms of Mutagenesis, 2008. **640**(1-2): p. 113-122.
251. Skocaj, M., et al., *Titanium dioxide in our everyday life; Is it safe?* Radiology and Oncology, 2011. **45**(4): p. 227-247.
252. Vandebriel, R.J. and W.H. De Jong, *A review of mammalian toxicity of ZnO nanoparticles.* Nanotechnology, Science and Applications, 2012. **5**(1): p. 61-71.
253. Guichard, Y., et al., *Cytotoxicity and genotoxicity of nanosized and microsized titanium dioxide and iron oxide particles in Syrian hamster embryo cells.* Ann Occup Hyg, 2012. **56**(5): p. 631-44.
254. Warheit, D.B., *How Meaningful are the Results of Nanotoxicity Studies in the Absence of Adequate Material Characterization?* Toxicological Sciences, 2008. **101**(2): p. 183-185.
255. Ong, K.J., et al., *Widespread Nanoparticle-Assay Interference: Implications for Nanotoxicity Testing.* PLoS ONE, 2014. **9**(3): p. e90650.
256. Samuel Reich, E., *Nano rules fall foul of data gap.* Nature, 2011. **480**(7376): p. 160-161.

257. Geys, J., B. Nemery, and P.H.M. Hoet, *Assay conditions can influence the outcome of cytotoxicity tests of nanomaterials: Better assay characterization is needed to compare studies.* Toxicology in Vitro, 2010. **24**(2): p. 620-629.
258. Hirsch, C., et al., *Nanomaterial cell interactions: Are current in vitro tests reliable?* Nanomedicine, 2011. **6**(5): p. 837-847.
259. Laurent, S., et al., *Crucial Ignored Parameters on Nanotoxicology: The Importance of Toxicity Assay Modifications and "Cell Vision".* PLoS ONE, 2012. **7**(1): p. e29997.
260. Gomaa, I.O., et al., *Evaluation of in vitro mutagenicity and genotoxicity of magnetite nanoparticles.* Drug discoveries & Therapeutics, 2013. **7**(3): p. 116-123.
261. Landsiedel, R., et al., *Gene toxicity studies on titanium dioxide and zinc oxide nanomaterials used for UV-protection in cosmetic formulations.* Nanotoxicology, 2010. **4**(4): p. 364-381.
262. Shukla, R.K., et al., *TiO(2) nanoparticles induce oxidative DNA damage and apoptosis in human liver cells.* Nanotoxicology, 2013. **7**(1): p. 48-60.
263. Gurr, J.R., et al., *Ultrafine titanium dioxide particles in the absence of photoactivation can induce oxidative damage to human bronchial epithelial cells.* Toxicology, 2005. **213**(1-2): p. 66-73.
264. Shi, H., et al., *Titanium dioxide nanoparticles: a review of current toxicological data.* Part Fibre Toxicol, 2013. **10**: p. 15.
265. Chen, T., J. Yan, and Y. Li, *Genotoxicity of titanium dioxide nanoparticles.* Journal of Food and Drug Analysis, 2014. **22**(1): p. 95-104.